CO-SELECTION OF METAL AND ANTIBIOTIC RESISTANCE IN THE GUT MICROBIAL COMMUNITY OF THE MUMMICHOG FISH (FUNDULUS HETEROCLITUS)

by

NICOLE A. LLOYD

A dissertation submitted to the

School of Graduate Studies

Rutgers, The State University of New Jersey

In partial fulfillment of the requirements

For the degree of

Doctor of Philosophy

Graduate Program in Microbial Biology

Written under the direction of

Tamar Barkay

And approved by

_____

_____

_____

_____

New Brunswick, New Jersey

October 2018

ABSTRACT OF THE DISSERTATION

Co-selection of Metal and Antibiotic Resistance in the Gut Microbial Community of the Mummichog Fish (*Fundulus heteroclitus*)

by NICOLE A. LLOYD

Dissertation Director:

Tamar Barkay, Ph. D.

Microbial resistance to antibiotics is one of the most pressing health care concerns we are currently facing. Antibiotic resistance can be selected for by metals through the process known as co-selection. Co-selection occurs through two primary mechanisms: i) co-resistance, when genes encoding both are located together in the genome and ii), cross-resistance, when the same mechanism provides resistance to both (e.g. efflux pump proteins). This thesis describes co-selection in the gut microbiota of a forage feeder fish, the mummichog (*Fundulus heteroclitus*). By comparing gut microbiota from fish from a mercury contaminated site and a relatively clean site, we established the mummichog gut as a reservoir of antibiotic and mercury resistant microbiota. We further examined three representative isolates with interesting antibiotic and metal resistant profiles. Genome analyses revealed few instance of co-resistance, and instead, presented various chromosomally-encoded resistance genes, including some of public health concern, (i.e. a bla_{OXA} carbapenemase), and contributions from cross-resistance. All three organisms contained a large number of efflux pump proteins, including multiple RND efflux pump operons. Testing of the strains shows that RND efflux pumps may be involved in

resistance to several classes of drugs. A transcriptomic study is in progress to understand the regulation of arsenate resistance and the potential involvement of RND efflux pumps under metal stress. Together, this work describes the abundance and inventory of antibiotic resistance genes and mechanisms in the mummichog gut microbiome and establishes the fish gut as a reservoir of such genes. This work further adds to the understanding of the role of RND efflux pumps in resistance to antibiotics, which is critical in understanding multi-drug resistance in Gram negative bacteria.

ACKNOWLEDGEMENTS

I would like to extend my gratitude to the many people who have helped me throughout my graduate school years. First and foremost, I must thank Dr. Tamar Barkay, for her guidance, encouragement, and support throughout the years. I thank Dr. Sylvie Nazaret for extending the warmest welcome to me in her lab in France, and for her mentorship in completing my thesis. I will always remember my experience in France, both for the productive time I had in the lab, and the amazing cultural experiences. Thank you to Dr. Nicole Fahrenfeld for her valuable input as a member of my committee and for the chance to get involved in projects in her lab. Thanks to Dr. Gerben Zylstra for helpful feedback as a member of my committee and for being a super supportive program director. Thanks to the Department of Biochemistry and Microbiology for financial support to attend conferences and the amazingly helpful staff in Lipman including Jessie, Kathy, Lindsay, Allison, Audrey, Tamara, and Peter. I would also like to acknowledge funding from the New Jersey Water Resources Research Institute and The Chateaubriand Fellowship from the Embassy of France in the United States.

I would like to also express my gratitude to those who have assisted me in various ways throughout the years: Dr. John Reinfelder for introducing me to research as an undergraduate, serving on my qualifying exam committee, and valuable feedback at lab meetings; Dr. Sharron Crane for statistical assistance, friendship, and making teaching an awesome experience; Dr. Sarah Janssen for assistance with mercury analysis. Thanks also to the Cooper lab and Roland Hagan at the Rutgers University Marine Field Station for help with my fish experiments.

I would like to thank and acknowledge my lab mate who has been there through it all, Javiera, for her support and the fun times we have shared during this unique experience. Thanks also to past and present members of the Barkay Lab, especially Spencer. Shout-out to my fellow biochemistry TA ladies: Kate, Brittany, Tiff, Jie, and Gina for their friendship and making teaching an enjoyable experience.

I would also like to acknowledge the support of the good friends I have made during my time at Rutgers: Ann, Aakansha, Ashley, and Fatima, for the life-changing times we have shared. Finally, I would like to thank my parents Margie and John, my sister Betty Lou, and my partner Ike for their love and continued support.

TABLE OF CONTENTS

LIST OF TABLES

LIST OF FIGURES

PREFACE

Chapter 2 has been published as "Co-selection of Mercury and Multiple Antibiotic Resistances in Bacteria Exposed to Mercury in the *Fundulus heteroclitus* gut Microbiome", Lloyd NA, Janssen SE, Reinfelder, JR, Barkay T. 2016. *Curr Microbiol*. Dec;73(6)834-842. PMID: 27620386.

Lloyd NA contribution: Figures 1, 2; Tables 1, 2, 3; Supplementary Tables 1-9; Supplementary Figures 1-3.

Chapter 3 has been accepted for publication as Lloyd NA, Nazaret, S, and Barkay T. "Whole Genome Sequences to Assess the Link Between Antibiotic and Metal Resistance in Three Coastal Marine Bacteria Isolated from the Mummichog (*Fundulus heteroclitus*) Gastrointestinal Tract" in *Marine Pollution Bulletin*. July 2018.

Lloyd NA contribution: Figures 1, 2; Tables 1, 2, 3; Supplementary Figures 1, 2; Supplementary Tables 1-16.

Chapter 4 is in preparation as Lloyd NA, Nazaret, S, and Barkay T. “Genome-Facilitated Discovery of RND Efflux Pump-Mediated Resistance to Cephalosporins in *Vibrio* spp. Isolated from the Mummichog Fish Gut” for submission in *Journal of Global Antimicrobial Resistance.* Lloyd NA participated in writing the manuscript and is directly responsible for those experiments dealing with the genome sequences and RND efflux pump inhibitors.

Chapter 1: Introduction

Antibiotic Resistance

Microbial resistance to antibiotics (ABs) is a growing problem that threatens the effective prevention and treatment of many infectious diseases. The Centers for Disease Control (CDC) report an estimated 2 million infections and 23,000 deaths in the United States are caused by AB resistant bacteria [1] every year. In his 1945 Nobel Prize acceptance speech, Alexander Fleming, the founder of penicillin, forecasted the current resistance crisis, and warned that bacteria will become resistant to antimicrobials due to overuse. We failed to heed Dr. Fleming's advice and today the quest for novel ABs is miniscule simply due to profitability issues. The lack of new effective antimicrobials exacerbates the looming challenge of microbial resistance, as addressed by a United States Surgeon General, Dr. Boris Lushniak. In 2014, he reported that AB resistant infections are a public health crisis and not only cause more deaths than AB susceptible infections, but also take longer and are more costly to treat [2]. Due to a lack of reliable data on AB resistant infection rates, it is difficult to estimate or predict morbidity and mortality. Nevertheless, antimicrobial resistance (AMR) poses an immense clinical and public health burden [3] and if we do not take steps to combat the problem, the consequences will only become more severe as bacteria become increasingly resistant to ABs.

Resistance to ABs can be mediated by genes present in the chromosome or by genes located on extra-chromosomal elements. Bacteria show resistance to ABs through typically four mechanisms: (i) reduction of membrane permeability to the drugs, (ii) enzymatic inactivation of the drug, (iii) efflux of the AB, and (iv) mutation of cellular

target genes rendering these targets less susceptible to the drug [4]. The spread of microbial resistance can be attributed to many factors. The widespread use of ABs in industries such as healthcare, agriculture, and aquaculture contribute to bacterial resistance by creating selective pressures in environments such as wastewater [5]. Bacteria transfer genes encoding resistance among different species through a process known as horizontal gene transfer (HGT). Additionally, heavy metal pollutants have been shown to increase AB resistance in the environment because of the demonstrated genetic linkage between genes encoding heavy metal and AB resistances in bacterial genomes [4]. This genetic linkage together with frequent genetic exchange creates a potentially disastrous reservoir of resistance genes in various locations such as the human body, hospitals, and the environment. Environmental reservoirs of resistance genes remain poorly understood [6]. In order to combat AMR, we need to fully understand the mechanisms of how bacteria obtain resistance determinants in the environment.

Mercury

Mercury (Hg) is a toxic heavy metal that poses global health and environmental risks. While Hg naturally occurs in the environment, anthropogenic activities continue to increase its input to land, the atmosphere, and water [7]. Anthropogenic sources of Hg include the burning of fossil fuels, mining, use in precious metal extractions, use in products (i.e. paint, electronics) and use by various industries [7]. Mercury is especially harmful for aquatic systems, as it can be methylated by microorganisms into methylmercury, a potent neurotoxic substance [7]. In addition, methylmercury in aquatic environments biomagnifies in the food web, leading to increased risk of human exposure by fish and shellfish-consumption.

Mercury has been used as a topical antimicrobial since the 15th century [8]. Additionally, Hg was used as a laxative, diuretic, antidepressant, and to treat sexually transmitted and skin infections. Further, it has been used as a pesticide and an antifungal agent in fertilizers [8]. In the developed world, the use of Hg as an antimicrobial has drastically declined, but it can still be found as a preservative in some vaccines [8].

Mercury Resistance

While Hg in high concentrations is toxic to many organisms, some microorganisms can adapt to its presence by employing Hg detoxification systems [9]. Mercury resistance is well characterized in different types of microorganisms and the most extensively studied system is the bacterial Hg resistance (*mer*) operon [10]. The proteobacterial *mer* operon contains several well-characterized genes involved in genetic regulation and the detoxification of Hg by reduction of cationic Hg [Hg(II)] to elemental volatile Hg [Hg(0)] by the mercuric reductase, MerA. The *mer* operon also encodes proteins involved in regulation (MerR or MerD), periplasmic Hg(II) scavenging (MerP), one or more inner membrane spanning proteins (MerT, MerC, MerE, MerF, MerG) implicated in Hg(II) transport into the cytoplasm, and organomercury degradation (MerB) [11].

Mobile Genetic Elements

Plasmids are extrachromosomal pieces of DNA found in Bacteria and Archaea. Plasmids are known to carry genes for AB and metal resistance, virulence factors, toxins, catabolic enzymes and more [12] and they can be classified by their function. For example, R plasmids code for resistance to ABs, degradative plasmids code for catabolic enzymes, and virulence plasmids increase pathogenicity of bacteria [12]. Plasmids may

be conjugative, i.e., they can transfer copies of themselves to other cells. R plasmids, which are known to carry resistance to Hg as well, can be conjugative and can also be mobilized by conjugative plasmids [12].

Other genetic elements that increase gene mobility and recombination found in bacterial genomes include insertion sequences and transposons [12]. Insertion sequences are able to make copies of themselves and insert into DNA and can thus become part of the bacterial chromosome. Transposons typically contain resistance genes as well as sequences that enable the element to make and move copies of itself [12]. Transposons and insertion sequences occasionally integrate with each other, which results in complex assemblies such as the Tn*21* transposon. The Tn*21* transposon is believed to have arisen when a transposable integron (In*2*) moved into a Hg resistance transposon related to Tn*501*[13]. Integrons, in contrast to transposons and insertion sequences, cannot move themselves, but can move gene cassettes into an insertion site, which then can incorporate itself into a larger genetic element such as a plasmid or chromosome [14]. Integrons are classified in several classes; the Class 1 integron is widely found and often associated with antibiotic resistance genes [15].

Co-selection of Metal and Antibiotic Resistance

Exposure to contaminants, especially metals, may promote the spread of antibiotic resistance in the environment through co-selection [4]. Co-selection occurs primarily through 1) co-resistance, when genes encoding for antibiotic and metal resistance are located together in the genome or on mobile genetic elements, 2) cross-resistance, when the same system (e.g. efflux pumps) confers resistance to both chemicals and 3) co-regulation, when different resistance genes are regulated by the same regulatory system.

Co-resistance

The phenomenon of co-resistance has been known for several decades [4]. Co-resistance is usually related to various HGT elements, such as plasmids, ICEs, transposons, and integrons. Horizontal transfer of antibiotic resistance genes has been widely studied, and conjugation is generally considered the most common mechanism [16]. Generally, plasmids encoding for resistance to ABs and other stressors, e.g., metals, are more commonly found in bacteria isolated from humans or domestic animals [17].

Cross-resistance and Efflux Pumps

The most common way by which cross-resistance is mediated is by multidrug efflux pumps. Efflux pumps are proteins that span the plasma membrane of bacteria and extrude various compounds from the cell. Efflux pumps are found across all domains of life and they are highly conserved among bacterial species [18]. While there is still a lack of knowledge on some of the specificities of these pumps, efflux systems have been identified as contributing to multiple antibiotic resistances in the *Enterobacteriaceae* [19].

Efflux pumps are known to extrude a wide-range of substances, including metals, antibiotics, biocides, plant signaling compounds, and cell-to-cell communication compounds [18]. Efflux pumps also contribute to host colonization. For example, the *acrAB* efflux pump in *E. coli* extrudes bile salts [20], suggesting this pump may have evolved for surviving in the harsh environment of the gut. Efflux pump genes are usually chromosomally-encoded. However, some narrow spectrum resistance efflux pumps are known to spread through HGT [21].

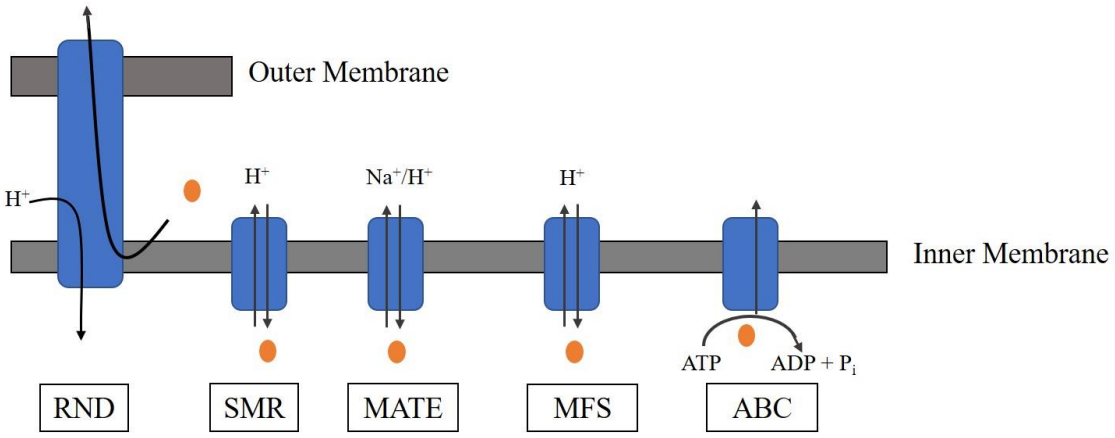

Figure 1.1 - Efflux pump structural families and their respective energy mechanisms. Modified from [21].

There are five primary structural families of efflux pumps (Figure 1.1), categorized based on the mode by which they are energized. The ABC (ATP Binding Cassette) family uses ATP to transport substrates. Only a few of this type have been identified as multidrug exporters in prokaryotes [21]. The Major Facilitator Superfamily (MFS) use the proton motive force (PMF). The EmrAB-TolC efflux pump in *E. coli* is an example from this group and is one of the most widely studied. The Small Multidrug Resistance (SMR) transporters also use the PMF. The Multidrug and Toxic compound Extrusion (MATE) family uses a Na^+/H^+ transport system and is commonly associated with resistance in Gram positive bacteria.

The Resistance Nodulation and cell Division (RND) superfamily plays a prominent role in AMR in Gram negative bacteria. RND efflux pumps consist of a tripartite system including an outer membrane protein (OMP), a membrane fusion protein (MFP), and the inner membrane protein (IMP). The AcrAB in *E. coli* (Figure 1.2) has been shown to export dyes, detergents, chloramphenicol, tetracyclines, macrolides, betalactams, fluoroquinolones, and organic solvents [18].

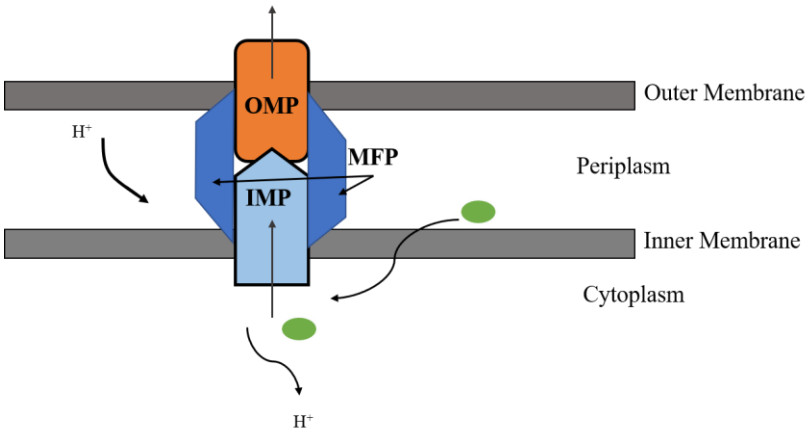

Figure 1.2 - Structure of a typical tripartite RND efflux pump system in a Gram-negative membrane. Examples of proteins include AcrA (MFP), AcrB (IMP), TolC (OMP) [22].

Co-regulation

The third way by which co-selection occurs is through the transcriptional co-regulation of resistance genes. For example, heavy metal ions can increase regulation of efflux systems (e.g. the AcrAB efflux pump in *E. coli*), which results in increased resistance towards antibiotics [23].

Efflux Pump Regulation

Efflux pump genes are usually expressed at low levels in the cell. However, there are a number of different effectors that can affect the expression. For example, non-physiological, inherited, high-level expression can be affected by mutations in genes involved in efflux pump regulation [21]. Further, one local regulator can act as a repressor or activator of different multidrug efflux systems [21]. Cell stress and quorum sensing molecules have also been shown to induce expression [21]. Global transcriptional regulators (e.g. SoxS, RobA, or RamA) can also affect activation [22].

Previous Work on Co-Selection

The connection between heavy metal resistance and AMR has been studied in fish and several other systems. Pathak and Gopal [24] studied metal resistance and AB resistance in several organs of the catfish (*Clarias batrachus*), not including the gastrointestinal tract. Although they did not test for resistance to Hg, they reported significant incidences of resistance to other heavy metals and ABs. In another study, Meredith et al. [25] examined Hg resistance and AMR in the GI tract of the feral brook trout (*Salvelinus fontinalis*), a fish that consumes invertebrates and other small fish. They showed broad-spectrum Hg resistance and multi-drug resistance in fish sampled from a pristine lake. Akinbowale et al. [26] studied skin and muscle tissues from rainbow trout (*Oncorhynchus* mykiss) collected from Australian fish farms and reported multi-drug resistant (MDR) isolates with tolerance to heavy metals other than Hg. A connection has been demonstrated in other systems as well, including sphagnum bogs. Wardwell et al. [27] isolated bacteria showing mercury and multi-drug resistance from Hg-containing sphagnum bogs in the northeastern United States. In summary, the connection between heavy metal resistance and multi-drug resistance is well-documented in various ecosystems and results suggest a genetic linkage between the two.

The connection between Hg resistance and AMR in the gut of a benthic forage feeder fish has not been studied. In 2008, McIntosh et al. [15] examined AMR and Hg resistance genes found on plasmids isolated from *Aeromonas salmonicida* obtained from fish farms in Canada. Detailed testing revealed that the isolates were resistant to eight ABs in addition to Hg [15]. The study found resistance genes organized into cassettes carried on large IncA/C plasmids and this plasmid was carried by all of the MDR strains

[15]. The Inc-type plasmids are a family of plasmids associated with *Enterobacteriaceae* that are known to encode genes for their own conjugative transfer in addition to providing resistance towards antimicrobial agents [28]. Because it is clear that the plasmids were spread by HGT, this study is an example of how HGT in aquatic environments contributes to the spread of AMR. In a recent study, Henriques et al. assessed co-selection in epiphytic bacteria from an estuarine salt marsh [29]. They observed that metal exposure selected for intrinsically resistant organisms and possibly mobile genetic elements, and established plant surfaces as a niche for co-selection.

A recent study on the antibiotic and metal resistome in *P. aeurginosa* found that multidrug efflux pumps play an important role in AMR, more so than any physical genetic link [30]. Another study reported on the increased extrusion of antibiotics via RND efflux pumps in marine biofilms exposed to heavy metals [31].

Vibrio* and *Shewanella

The Vibrionaceae class is known to make up a large portion of the wild mummichog gut intestinal microbial community [32]. The two aquatic genera on which this study is focused, *Shewanella* and *Vibrio*, are both opportunistic pathogens and are both considered vehicles of AMR [33, 34]. *Shewanella* species (primarily *S. algae* and *S. putrefraciens*) have been implicated in human infections [35] and are known to harbor resistance genes for antibiotics of public health concern [33]. Likewise, *Vibrio* are important reservoirs and vehicles of AMR genes [34] due to their abundance and diversity in coastal waters, ability to develop and acquire AMR in response to selective pressure, and their ability to spread resistance genes by HGT [36]. *V. parahaemolyticus*

thrives in marine, estuarine, and aquaculture environments and is a causative agent of seafood-borne food poisoning [37].

Objective and Hypotheses

The overall objective of this dissertation was to investigate the mechanisms of co-selection (co-resistance and cross-resistance) in the gut microbial community of a benthic, forage-feeder fish, the mummichog (*Fundulus heteroclitus*). We hypothesized that co-selection of AMR genes by metals occurs in the gut microbial community of fish living in heavy metal contaminated environments. The gastrointestinal tract is conducive to HGT due to the selection pressure of heavy metals, the abundance of nutrients in, and the stable temperature of, the fish gut. We hypothesized that genes encoding for resistance to antibiotics and metals would either be co-located in the genome, and potentially on mobile genetic elements (co-resistance), and that efflux pumps would contribute to the phenotype of metal and antibiotic resistance (cross-resistance).

Specific Objectives:

1. Assess the co-selection of Hg and multi-drug resistance in bacteria isolated from the mummichog gut microbial community

2. Investigate the mechanisms underlying the association between antibiotic and metal resistance in aquatic bacteria isolated from the mummichog gut microbial community using whole genome sequencing

3. Assess the role of efflux pumps (cross-resistance) in co-selection

Chapter 2: Co-selection of Mercury and Multiple Antibiotic Resistances in Bacteria Exposed to Mercury in the *Fundulus heteroclitus* Gut Microbiome

Lloyd, NA, *et al*. 2016. *Curr Microbiol*. PMID: 27620386

Abstract

The emergence and spread of antibiotic-resistant pathogenic bacteria is currently one of the most serious challenges to human health. To combat this problem, it is critical to understand the processes and pathways that result in the creation of antibiotic resistance gene pools in the environment. In this study, we examined the effects of mercury (Hg) exposure on the co-selection of Hg and antibiotic-resistant bacteria that colonize the gastrointestinal tract of the mummichog (*Fundulus heteroclitus*), a small, estuarine fish. We examined this connection in two experimental systems: (i) a short-term laboratory exposure study where fish were fed Hg-laced food for 15 days and (ii) an examination of environmental populations from two sites with very different levels of Hg contamination. In the lab exposure study, fish muscle tissue accumulation of Hg was proportional to food Hg concentration (R^2 = 0.99; $P < 0.0001$). In the environmental study, fish from the contaminated site contained three-fold more Hg compared to fish from the reference site ($P < 0.05$). Further, abundance of the Hg resistance gene mercuric reductase was more than eightfold higher ($P < 0.0001$) in DNA extracts of ingesta of fish from the contaminated site, suggesting adaptation to Hg. Finally, resistance to three or more antibiotics was more common in Hg-resistant as compared to Hg-sensitive bacterial colonies that were isolated from fish ingesta ($P < 0.001$) demonstrating co-selection of Hg and antibiotic resistances. Together, our results highlight the possibility for the

creation of antibiotic resistance gene pools as a result of exposure to Hg in contaminated environments.

Introduction

Microbial resistance to antibiotics is a pressing public health concern that threatens to reverse the last 70 years of medical advancements. The Centers for Disease Control report that an estimated 2 million infections and 23,000 deaths in the United States are caused by antibiotic-resistant bacteria each year [1]. Not only are they more deadly, but infections caused by antibiotic-resistant bacteria also take longer and are more costly to treat [2]. The widespread use of antibiotics in industries such as healthcare, agriculture, and aquaculture contributes to the spread of antibiotic resistance by selecting for antibiotic-resistant bacteria [7]. This selective pressure eliminates the bacteria that are sensitive, thus stimulating the propagation of resistant members in a population. Moreover, the spread of resistance in microbial communities is accelerated by the carriage of antibiotic resistance genes on mobile genetic elements such as plasmids and transposable elements [38]. Since these elements carry fitness-enhancing genes for other environmental stressors, antibiotic resistance may be co-selected indirectly by exposure to various toxic substances such as heavy metals [39]. This mode of co-selection has been termed co-resistance by Baker-Austin et al. [4] to distinguish it from cross-selection whereby low specificity efflux pumps render resistance to drugs and toxic metals [7].

The demonstration that metal exposure has resulted in co-resistance to antibiotics requires evidence that (i) exposure to metals has taken place, (ii) this exposure resulted in the selection of metal-resistant bacteria, (iii) the metal-resistant bacteria are more

resistant to antibiotics than metal sensitive strains, and (iv) both metal and antibiotic resistance genes are carried on the same mobile genetic elements. Previous studies have shown that increased frequency of antibiotic resistance [requirements (i) and (ii) above] was related to copper and zinc concentrations in pig manure [40] and in agricultural soils [41], to mercury (Hg) concentrations in stream sediments [42], and among gold miners in French Guyana [43]. Mercury- and antibiotic resistant strains, naturally present in the oral cavity [44], are highly enriched by exposure to Hg in dental amalgam; moreover, this exposure affects selection of co-resistant strains not only among oral flora but also in the intestinal microbiome [45]. However, only a few studies (e.g., [46]) demonstrated that resistance to antibiotics was more prevalent among metal-resistant than sensitive strains [requirement (iii)]. The co-carriage of metal and antibiotic resistance genes on conjugative plasmids [15, 39], transposons [47], and integrons [48] is well-documented [requirement (iv)] and co-resistance to Hg and several antibiotics in aerobic heterotrophic bacteria from mine tailing ponds was attributed to co-carriage on large conjugative plasmids [49]. Previous research clearly demonstrated co-resistance of Hg and antibiotics among gastrointestinal (GI) tract microbes of feral brook trout *Salvelinus fontinalis* [25], a predatory fish exposed to Hg through the food chain.

Mercury is a highly toxic metal known to biomagnify in the aquatic food web leading to high exposure risks for humans. Despite the toxicity and abundance of anthropogenic and natural sources of Hg in the environment, some microorganisms have adapted to its presence by employing detoxification systems [9]. The most extensively studied Hg detoxification mechanism is bacterial reduction of Hg(II) to the volatile elemental form mediated by the *mer* system [10]. This system is particularly suited for

the study of the role of co-resistance on the dissemination of antibiotic resistance because genes encoding the *mer* system often travel on mobile genetic elements with antibiotic resistance genes [47, 48]. Furthermore, conjugative and mobilized plasmids captured by the exogenous plasmid isolation approach [50] are often Hg resistance plasmids (e.g., [51]). A recent genomic survey of thousands of bacterial genomes and plasmids showed that among biocide/metal resistance genes, resistances to Hg and quaternary ammonium compounds were commonly linked to antibiotic resistance genes [17]. Here we describe a fish exposure study that was designed to test if exposure to Hg selects for Hg-resistant bacteria and if this selection results in the co-selection of antibiotic resistances.

In this study, we examined the effect of environmental and laboratory exposure to Hg on the selection of Hg and antibiotic-resistant bacteria among microbes that colonize the gastrointestinal (GI) tract of the mummichog (*Fundulus heteroclitus*), a small, estuarine fish. Mummichogs forage for benthic invertebrates which directly exposes them to Hg and other contaminants in sediments [52]. The GI tract of this organism may serve as a model in which to study co-resistance as a pathway for the enrichment of antibiotic resistance because it provides an environment conducive for genetic exchange: a stable temperature, abundance of microbial growth substrates, and a plethora of bacteria that may be directly exposed to Hg. Therefore, relating antibiotic resistance phenotypes of bacteria in the GI tract to Hg exposure may shed light on the extent that Hg contamination may co-select for antibiotic resistance in the environment.

Materials and Methods

An expanded version of the materials and methods is available in Appendix A.

Laboratory Hg Exposures

To prepare Hg-laced fish food, 9 g of TetraMin Tropical Fish Food Flakes (Tetra, Blacksburg, VA) was soaked in 10 mL $HgCl_2$ solutions for 24 h and then dried in an oven (70°C) for 2 days. A control was treated in a similar manner, but prepared in the absence of Hg. Dried food stocks were homogenized using a Teflon mortar and pestle into pieces small enough for fish to eat, approximately 1 mm [53]. Concentrations of total Hg (THg) in the food after treatment were 24.4 ± 4.2 μg g^{-1} THg for the low exposure and 132 ± 4.1 μg g^{-1} THg for the high exposure treatment. The control food with no Hg amendments had a background concentration of 0.08 ± 0.01 μg g^{-1} THg and 0.026 ± 0.004 μg g^{-1} MeHg (Table 2.1). Selection of Hg food concentrations was based on the known Hg levels in Berry's Creek (BC), which is near an EPA Superfund site in the Hackensack Meadowlands, NJ, where THg concentrations of 42–1360 ng L^{-1} in surface waters [54] and 20–51 mg kg^{-1} in sediments [55] have been recorded.

Mummichogs for the laboratory feeding experiment were trapped without bait in tidal channels among the salt marshes of Great Bay (GB), Tuckerton, New Jersey, in January 2014. Upon arrival in the laboratory, fish were randomly separated into a control, low Hg exposure, or high Hg exposure aquaria. Fish were fed for 15 days during which each aquarium received 0.45 g of fish food per day, in an attempt to provide the recommended feeding level of 0.5–1.0% of fish body weight per day [56]. At the completion of the experiment, it was determined that each aquarium received between 1.0 and 1.8% of fish body weight per day.

Environmental Hg Exposures

Mummichogs for the examination of environmental Hg exposures were collected from BC, part of the Hackensack River estuary, a legacy Hg-contaminated site in the Hackensack Meadowlands [57]. As a reference site with little anthropogenic input, we sampled fish from GB, Tuckerton, NJ. Fish were trap-netted in GB in June 2014 and August 2014 (Fig. 2.S1). Fish collected in June were analyzed for Hg concentration, while fish collected in August were used for the Hg resistance and antibiotic resistance experiments. A previous study has shown no significant increase in fish Hg tissue concentrations over a period of weeks when mummichogs were exposed to Hg-contaminated sediments [58]. Mummichogs from BC were captured via cast net in July 2014. No bait was used to trap any of the fish collected for this study. During transport to the lab, fish were stored in an aerated bucket containing site water.

Processing of Fish

Laboratory and environmentally collected fish were sacrificed at the end of the 15-day exposure experiment or within 2 h after field collection according to the American Veterinary Medical Association Method for Humane Euthanasia for Finfish [59], including euthanasia in 0.4% tricaine methanesulfonate. Prior to dissection, the length and weight of each fish were determined (Tables 2.S1–2.S5). The intact GI tract was then surgically removed and its contents aseptically transferred to a sterile microfuge tube. Additionally, a muscle tissue sample was taken and freeze dried for Hg analysis. All applicable international, national, and/or institutional guidelines for the care and use of animals were followed.

Analysis of Total Hg and Methylmercury

Total Hg was quantified in fish tissue, fish food, aquarium water, and site water via cold vapor atomic fluorescence spectroscopy (CVAFS) [60] using a MERX-T Hg Analyzer (Brooks Rand Laboratories). Analysis of methylmercury (MeHg) was performed by CVAFS following isothermal gas chromatographic separation of ethylated derivates according to Liang et al. [61] using a Tekran 2500. For further details on the procedures, see Appendix A.

Collection of Gut Ingesta

Fish GI tracts were washed in sterile 0.85% sodium chloride solution before gut contents were extracted using tweezers into sterile pre-weighed 1.5 mL microfuge tubes. Gut ingesta from 4 to 7 fish were pooled to obtain enough biomass for plating. Samples were placed on ice until processing, which was performed on the same day no longer than 4 h following fish euthanasia. Gut ingesta were diluted 1:10 in sterile saline. Remaining ingesta was stored in 50% glycerol at -80°C.

Growth Media Preparation

Tryptic soy agar (TSA) plates were prepared using trypticase soy broth and 2% agar. TSA plates amended with Hg (TSA-Hg plates) were prepared by addition of $HgCl_2$ to autoclaved media that was cooled down to 60 °C before plates were poured. While the targeted concentration of Hg was 25 µM, concentrations of Hg in stocks were routinely analyzed to determine actual concentrations of Hg for every batch of prepared plates and actual Hg concentrations are reported throughout this manuscript.

Testing of Colonies for Antibiotic Resistance

To assess resistance to antibiotics and Hg, colonies were randomly chosen from the initial TSA and TSA-Hg plates on which gut ingesta dilutions had been plated. The

colonies were spot plated on the following: TSA-Hg plates, individual plates containing each antibiotic (Table 2.S6), and a TSA plate with no amendments. Antibiotics were chosen based on their modes of action (Table 2.S7). Colonies that failed to grow on the TSA plates with no amendments were not used in any analysis. A colony was considered resistant to Hg and/or an antibiotic if growth was apparent after 5 days of incubation at 23°C. Because the minimum inhibitory concentrations of antibiotics for environmental bacteria are not well known [62], we based the tested concentrations on those reported in a variety of studies [27, 45, 63-65].

DNA Extractions

DNA was extracted from thawed fish gut ingesta samples using the PowerLyzer PowerSoil DNA Isolation Kit (Mo Bio Labs, Carlsbad, CA). Due to the small sample size, ingesta from several fish were combined prior to extraction to obtain sufficient quantities of DNA for qPCR analysis. Unfortunately, we did not have sufficient ingesta from fish collected in the exposure experiment for DNA extraction and gene quantitation by qPCR.

Quantitative PCR (qPCR)

qPCR analysis was performed to quantify glutamine synthetase (*glnA*) and mercuric reductase (*merA*) genes in pooled ingesta samples. The primer set GS2γ and GS1 β [66] was used to quantify the number of *glnA* copies, an estimate of the total number of bacteria in the sample, and primers MerAF and MerA2R were used [67] to quantify *merA*, the gene specifying the central function of the *mer* system. This primer set was designed to capture the diversity of *merA* among the proteobacteria (A. Poulain, personal communication). Samples were analyzed in triplicate and standard deviations (1

SD) of the triplicate readings are reported in the results. For further details on the procedure, see Appendix A.

Results

Exposure of Fish in the Lab: Aquarium Experiment

Mummichogs exposed to Hg in the laboratory, which were collected in winter, were smaller than those collected in the summer (Tables 2.S1–2.S5). At the end of the 15-day exposure period, the average mass of the fish from all treatments (n = 52) was 2.0 ± 2.7 g and the average length was 40 ± 8 mm (Table 2.1) compared with 6.7 ± 3.2 g and 66 ± 3 mm for the summer fish (n = 36) (Table 2.2). In all experiments, fish had little gut contents and therefore ingesta of 1–5 fish were pooled to obtain 4–5 samples for each treatment of 0.03–0.12 g each.

Table 2.1- Concentrations of total Hg (THg) in mummichog muscle tissues and in fish aquarium water and fish lengths and weights at the end of a 15-day laboratory feeding experiment

Treatments	THg in food ($\mu g\ g_{dw}^{-1}$)	MeHg in food ($\mu g\ g_{dw}^{-1}$)	Mean fish length (mm)	Mean fish weight (g)	THg in fish muscle ($\mu g\ g_{ww}^{-1}$)	MeHg in fish muscle ($\mu g\ g_{ww}^{-1}$)	THg in fish aquarium water ($ng\ L^{-1}$)
Control	0.08 ± 0.01 (n = 2)	0.026 ± 0.004 (n = 3)	38.0 ± 3.6 (n = 18)	1.34 ± 0.40 (n = 18)	0.031 ± 0.015 (n = 5)	0.019 ± 0.002 (n = 4)	0.16 ± 0.20 (n = 2)
Low Hg exposure	24.4 ± 4.2 (n = 2)	N.D.	45.0 ± 13.0 (n = 17)	2.5 ± 2.9 (n = 17)	0.041 ± 0.010 (n = 4)	0.033 ± 0.013 (n = 4)	16.55 ± 0.50 (n = 2)
High Hg exposure	131.6 ± 4.1 (n = 2)	N.D.	39.0 ± 4.0 (n = 18)	1.97 ± 3.80 (n = 18)	0.149 ± 0.012 (n = 4)	0.013 ± 0.008 (n = 4)	3.97 ± 2.50 (n = 2)

Concentrations of THg and methylmercury (MeHg) in mummichog food throughout the experiment are also shown. Values are means ± 1 SD

Table 2.2 - Fish lengths and weights of mummichogs collected for field study

Sampling location	Mean fish length (mm)	Mean fish weight (g)	THg in fish muscle ($\mu g\ g_{ww}^{-1}$)	MeHg in fish muscle ($\mu g\ g_{ww}^{-1}$)	THg in water at sampling site ($ng\ L^{-1}$)	THg in sediment at sampling site ($mg\ kg_{dw}^{-1}$)
Berry's Creek (BC)	69.5 ± 9.5 (n = 18)	8.2 ± 3.7 (n = 18)	0.166 ± 0.072 (n = 12)	0.11 ± 0.01 (n = 4)	20.7 ± 1.9 (n = 2)	12.3 ± 4.0 (n = 2)
Great Bay (GB)	71.6 ± 6.8 (n = 18)	9.1 ± 2.5 (n = 18)	0.058 ± 0.017 (n = 12)	0.04 ± 0.01 (n = 4)	28.0 ± 6.3 (n = 2)	0.39 ± 0.03 (n = 2)

Concentrations of total Hg (THg) in mummichog muscle tissues, sampling site water, and sediment are shown, along with concentrations of methylmercury (MeHg) in mummichog muscle tissue. Values are means ± 1 SD of the indicated number of samples.

Accumulation of Hg in Aquarium-Exposed Fish

After 15 days, accumulated Hg in fish muscle was directly proportional to the amount of Hg in the food for each treatment (Tables 2.1, 2.S1, 2.S2, 2.S3; Fig. 2.1). Muscle tissue from the high Hg exposure fish (132 μg g^{-1}) contained 0.149 ± 0.012 μg g^{-1} THg compared to 0.041 ± 0.010 μg g^{-1} in the low exposure and 0.031 ± 0.015 μg g^{-1} in the control fish. Therefore, the accumulation of Hg in fish muscle was nearly five-fold higher after 15 days of exposure compared to the control. The high variability of fish muscle Hg concentrations, as indicated by large standard deviations (8–48% of the means) may be attributed to the natural variability of various physiological processes, including ingestion, assimilation, and excretion, among individual fish. The difference in Hg tissue accumulation among the three treatments was significant ($P < 0.0001$, one-way ANOVA) clearly showing that fish exposure to Hg resulted in tissue accumulation. Furthermore, the Hg concentration in the fish tissue increased in a linear relationship to the Hg concentration in the food (Fig. 2.1), connecting consumption of contaminated food to tissue accumulation. There was no significant difference ($P > 0.05$, one-way ANOVA) in tissue MeHg accumulation between fish exposed to different levels of Hg (Table 2.1).

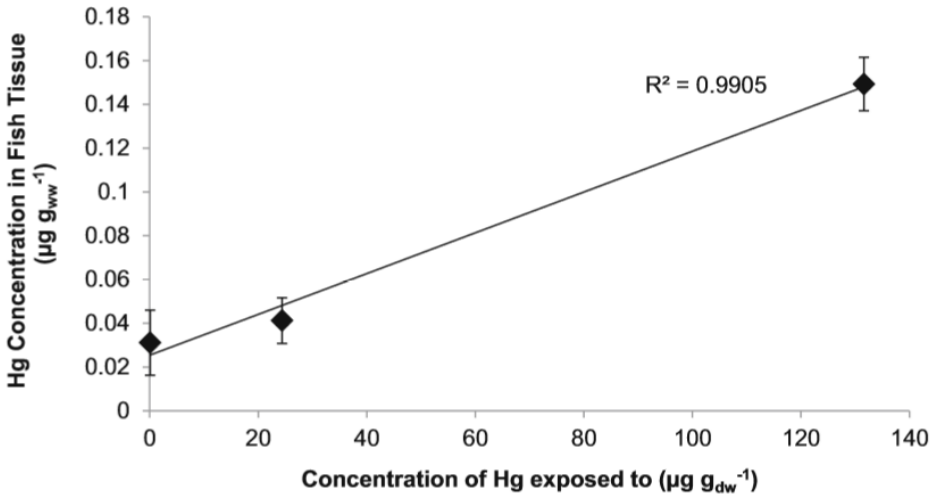

Figure 2.1 - Effect of Hg exposure on Hg tissue accumulation in mummichogs (*F. heteroclitus*) exposed to the indicated Hg concentrations for 15 days in the aquarium study. Values are means ± 1 SD of all determinations; see Table 2.1 for number of replicate analyses

At the completion of the experiment, unfiltered water samples from each aquarium were analyzed for Hg concentration (Table 2.1). Results showed concentrations lower than those recorded in GB field samples and little consistency between Hg concentration in food and water. The most highly dosed aquarium had a lower Hg concentration, 3.97 ng L^{-1} , than the low exposure aquarium, 16.55 ng L^{-1} , suggesting that release from food added little Hg to the aquarium water. Together, the data suggest that the main and perhaps only exposure route of fish to Hg was via ingestion of Hg-amended food.

Linked Antibiotic and Hg Resistances in Bacterial Isolates from the Fish GI Tract

Co-selection of Hg and antibiotic resistance was tested by randomly picking colonies of aerobic heterotrophic GI bacteria from plates on which diluted ingesta was plated and spot transferred to plates each containing a different antibiotic or 12.5 µM Hg (Table 2.S8). A total of 136 colonies, 53 Hg-resistant (HgR) and 83 Hg-sensitive (HgS)

were thus tested. The results indicate that colonies resistant to 3 or 4 antibiotics are almost twice as likely to be HgR than HgS, 32 and 18%, respectively, though this association was not statistically significant ($P > 0.05$, χ^2 test) and therefore the results are not shown. There was no clear connection between Hg resistance and antibiotic resistance among the three different levels of Hg exposure. However, these results suggest a connection between Hg exposure and multi-drug resistances among ingesta bacteria.

Fish Exposed to Hg in Contaminated and Reference Sites in NJ: Field Samples

To examine if long-term exposure to Hg resulted in tissue accumulation and in selection of Hg and antibiotic-resistant GI microbiota, as was observed in the short-term exposure, mummichogs were collected from two field sites in New Jersey. Total Hg concentrations in the sediment clearly reflected the contamination status of the two sites with 12.3 ± 4.0 mg kg_{dw}^{-1} in BC and 0.39 ± 0.03 mg kg_{dw}^{-1} in GB, while water concentrations at the time of sampling were 20.7 ± 1.9 and 28.0 ± 6.3 ng L^{-1} for BC and GB, respectively (Table 2.2). The Hg concentrations in the sediment are of more relevance to this study because mummichogs forage in the sediment and are therefore exposed to Hg in their food.

Accumulation of Hg in Fish Tissue

Fish from both sites were of similar size and weight (Table 2.2) and about twice as long and 4–5 times heavier than the mummichogs that were exposed in the aquarium experiment (Table 2.1). Muscle tissue accumulation of THg in BC fish, 0.166 ± 0.072 µg g^{-1} , was almost three times higher than fish from GB (0.058 ± 0.017 µg g^{-1} , Tables 2.2, 2.S4, 2.S5). Levels of THg in BC fish were greater than the high Hg exposure aquarium

treatment while those in GB fish were between the low and high Hg exposure treatments. The accumulation of THg in fish from the two sites was significantly different (paired *t* test, $P < 0.05$). Muscle tissue MeHg concentrations were low in both populations of mummichogs (Table 2.2) with 0.11 ± 0.01 μg g^{-1} in BC and 0.04 ± 0.01 μg g^{-1} in GB. The proportion of THg as MeHg in mummichog muscle tissue was similar in both sites: 66% in BC and 69% in GB. The relatively high percentage of THg that is not MeHg in mummichog muscle tissue is expected since these are predominantly benthic detritus feeders and are low in the aquatic food chain [68].

Selection of Hg-Resistant Microbes in Fish Ingesta

Selection for Hg resistance among cultured aerobic heterotrophic bacteria was examined in fish ingesta from both the aquarium exposure and field studies (See Appendix A for methods). As observed in the aquarium exposure study, there was no difference in the number of HgR bacteria between the two study sites (Table 2.S9) even though the proportion of resistant organisms in both sites was much higher, about half of all CFU, as compared to fish exposed in aquaria, <2% (Table 2.S8). The difference between the two sites was not significant ($P > 0.05$, two-way ANOVA).

Because only a small proportion of the microbial community from any environment can be cultured aerobically on rich growth medium such as TSA [69], it was possible that adaptation to Hg in the fish ingesta did not occur among cultured aerobic heterotrophs. Therefore, we quantitated the copy number of *merA*, the gene encoding mercuric reductase [67] in DNA extracts of fish ingesta to measure the abundance of Hg resistance genes in the whole community. The abundance of *glnA*, a house-keeping gene encoding for *glnA* in DNA extracts was used as a measure of total microbial biomass.

Ingesta from several fish were combined (Table 2.3) to obtain sufficient amounts of DNA for this analysis and results represent a single sample from each site analyzed in triplicate. qPCR results show that the ratio of *merA*/*glnA* gene copy number was 1/6 in BC and 1/52 in GB, suggesting adaptation to Hg in the GI tract of fish from the contaminated site, BC, as *merA* enrichment in community DNA extracts is a hallmark of adaptation to Hg [70]. Although analysis of more samples is desirable, the highly significant difference in *merA* abundance between fish ingesta from the two sites, (z = -8.139, P < 0.0001, z-test), strongly supports our conclusion.

Table 2.3 - Number of *merA* and *glnA* in ingesta DNA extracts and ratios of *merA*/*glnA* indicated *merA* gene abundance

Sample	DNA extracted from ingesta of:	*glnA* copy number/ng DNA[a]	*merA* copy number/ng DNA	Relative *merA* abundance (*merA*/*glnA*)
GB – 1	6 fish combined	678 ± 276	13 ± 2	1/52
BC – 1	18 fish combined	253 ± 72	40 ± 7	1/6

[a] Average and standard deviation of triplicate qPCR analyses

Co-occurrence of Hg and Antibiotic Resistances Among Ingesta Isolates

We examined the co-occurrence between Hg and antibiotic resistances by testing HgR and HgS colonies for their resistance to 5 (GB) and 6 (BC) antibiotics (Table 2.S6). Compared to the exposure study, we sought to expand the number of antibiotics tested and include those of public health concern. A total of 181 ingesta colonies (84 HgR and 97 HgS) were tested from BC and a total of 106 colonies (80 HgR and 26 HgS) were tested from GB. As was observed above for the aquarium-exposed mummichogs, a larger proportion of the resistant strains were resistant to at least three antibiotics (Fig. 2.2). For GB colonies, these proportions accounted for 68 and 23% of the HgR and HgS colonies, respectively, and for BC, these proportions were 84 and 55%. Interestingly, overall a higher percentage of multi-drug resistance was observed among colonies from the

contaminated BC site compared to GB. Mercury resistance was significantly associated with resistance to multiple antibiotics in both sites (χ^2 test, BC: $P < 0.0001$; GB: $P < 0.001$).

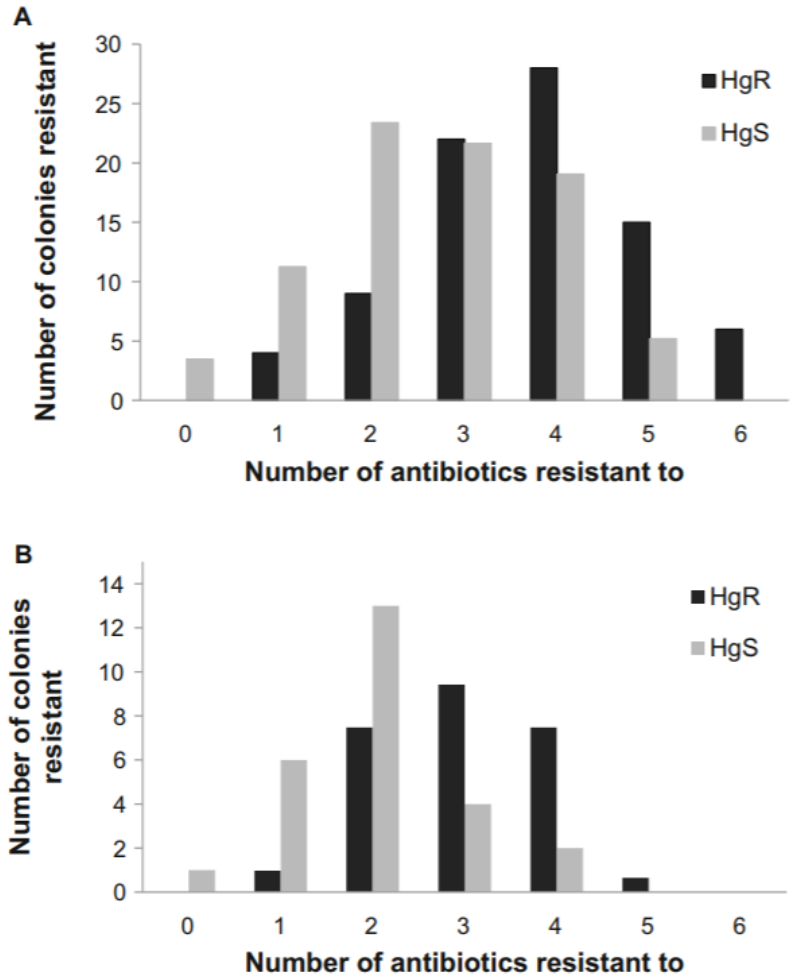

Figure 2.2 - Co-selection of Hg and antibiotic resistances in field studies. The graphs depict the patterns of Hg and antibiotic resistance in the field sites BC (**a**) and GB (**b**). Colonies were scored as either HgR or HgS , and the number of antibiotic resistances was counted.

Discussion

This study examined the effects of Hg exposure on the Hg and antibiotic resistances of the gut microbiota of a small estuarine fish through a short-term laboratory exposure study and examination of environmental populations from two sites with very different levels of Hg contamination. We report that (i) Hg exposure resulted in increased Hg concentrations in fish muscle tissue, (ii) gut microbiomes of exposed fish had an increased abundance of the *merA* gene, suggesting adaptation to Hg, and (iii) HgR bacteria from fish caught in the environment were more likely to be resistant to multiple antibiotics as compared to HgS bacteria. Together, our study shows that the creation of antibiotic-resistant gene pools, likely by co-selection with Hg resistance, may occur in the environment.

Fish exposure to Hg was evident by the accumulation of Hg in fish tissue. In the aquarium study, Hg concentrations in fish muscle were directly related to the amount of Hg in the food (Fig. 2.1). Similarly, Hg concentrations in field collected fish corresponded to the degree of Hg contamination at each site with BC fish containing three-fold more Hg than GB fish. This is consistent with the 32-fold higher sediment Hg concentrations in BC as compared to GB (Table 2.2). Mummichogs are known to feed on sediment detritus [71] and others have reported concentrations of Hg in BC mummichogs spanning a range of 0.5–1.1 μg g^{-1} [72]. A substantial proportion of the accumulated Hg in fish tissue was in the inorganic form. As mummichogs feed relatively low in the estuarine food chain, the proportion of MeHg of THg in their tissues likely reflects its amount in their food and the dynamics of Hg intake and removal.

That Hg accumulated in mummichog tissue is not related to biomagnification is strongly suggested by the absence of correlations between fish length and weight and tissue Hg content (Figs. 2.S2, 2.S3); such correlations are commonly observed in predatory fish [25]. For the short-term laboratory exposure study, close to 33% of the Hg in the food was MeHg prior to dosing with inorganic Hg. A majority of the THg in the control and low exposures was in the methylated form, while the fish from the high exposure aquarium contained a much lower proportion of MeHg: <10% (Table 2.1). In a previous study, mummichogs that were collected from a reference site and incubated in aquaria containing sediments from our polluted site, BC, accumulated as much as 0.11 μg g^{-1} Hg, almost all as MeHg, after 2 weeks of exposure [58]. Thus, a short-term incubation may result in the preferential accumulation of MeHg by fish, possibly due to removal of inorganic Hg and retention of MeHg [73], as well as to different partition patterns into fish fillets [74]. In the highly dosed fish, the MeHg originally present in the food, 0.08 ± 0.01 μg g^{-1}, was diluted more than 5000 times by inorganic Hg, likely leading to the observed lower proportion of MeHg in their tissues. The possibility of methylation by microbes in the fish gut, although rarely observed [75], could also contribute to MeHg accumulation patterns. In both studies, fish tissue Hg concentration was directly related to their exposure (Fig. 2.1; Table 2.2).

We present strong evidence that the fish were exposed through their food. First, the fish aquaria were given the appropriate amount of food to prevent excessive food debris as suggested by the little accumulation of Hg in aquarium water. At the completion of the experiment, water Hg was at most 17 ng L^{-1} (Table 2.1), less than its concentration in the water at both field sites (Table 2.2). In the field studies, fish from BC accumulated

an average Hg concentration of 0.166 ± 0.072 μg g^{-1}, compared to fish from GB that accumulated 0.058 ± 0.017 μg g^{-1} (Table 2.2). This three-fold difference in tissue Hg concentration is most likely related to sediment Hg concentration because (i) mummichogs are sediment feeders [71] and (ii) BC sediment had 32 times more Hg than GB sediment (12.3 ± 4.0 and 0.39 ± 0.03 mg kg_{dw}^{-1}, respectively; Table 2.2). We therefore conclude that the mummichogs' GI tracts contained Hg at levels that reflected concentrations in their food, thus potentially exposing GI microbes to Hg toxicity.

Evidence that Hg toxicity leads to the enrichment of resistant populations in the impacted microbial community may be obtained by observations of increased proportions of HgR microbes [9, 76, 77] or of presence [70] and expression [78] [79] of *mer* gene homologs. When these two approaches were applied here, the molecular approach clearly showed an enrichment of *merA*, specifying the major function of the *mer* system, in BC as compared to GB fish (Table 2.3).

On the contrary, the culturing approach clearly showed no relationships between fish exposure and the proportion of HgR microbes among the total number of heterotrophic aerobes; this trend was common to the aquarium exposure and the field studies (Tables 2.S7, 2.S8). The discrepancy between the results of the plating experiment (no enrichment for Hg resistance) and the qPCR (almost nine-fold enrichment of *merA* in ingesta from BC fish relative to GB fish) may be explained by low culturability of ingesta microbes that do not contain *merA*. Consistent with this suggestion, HgR isolates obtained from ingesta rarely contained *merA* homologs (Lloyd *et al*., manuscript in preparation). Less than 1% of all microbes in the environment are culturable [80] and plating results may not represent the entire community in the fish gut.

The molecular qPCR-based approach scored the presence of *merA* in the microbial microbiome of the gut ingesta, not only those microbes that could be cultured. Thus, prior studies reporting no significant co-selection of antibiotics with metal resistances (e.g., [41] [42]) may have underestimated its occurrence by targeting only cultured strains.

The five most abundant core species, those shared by the gut metagenomes of four individual mummichogs that were collected near Sapelo Island, GA, USA, included *Vibrio* sp., *Photobacterium* sp., *Pseudomonas* sp., *Halomonas* sp., and *Propionibacterium* sp. [32]. Several cultured isolates from the BC and GB ingesta (Lloyd, unpublished), and numerous *mer*-carrying genomes [81], are affiliated with these genera. It is therefore not surprising that *merA* homologs were detected in the fish ingesta; their enrichment in BC samples, where sediment and fish tissue Hg concentrations were significantly higher than those in GB, is a clear indication for the selection of resistant gut populations, likely as a result of Hg exposure.

Mercury-resistant bacterial colonies that were isolated from BC and GB fish ingesta were more likely to be resistant to several antibiotics as compared to HgS colonies (Fig. 2.2); results of the exposure study suggested a similar trend, although they are not statistically significant. These results clearly suggest that selection for Hg resistance inadvertently enriched for multi-drug-resistant strains, consistent with the findings of Wireman *et al*. [46] who studied co-selection among gram-negative fecal bacteria.

While a significant connection between Hg resistance and multidrug resistance in colonies from the Hg-contaminated BC site was expected, the GB site may experience other selective pressures for antibiotic and Hg resistances, e.g., pesticides may select for

antibiotic resistance [62]. Our sampling sites, even the so-called ‘‘cleaner’’ GB site, are exposed to multitude of contaminants, including industrial and domestic runoffs, from variable sources [82-84] leaving open the possibility that other effectors may select for antibiotic and HgR bacteria in these fish.

The most plausible explanation for the co-selection of Hg resistance and multi-drug resistance is genetic co-occurrence of resistance genes in the genomes of gut microbes. When such co-occurrences occur on mobile genetic elements, selective pressure for one gene that under the prevailing environmental conditions enhances fitness could lead to enrichment and spread by horizontal gene transfer of all genes, potentially creating an antibiotic resistance gene pool as a result of exposure to unrelated contaminants. This process may be particularly important in environments that are conducive for horizontal gene transfer such as the fish GI tract. This indirect path to the enhancement and spread of antibiotic resistance should be integrated into our thinking of how to best address this looming public health challenge.

Chapter 3: Whole Genome Sequences to Assess the Link Between Antibiotic and Metal Resistance in Three Coastal Marine Bacteria Isolated from the Mummichog (*Fundulus heteroclitus*) Gastrointestinal Tract

Submitted to *Marine Pollution Bulletin*, June 2018.

Abstract

Antibiotic resistance is a global public health issue and metal exposure is known to select for antibiotic resistance through co-selection. Here, we examined genome sequences of three multi-drug and metal resistant bacteria: one *Shewanella* sp., and two *Vibrio* spp., isolated from the gut of the mummichog fish (*Fundulus heteroclitus*). Our primary goal was to understand the genetic mechanisms of co-selection. Phenotypically, the strains showed elevated resistance to arsenate, mercury, and various types of β-lactams. The genomes contained genes of public health concern including one carbapenemase ($bla_{\text{OXA-48}}$). Our analyses indicate that co-selection may be mediated by co-resistance, cross-resistance, and co-regulation. Co-resistance is supported by the presence of resistance genes on genomic islands, although most resistance genes were chromosomally located. Moreover, many efflux pump gene homologs amongst the three genomes indicates that cross-resistance and/or co-regulation may further contribute to resistance. We suggest that the mummichog gut microbiome may be a source of clinically relevant antibiotic resistance genes.

Introduction

Antimicrobial resistance (AMR) is a pressing public health concern that threatens the usage of effective antibiotic therapies and the global healthcare system. Multidrug resistance (MDR) in Gram-negative bacteria is currently increasing at an alarming rate [85]. AMR genes are found in many environments [86] including ancient (30,000 year-old) permafrost sediments [87]. Environmental reservoirs of resistance genes remain poorly understood [6]. In order to combat the growing threat of AMR, it is important to understand the processes and pathways by which MDR is created and spread in the environment.

The aquatic environment is increasingly being recognized as an important reservoir for AMR genes [88]. Exposure to a plethora of persistent contaminants, including metals, promotes the selection of resistant indigenous microbiota. Coastal marine environments, at the boundary between terrestrial, freshwater, and marine environments, are of particular importance in this paradigm as they are locations with large and rapidly growing population centers [89]. The release of contaminants to productive coastal ecosystems where antibiotic resistance genes (ARG) may spread and be selected for, may lead to the exposure of large human population centers to MDR bacterial pathogens [90]. For this reason, estuaries, typical ecosystems at the land-sea boundary, have been a focus of much research on the effect of environmental contamination on the spread of AMR and ARG for quite some time [5].

Exposure to contaminants, especially metals, may promote the spread of antibiotic resistance in the environment through a process known as co-selection [4]. Co-selection is mediated through several mechanisms including co-resistance, cross-resistance, and

co-regulation. Co-resistance occurs when genes encoding for antibiotic and metal resistances are located proximally to each other in a genome, particularly on mobile genetic elements. Horizontal gene transfer of ARGs has been widely studied, and conjugation is generally considered the most common mechanism [16]. Generally, co-resistance plasmids are commonly found in bacteria isolated from humans or domestic animals [17]. Another mechanisms by which co-selection occurs is via cross-resistance, when the same system (e.g. MDR efflux pumps) confers resistance to both antibiotics and metals [4]. Multidrug efflux pumps are wide-spread and well-conserved elements thought to have evolved for life in enteric environments [18]. They are known to extrude a wide range of substrates from the cell, not only antibiotics and metals, but also plant-produced compounds, quorum sensing signals, and bacterial metabolites [18]. While there is still a lack of knowledge on some of the specificities of these pumps, particularly about how they are regulated, efflux systems have been identified as contributing to multiple AMR in *Enterobacteriaceae* [19]. The third way by which co-selection occurs is through the transcriptional co-regulation of resistance genes. For example, heavy metal ions can increase regulation of efflux systems (e.g. the AcrAB efflux pump in *E. coli*), which results in increased resistance towards antibiotics [23]. While numerous studies have documented the occurrence of AMR among environmental microbes (e.g., [88, 91] and reviewed in: [65]), few have examined the molecular mechanisms responsible for this phenomenon.

We previously reported on the isolation of multi-drug and mercury resistant bacteria from the mummichog (*Fundulus heteroclitus*) gastrointestinal tract and showed that mercury resistant strains were more likely than sensitive strains to be MDR [92].

These results led us to consider the mechanisms that facilitate co-selection of metal and antibiotic resistances in our isolates. Here we used the power of whole genome sequencing to identify antibiotic resistance genes and their association with metal resistance genes in two *Vibrio* spp. and one *Shewanella* sp., which are known to make up a large portion of the wild mummichog gut intestinal microbial community [32]. These strains belong to genera that include opportunistic pathogens and are considered vehicles of AMR [93, 94]. *Shewanella* spp., primarily, *S. algae* and *S. putrefraciens*, have been implicated in human infections [35] and are known to harbor ARGs of public concern [33]. *Vibrio* are abundant in coastal waters, and their ability to develop and acquire AMR in response to selective pressure and to further spread ARGs by horizontal gene transfer has been documented [36].

Our results indicate that while the aquatic bacteria studied did indeed harbor many AMR genes of clinical importance, evidence for co-resistance in the genomes was scarce. Rather, we found evidence to support chromosomally-encoded resistance as well as cross-resistance and/or co-regulation as mechanisms of co-selection of AMR and metal resistance.

Methods

Isolation

Strains were isolated from mummichog (*Fundulus heteroclitus*) gut ingesta collected from Berry's Creek in Bergen County, New Jersey, and Great Bay, part of Rutgers University Marine Field Station in Tuckerton, New Jersey during the summer of 2014. For details on isolation methods, refer to [92]. To taxonomically identify the

strains at the genus level, colony PCR of the partial 16S rRNA gene was performed using the 27F/519R universal primers [95] and the sequences were compared to NCBI [96].

Antibiotic Susceptibility Testing

Antibiotic susceptibility to the following 14 compounds (0.125-64 µg/mL) was carried out by the broth microdilution method according to the guidelines of the Clinical Laboratory Standards Institute (CLSI) using microtiter plates: cefazolin, cefoperazone, cefradine, ceftazidime, kanamycin, meropenem, nalidixic acid, penicillin, sulfamethoxazole, streptomycin, tetracycline, ticarcillin, ticarcillin-clavulanic acid, and vancomycin. Additionally, all strains were tested by the disk diffusion method for their susceptibility to amikacin (30 µg), aztreonam (30 µg), cefepime (30 µg), cefoxitin (30 µg), cefpirome (30 µg), ceftazidime (30 µg), chloramphenicol (30 µg), ciprofloxacin (5 µg), doripenem (10 µg), gentamicin (15 µg), imipenem (10 µg), levofloxacin (5 µg), meropenem (10 µg), minocycline (30 µg), netilmicin (30 µg), ofloxacin (5 µg), pefloxacin (5 µg), piperacillin (75 µg), piperacillin-tazobactam (75/10 µg), rifampicin (30 µg), tetracycline (30 µg), ticarcillin (75 µg), ticarcillin-clavulanic acid (75/10 µg), tobramycin (10 µg), trimethoprim-sulfamethoxazole (1.25/23.75 µg). Testing was performed according to the guidelines of the CLSI using commercially available disks (Bio-Rad, Marne-la-Coquette, France). Since resistance profiles are not well established for environmental bacteria, prior reports including the *Enterobacteriaceae* table [97], clinical break points [98], and *Vibrio* breakpoints [99] were used in combination to determine resistance.

Metal Susceptibility Testing

Metal resistance testing was carried out using the Bioscreen C (Oy Growth Labs Ab Ltd), an automated microbiology growth curve analysis system. Pre-cultures were grown on solid tryptic soy agar media overnight at 28°C. Colonies were suspended in tryptic soy broth liquid media to a McFarland standard of ~1.5 measured using the Densicheck system (bioMérieux, Craponne, France). Approximately 4.5 x 10^6 CFU/mL were inoculated into Bioscreen C honeycomb plates containing various concentrations of the following (freshly prepared) metals: nickel chloride hexahydrate (1-16 mM), cadmium chloride hemi(pentahydrate) (0.31-10 mM), mercury (II) chloride (12.5-200 µM), potassium arsenate (3.12-200 mM), and sodium arsenite (3.12-50 mM), with uninoculated media as a negative control, and cultures grown in the absence of metals as a positive control. Assays were run in triplicate wells. Bioscreen plates were incubated at 28°C, with agitation, and OD at 600 nm measurements were taken every 20 minutes.

Growth Rate Calculations

Growth rates (μ) of the triplicate wells from the Bioscreen C assays were determined using the grofit package for R [100]. Briefly, media blanks were subtracted from absorbance readings from raw Bioscreen data. These corrected values were analyzed in grofit. The averages and standard deviations of the growth rates were visualized in Microsoft Excel.

DNA Extraction

Strains were grown overnight in LB liquid media amended with 100 µg/mL ampicillin. Genomic DNA was extracted using the QIAamp DNA Mini Kit (Qiagen). Plasmid DNA was extracted using the Macherey-Nagel Plasmid DNA purification kit

(Macherey-Nagel, Hoerdt, France). Samples were sent to Molecular Research DNA Labs in Shallowater, TX, USA, for sequencing according to company protocols.

Annotation and Analysis

Reads were assembled into contigs using SPAdes Genome Assembler [101]. Genomes were annotated using the NCBI Prokaryotic Pipeline [102] and genome sequences are available under the assembly numbers reported in Table 1. Average Nucleotide Identity (ANI) [103] was calculated using the whole genome sequences. Genomes were examined using Geneious version 10 (www.geneious.com; [104]). Genomic Islands were identified using IslandViewer4 [105]. Putative AMR genes were detected by a blast [96] search using ARG-ANNOT V3 March 2017, accessed November 2017 [106]. Putative metal resistance genes were detected by a blast search using the experimentally-confirmed BacMet metal resistance genes database version 1.1 [107] accessed December 2017. Gene homologs from both databases with E values < $10e^{-20}$ are reported. Efflux pump genes were identified using the BacMet database as well as manual scanning of the genome annotations. Metal resistance and antibiotic resistance genes were referenced with results of IslandViewer 4, to visualize if any resistance gene determinants were also on putative genomic islands. To determine the sub-groups of the p-type ATPase proteins, 80 representative p-type ATPases [108] were downloaded from UniProtKB [109], and a phylogenetic tree (not shown) was built from the alignment of the proteins.

Results

Taxonomic Identification and Genomic Properties

Among the 52 bacteria we isolated from the mummichog gut microbiome, the two most dominant taxa were *Vibrio* (62%) and *Shewanella* (21%) (Fig. 3.S1). The Vibrionaceae class is known to make up a large portion of the wild mummichog gut microflora [32]. *Shewanella* sp. BC20 was isolated from the gut ingesta of fish collected from Berry's Creek, an EPA superfund site contaminated with mercury and arsenic, located in New Jersey, USA [57]. *Vibrio* spp. T9 and T21 were isolated from the gut ingesta of mummichog fish collected from Great Bay, New Jersey, USA, a relatively uncontaminated site [92]. The average nucleotide identities (ANI) with scores above 95% were used to identify the available genome to which our strains were most closely related. Of those available in NCBI as of May 2016, *Shewanella* BC20 was most closely related to *Shewanella* sp. MR-4, a strain isolated from the water column of the Black Sea at a depth of 5 m [110]. *Vibrio* sp. T9 was most closely related to *Vibrio antiquarius* EX25, a *Vibrio* isolated from hydrothermal vents [111], and *Vibrio* sp. T21 was most closely related to *Vibrio parahaemolyticus* FORC 018, a strain isolated from sea bass in South Korea (Table 1). *Shewanella* sp. BC20 had an average G+C% of 48.0%, which is identical to that reported for *Shewanella* sp. MR-4. (GenBank Accession CP000446.1). The genome of *Shewanella* sp. BC20 contained no plasmids (Table 3.1). The average G+C% of the two *Vibrio* strains, *Vibrio* spp. T9 and T21, were 45.0 and 45.4%, respectively, which is within the normal range for *Vibrio* species [111]. Strain *Vibrio* sp. T9 contained one 120 kb plasmid, with a G+C% of 44.7%, close to that of the

chromosome. The plasmid showed 94% nucleotide identity (with 65% query cover) to *V. alginolyticus* ATCC 33787 plasmid pMBL128 (Accession number CP013486.1).

Table 3.1. Genome features of the three strains sequenced in this study

	Strains		
	***Vibrio* sp. T9**	***Vibrio* sp. T21**	***Shewanella* sp. BC20**
Isolated from	Great Bay	Great Bay	Berry's Creek
NCBI Assembly ID	GCF_003123985.1	GCF_003123995.1	GCF_003129585.1
Genome coverage	41X	49X	59X
Closest Available Genome and ANI score (%)	*Vibrio antiquarius* EX25 (98.30%)	*Vibrio parahaemolyticus* FORC 018 (98.19%)	*Shewanella* sp. MR-4 (95.14%)
Chromosome size (megabase pairs)	5.2	4.9	4.7
Chromosomes	2	2	1
Plasmids	1	none	none
Plasmid size and GC%	120 kb 44.7		
Protein-CDSs	4,891	4,525	4,099
GC (%)	45.0	45.4	48.0
# contigs	70	77	54

Antibiotic Susceptibility Profiles

Resistance to 33 antibiotics was tested using established procedures, a combination of the disc method and the microdilution method (Tables 3.2, 3.S1). Of those drugs tested with both the disc method and the microdilution method, we obtained consistent results among carbapenems, penicillins, tetracyclines, and most cephalosporins. All three strains were resistant to ceftazidime using the MIC method, but sensitive in the disk method. Inconsistencies between results obtained with different types of antimicrobial testing methods were previously reported [112]. All three strains showed broad resistance to β-lactams, primarily cephalosporins and penicillins. The two *Vibrio* strains were intermediately resistant to aminoglycosides. The resistance profile of

Shewanella sp. BC20 was varied, including resistance to carbapenems as well as to vancomycin. All strains were sensitive to tetracycline and chloramphenicol.

Table 3.2. Antibiotic MICs/measures of zone of inhibition profiles and resistance interpretation of the three strains

		Vibrio sp. T9		*Vibrio* sp. T21		*Shewanella* sp. BC20	
Class	**Drug**	**Zone of Inhibition (mm)***	**Interpretation**	**Zone of Inhibition (mm)**	**Interpretation**	**Zone of Inhibition (mm)**	**Interpretation**
Carbapenems	Doripenem	≥ 24	S**	≥ 24	S	≤ 21	R
Carbapenems	Imipenem	≥ 22	S	≥ 22	S	≤ 16	R
Carbapenems	Meropenem	≥ 22	S	≥ 22	S	≤ 16	R
Penicillins	Piperacillin	≤ 17	R***	≤ 17	R	≤ 17	R
Penicillins	Piperacillin – Tazobactam	≥ 20	S	≥ 20	S	≤ 17	R
Penicillins	Ticarcillin	≤ 23	R	≤ 23	R	≤ 23	R
Penicillins	Ticarcillin – Clavulanic Acid	≤ 23	R	≤ 23	R	≤ 23	R
Fluoroquinolones	Ofloxacin	≥ 22	S	≤ 22	I	≥ 22	S
Aminoglycosides	Amikacin	≥ 17	S	≤ 17	I	≥ 17	S
Aminoglycosides	Tobramicin	≤ 17	I	≤ 17	I	≥ 17	S
Phenicols	Chloramphenicol	≥ 17	S	≥ 17	S	≥ 17	S
Class	**Drug**	**MIC***	**Interpretation**	**MIC***	**Interpretation**	**MIC***	**Interpretation**
Carbapenems	Meropenem	0	S	0	S	16	R
Cephalosporins (3rd)	Cefoperazone	64	R	64	R	32	R
Cephalosporins (3rd)	Ceftazidime	64	R	64	R	64	R
Cephalosporins (1st)	Cefazolin	0.5	S	4	S	64	R
Cephalosporins (1st)	Cefradine	8	S	64	R	2	S
Penicillins	Ticarcillin	64	R	64	R	64	R
Penicillins	Penicillin	64	R	64	R	64	R
Penicillins	Ticarcillin - Clavulanic Acid	16	R	32	R	64	R
Glycopeptides	Vancomycin	2	S	8	S	32	R
Quinolones	Nalidixic Acid	0.5	S	1	S	2	S
Sulfonamides	Sulfamethoxazole	2	S	8	S	64	****
Tetracyclines	Tetracycline	0	S	0.125	S	1	S

*Levels of resistance are reported in MIC µg/mL (for those tested with the microdilution method) or zone of inhibition in mm (for those tested with the disc method).

**Organisms are reported as S (sensitive), I (intermediate), or R (resistant) as established by common standards. For a complete list of all antibiotics tested, and sources for common standards used in determining break points, see Table 3.S1.

***Shading indicates that a resistance gene homolog potentially conferring resistance to that antibiotic was found in the genome regardless if the strain was phenotypically resistant or sensitive to that drug.

****Comparable resistance breakpoints for this drug could not be found.

Table 3.3. Antibiotic resistance gene homologs with clinical relevance and their respective locus tags in the three genomes

			***Vibrio* sp. T9**	***Vibrio* sp. T21**	***Shewanella* sp. BC20**
Antibiotic Class	**Putative gene**	**Substrates/ Function**	**Locus**	**Locus**	**Locus**
β-lactam	class A β-lactamase (CARB)	Penicillins, cephalosporins, carbenicillin [113]	CBX98_10150	CCD93_08640	
	class B metallo β-lactamase	Broad spectrum, including carbapenems, [114]	CBX98_12520	CCD93_19270	CBX96_13965
	class C β-lactamase	Cephalosporins [115]	CBX98_08735		CBX96_05400
	class D β-lactamase (*bla*$_{OXA48}$)	Penicillins and carbapenems [115]			CBX96_07750
Tetracycline	*tet34*	Oxytetracycline mechanisms [116]	CBX98_18940	CCD93_18545	
	tet35	Efflux of tetracycline [117]	CBX98_02340	CCD93_18785	
Fluoroquinolone	*qnrS*	Quinolones [118]	CBX98_12495	CCD93_19295	

Antibiotic Resistance Genes

Overall, our analysis identified 70 potential AMR gene homologs in *Shewanella* sp. BC20, 78 were identified in *Vibrio* sp. T21, and 89 in *Vibrio* sp. T9 (Tables 3.S2, 3.S3, 3.S4). AMR gene homologs of clinical relevance are reported (Table 3.3). All four Ambler classes of β-lactamases were identified amongst the three strains. All three harbored class B metallo-β-lactamases. *Vibrio* sp. T9 contained a class C β-lactamase located on a genomic island (Fig. 3.1). Strains *Vibrio* spp. T9 and T21 both contained class A carbenicillin hydrolyzing β-lactamases (CARB). The amino acid % identity of the two CARB genes was 88.3%, indicating they are closely related but not identical (Table 3.3). *Shewanella* sp. BC20 harbored a class C β-lactamase as well as an extended spectrum β-lactamase (ESBL), $bla_{\text{OXA-48}}$. The two *Vibrio* spp. harbored tetracycline (*tet34* and *tet35*) and chloramphenicol resistance genes yet were susceptible to those drugs (Tables 3.2, 3.3). *Vibrio* spp. T9 and T21 harbored *qnrS*, which confers resistance to quinolones (Table 3.3). The *Vibrio* spp. were phenotypically sensitive to nalidixic acid and most of the fluoroquinolones tested, however *Vibrio* sp. T21 was intermediately resistant to ofloxacin (Table 3.2, 3.S1). Further, the genomes harbored many efflux pump gene homologs from various families including ABC, MATE, MFS, RND, and in the *Vibrio* spp., SMR (Tables 3.S5, 3.S6, 3.S7). The type and abundance found in each were comparable to reference strains (Fig. 3.S2). Notably, *Shewanella* sp. BC20 contained 13 operons for RND efflux pumps, *Vibrio* sp. T9 contained 12, and *Vibrio* sp. T21 contained 13.

Metal Resistance Profiles

Compared to other metal resistance studies in *Vibrio*, *Vibrio* spp. T9 and T21 were resistant to cadmium (5 mM) (data not shown) [37] and arsenate (100 mM) [119]. *Vibrio* sp. T21 was also resistant to mercury (50 µM) (Fig. 3.2 A-B) [37]. *Shewanella* sp. BC20 was able to grow with 50 mM arsenate and 25 µM mercury (Fig. 3.2 C). All three strains were sensitive to the tested concentrations of arsenite and nickel.

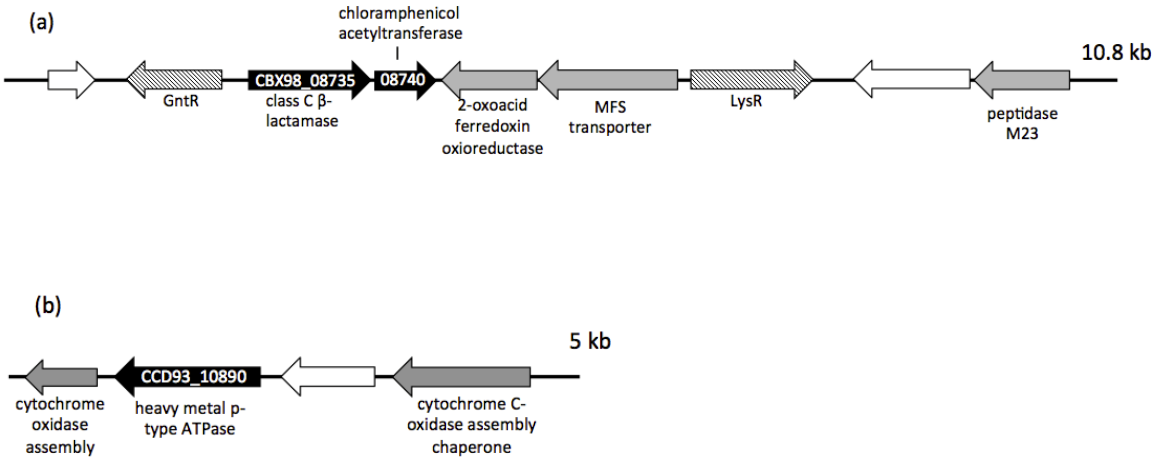

Figure 3.1. Genomic Islands containing genes of interest located in *Vibrio* sp. T9 (A) and *Vibrio* sp. T21 (B). The genomic island in (A) contains two antibiotic resistance genes and the island in (B) contains one metal resistance gene (colored black). Hypothetical proteins are colored white, genes involved in transcriptional regulation are shaded with diagonal lines, and all other genes are in grey. Arrows indicate direction of transcription.

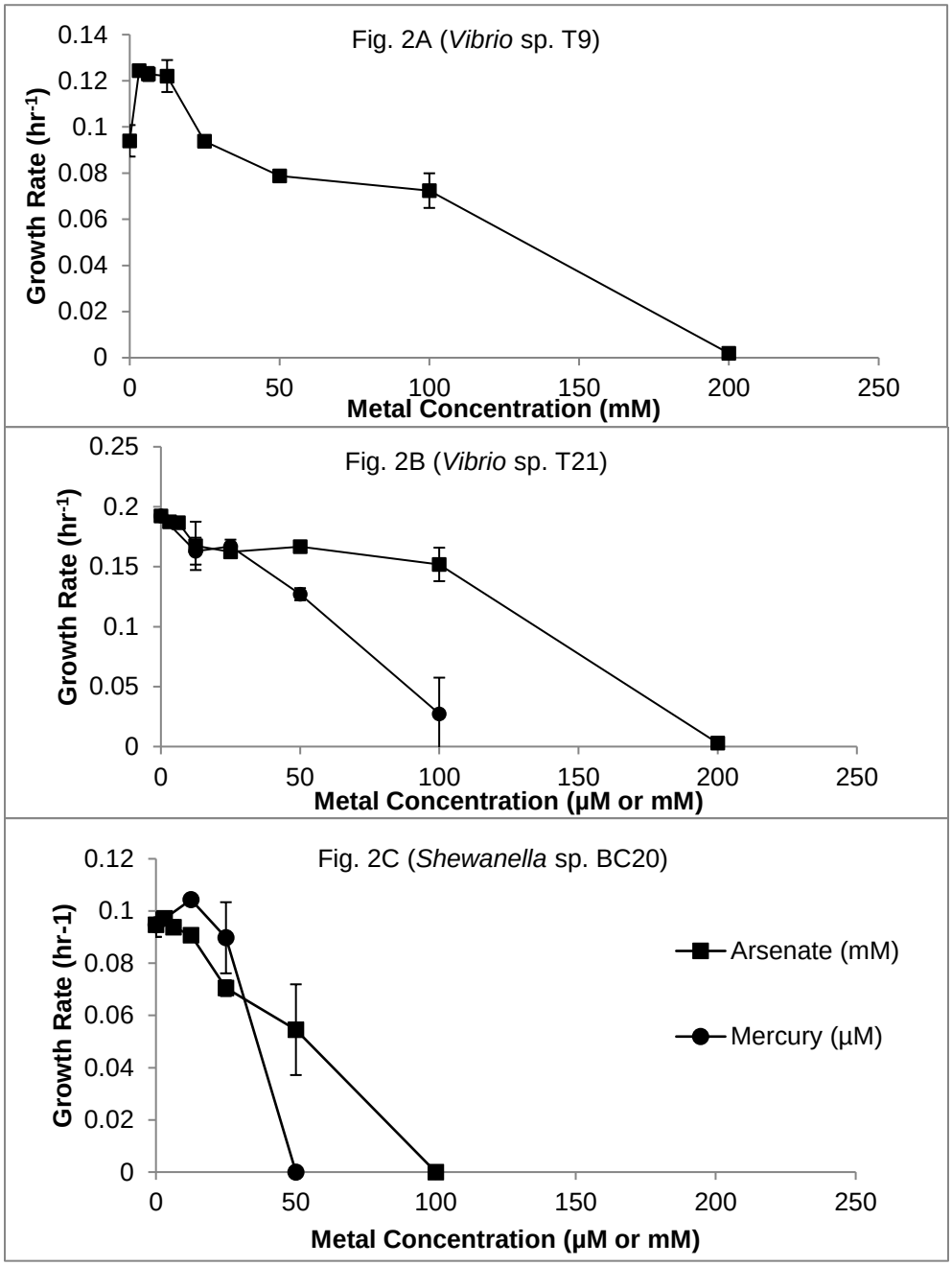

Figure 3.2 A-C. Effect of increasing concentrations of arsenate and mercury on growth rates of the three mummichogs bacterial isolates. Each point represents average growth rates of 3 replicates ± standard deviation.

Metal Resistance Genes

The genomes of the three strains contained operons for arsenate resistance and metabolism (i.e., arsenite oxidation/arsenate reduction) (Table 3.S8, 3.S9). They also contained genes for various P-type ATPases (Table 3.S10). *Vibrio* spp. T9 and T21 each contained two P_{1B-1}-ATPases and one P_{1B-2}-ATPase. *Shewanella* sp. BC20 contained two P_{1B-1}-ATPases. Not including efflux pump genes, in total, *Shewanella* sp. BC20 contained 148 homologs for genes involved in metal resistance, while *Vibrio* sp. T9 had 149, and *Vibrio* sp. T21 had 154 (Tables 3.S11, 3.S12, 3.S13). The most abundant metal resistance genes amongst all three genomes were gene homologs for zinc, iron, copper, and nickel resistance.

Genomic Islands and the Mobilome

We searched for genomic islands in the strains, and more specifically, the carriage of antibiotic and metal resistance genes on such islands as possible evidence for co-resistance. The genome of *Shewanella* sp. BC20 contained 16 genomic islands with one metal resistance gene (Table 3.S14). *Vibrio* spp. T9 and T21 contained 29 and 23 genomic islands, respectively (Table 3.S15, 3.S16). *Vibrio* sp. T9's genome had one 10 kb genomic island that harbored genes encoding for a chloramphenicol acetyltransferase, a class C β-lactamase, and an MFS transporter (Fig. 3.1), all genes involved in AMR. *Vibrio* sp. T21's genome contained two genomic islands of interest: a large element (~25 kb) containing an MFS transporter gene, multidrug ABC transporter gene, and genes involved in horizontal gene transfer (IS3 family transposase) and a smaller genomic island (~5 kb), which contained a heavy metal translocating P-type ATPase (Fig. 3.1). Some of the metal resistance genes were located on genomic islands in the *Vibrio* spp.

genomes: three in *Vibrio* sp. T9 and four in *Vibrio* sp. T21 (Table 3.S12, 3.S13). All other metal resistance and AMR genes are located elsewhere in their respective genomes with no proximity to other AMR genes or to genes suggestive of horizontal transfer. We were unable to identify any genes of interest in proximity to phage genes.

Discussion

The aim of our study was to examine the genetic underpinning of co-selection in multi-drug and metal resistant bacteria isolated from the intestinal microbial community of the mummichog, a common coastal fish. Overall, our results indicate that co-selection is mediated by a variety of factors, including co-resistance, cross-resistance, and intrinsic resistance genes. Phenotypically, strains were resistant to various classes of antibiotics (primarily different types of β-lactams) as well as to metals. The genome sequences revealed carriage of efflux pump gene homologs, metal resistance, and AMR genes, including genes of public health concern.

The ease by which gene sequences are now obtained by metagenomic approaches has recently led to studies on the abundance and distribution of AMR genes in environmental samples (e.g. [120], [121]). While these studies have been useful in assessing hot spots where AMR is likely (e.g., [122]) they cannot identify the organisms and the mechanisms of gene transfer that partake in ARG transfer from environmental strains to clinical microbes [123]. Additionally, even though metatranscriptome surveys may inform on the expression of ARGs in the environment (e.g., [124]) how this expression is related to mobilome activities and microbial metabolism cannot be deciphered from such studies. As this information is crucial for the understanding of the ecological framework that underpins the spread of AMR, metagenomic approaches must

be complemented by pure culture studies that shed light on resistant taxa, their ARGs, and potential to mobilize these genes to clinical isolates.

Because MDR among Gram-negative bacteria is of public health concern [125], we chose to study three Gram-negative bacteria that represent dominant taxa, *Vibrio* spp. and *Shewanella* spp., in our collection [92] as well as in the mummichog microbiome [32]. Our approach compared genotype (i.e., gene presence) with phenotype to gain an understanding of the carriage, expression, and location of antibiotic and metal resistance genes within the genomes.

Shewanella sp. BC20, isolated from a heavy-metal contaminated estuary, showed resistance to carbapenems, cephalosporins, and penicillins; three classes of drugs to which *Shewanella* are commonly susceptible [93]. The strain showed an elevated resistance profile compared to the 28 out of the 33 environmental *Shewanella* isolates tested by Tacao et al. [126], with resistance to 9 of the antibiotics reported. Further, the *Shewanella* sp. BC20 genome harbors a class D β-lactamase, $bla_{\text{OXA-48}}$, with the same upstream and downstream genetic context that others have reported [126]. Numerous reports suggest the occurrence of $bla_{\text{OXA-48}}$ in environmental *Shewanella* spp. [127] and its horizontal mobility and expression in human pathogens [128]. One of the other isolates studied, *Vibrio* sp. T21, was intermediately resistant to ofloxacin (Table 2), a fluoroquinolone antibiotic. Resistance to ofloxacin has been attributed to a mutation in the *gyrB* gene [129] and possession of quinolone resistance genes has been described among fish-associated *Aeromonas* spp. [130]. Quinolones are synthetic antibiotics commonly recommended and used in treatment of Vibrionosis, including *V. parahaemolyticus* infections [131].

We identified members of all four Ambler classes of β-lactamases. Notably, all three strains harbored class B metallo-β-lactamases (MBLs), which confer resistance to almost all classes of β-lactam antibiotics. The so-called "New Delhi MBL", is considered a threat to global public health as it is easily mobilizable and has been found in many countries world-wide [132]. Studies have reported on previously unknown MBLs in soil microbiota, which present a clinical threat if acquired by pathogenic bacteria [133]. Thus, the occurrence of this gene among environmental organisms may contribute to community-acquired colonization as well as infections [134], and suggests the mummichog gut as a reservoir of clinically relevant antibiotic resistant organisms and their associated resistance genes. In order to understand this connection, we looked at the genetic linkage between metal and antibiotic resistance in the genomes. We expected evidence for co-selection suggesting horizontal gene transfer and selection due to heavy metal stress. This expectation was based on: 1) metal resistance genes are often found on mobile genetic elements [15], 2) the association of metal and antibiotic resistance genes on conjugative plasmid is well-documented [135] , and 3) the fish gut with its abundant nutrients and stable temperature is conducive to microbial growth and gene transfer [136].

Indeed, we identified two cases where AMR and metal resistance genes were located on genomic islands, clusters of genes of probable horizontal origin [105]. *Vibrio* sp. T9 contained a 10.8 kb genomic island with both a class C β-lactamase and a chloramphenicol acetyltransferase gene (Fig. 3.1A) and *Vibrio* sp. T21 had a P_{1B-1}-ATPase, possibly specifying cadmium resistance, on a 5 kb genomic island (Fig. 3.1B). These putative genomic islands do not carry mobilome gene homologs (those involved in

conjugation, phage, or transposition). Moreover, we were unable to identify other cases where genes of interest were proximally located to mobilome genes. The one large (~120kb) plasmid in *Vibrio* sp. T21, contained no mobilome, antibiotic, or metal resistance genes. This plasmid did not have any gene homologs indicating potential for conjugation, indicating the plasmid may not be transferrable.

Genome sequences suggest that cross-resistance (efflux pumps) may contribute to co-selection. Each genome harbored many efflux pump gene homologs (66 in *Shewanella* sp. BC20, 128 in *Vibrio* sp. T9 and 117 in *Vibrio* sp. T21 (Tables 3.S5, 3.S6, 3.S7). RND efflux pumps have been implicated in Gram-negative MDR, and both the *Shewanella* sp. BC20 and *Vibrio* sp. T21 contained an elevated number of RND operons compared to previous reports (Lloyd *et al*., in preparation). This result is consistent with a recent report on the dominance of efflux pump-based cross-resistance in the whole genome sequence of an environmental *Pseudomonas* strain from a metal-contaminated estuary [30] and the increased extrusion of antibiotics *via* RND efflux pumps in marine biofilms exposed to heavy metals [31]. These results highlight the need to examine cross-resistance, as well as co-regulation, as a mechanism of co-selection, which is currently under investigation in our lab. The environmental selection of resistant strains may be the strongest driver of co-selection as was suggested by Forsberg *et al*. [137] who assert that the primary determinant of ARG content in soil is microbial community composition rather than horizontal gene transfer of resistance genes.

One advantage of examining co-selection in three individual genomes over community analyses or PCR amplification assays is that it provides direct evidence for co-selection in individual organisms [16]. We tested resistance of three strains to many

different antibiotics using two standard methods; the genome sequences of these strains informed us on the presence and/or absence of corresponding resistance genes (Tables 3.2, 3.S1). There were several cases where the strains harbored resistance genes but were scored as sensitive to the drug (i.e., *tet* genes in *Vibrio* spp.) (Table 3.3). There were other cases where the strains did not harbor known resistance genes but were scored as intermediately resistant to the drug (i.e., aminoglycosides in *Vibrio* spp.). Thus, if a study scores only gene presence it may either over- or under-estimate AMR. This conclusion is in agreement with recent recommendations for essential verifications if whole genome sequences of pathogens are to serve in AMR profiling in the clinical lab [138].

All three strains contained an arsenal of putative metal resistance genes (Tables 3.S11, 3.S12, 3.S13). Notably, the genomes contain homologs to genes known to specify resistance to arsenate, cadmium, and mercury. All three genomes contained arsenate detoxification genes, *arsC, arsR, ACR3*, and arsenate respiration genes (Table S8, S9). P-type ATPases encoding for the efflux of mono- (P_{1B-1}-ATPases) and di-valent (P_{1B-2}-ATPases) cations [108] were identified amongst all three genomes. *Vibrio* spp. T9 and T21 contained P_{1B-1}-ATPases (2 copies) and P_{1B-2}-ATPase (1), while *Shewanella* sp. BC20 contained only P_{1B-1}-ATPases (2) (Table 3.S10) possibly explaining why the *Vibrio* spp. were resistant to cadmium, while *Shewanella* sp. BC20 was sensitive. Interestingly, in *Vibrio* sp. T21, one of the P_{1B-1}-ATPases was located on a predicted genomic island (Fig. 3.1B).

Conclusions

In summary, the co-occurrence of multiple antibiotic and metal resistances in three coastal bacterial isolates adds to numerous reports (e.g., [16, 29]). Coastal marine

environments are zones where high microbial productivity, anthropogenic contaminants, and high human population density may converge to create a hot spot for the selection of AMR and its subsequent inheritance among pathogenic bacteria.

Our results have implications in both the environment and clinic. Some of the resistance genes identified here were previously shown to occur in human pathogens. Our results provide information on the antibiotic and metal resistome of the mummichog intestinal microbial community, a potential reservoir of antibiotic resistant genes, and opportunistic human pathogens including *Vibrio parahaemolyticus* and *Shewanella* spp. Our findings contribute to the understanding of co-selection in the environment and can also be used to assess the threat of potential emerging MDR zoonotic infections, as well as predict the composition of the resistant community in the environment.

Chapter 4: Genome-facilitated Discovery of RND Efflux Pump-Mediated Resistance to Cephalosporins in *Vibrio* spp. Isolated from the Mummichog Fish Gut

Abstract

The extensive overuse of antibiotics in aquaculture contributes to the spread of resistance in aquatic microorganisms, including *V. parahaemolyticus*, a causative agent of food-borne illness. An increase in resistance to third-generation cephalosporins in *Vibrio* has been recently reported. By sequencing the genomes of two *Vibrio spp*. isolated from the mummichog fish gut we discovered RND efflux pump-mediated resistance to first- and third-generation cephalosporins in these strains. *Vibrio* sp. T21 was most similar to *V. parahaemolyticus*, and *Vibrio* sp. T9 to *V. antiquarius*. We identified 13 and 12 RND operons, respectively, with *V. parahaemolyticus* T21 containing an additional RND operon compared to other *V. parahaemolyticus* strains. Both the inner-membrane protein (IMP) and the membrane facilitator protein (MFP) of this operon are homologous to VexD and VexC, respectively, an RND operon in *V. cholerae*. More generally, the other RND proteins in our strains show homology to RND efflux pumps characterized in *E. coli* and *V. cholerae*. In *V. parahaemolyticus* T21, we observed decreased resistance to cefoperazone and cephradine, and in *V. antiquarius* T9, decreased resistance to cefoperazone and cefsulodin in the presence of PAβN, an RND efflux pump inhibitor. This work highlights the need for further research into this unique *V. parahaemolyticus* operon, and more generally, RND efflux pumps in *Vibrio* species, as *Vibrio* often cause seafood-borne illness.

Introduction

Microbial resistance to antibiotics is a major public health concern. The over-usage of antibiotics increases the spread of resistance by selecting for resistant bacterial populations. This problem is further exacerbated by horizontal gene transfer of antibiotic resistance genes, which has been well-documented in Gram-negative bacteria. While many antibiotic resistance genes are naturally occurring in the environment, the environment is increasingly being recognized for its role in the selection of antibiotic resistance [139]. The spread of antibiotic resistance genes in the environment is promoted by anthropogenic activities such as metal contamination [16, 23], farming [140], and antibiotic usage in aquaculture [141]. Some aquatic environments, especially those with anthropogenic input, are conducive for the genetic transfer of antibiotic resistance determinants in part due to high concentrations of bacteria and presence of bacteriophages that facilitate genetic transfer [142].

The growing aquaculture industry is a challenge for the spread of antibiotic resistance. In this sector, antibiotics are used without regulation [142] and in excess to prevent and treat infections to ensure continuous production of seafood [143]. It is estimated that up to 80% of antibiotics enter the environment unaltered, leading to the selection of resistant organisms [144]. A recent study on the adaptation of microbial populations to antibiotic treatment in a high-intensity catfish production system showed that 21 antibiotic resistant genes were under selection, with a majority of them classified as efflux pumps [145]. The overuse of antibiotics in aquaculture seems like it has the potential to pose risk to human health, as exposure to multi-drug resistant (MDR) bacteria is possible via consumption of seafood and exposure to water.

Vibrios, commonly associated with marine animals including fish, shellfish, and shrimp, are ubiquitous in aquatic environments. One of the most well-known examples is *V. cholerae*, the causative agent of cholera, of which outbreaks are often initiated in coastal brackish waters. Other species of *Vibrio* cause disease in humans, including *V. parahaemolyticus* which is among the leading causes of seafood-borne infections in the United States [146]. Cases of Vibrionosis are currently rising in the United States, with the last major outbreak reported in 2013 [147]. Many studies report on the multi-drug resistance of *V. parahaemolyticus* and *V. vulnificus* isolated from aquatic environments, including recreational and commercial areas of the Chesapeake Bay and Maryland Coastal Bays [148], as well as aquaculture operations. With approximately 90% of global aquaculture production in Asia, it is concerning that numerous food-borne outbreaks in several different Asian countries have been attributed to *Vibrio* contamination of seafood [149], including shrimp from Shanghai fish markets [37], and shellfish raised in Malaysia [150].

Cephalosporins, amongst the most widely-prescribed antibiotics, constitute a large group of β-lactam antibiotics [151]. The first-generation cephalosporins were created in the 1960s and the efficacy of these drugs drastically decreased with the spread of class A β-lactamases [152]. In the 1980s, third-generation cephalosporins were developed, and currently their efficacy is threatened by the spread of class C β-lactamases [152]. A recent survey of *V. parahaemolyticus* isolates worldwide revealed high rates of resistance to gentamicin and ampicillin, and emerging resistance to third-generation cephalosporins [153]. Recent reports suggest that the burden of third-generation cephalosporin resistance may be underestimated [154]. Surveillance data provided by the United States Centers for

Disease Control and Prevention shows between 1990 to 2010, quinolones and cephalosporins were the most commonly prescribed antibiotics for Vibrionosis in the United States [131]. Cephalosporin antibiotics, in combination with doxycycline, are currently recommended for treatment of *Vibrio* infections, despite reports of increased cephalosporin resistance [155]. Resistance to β-lactam antibiotics including penicillins and cephalosporins is mediated by β-lactamases in *Vibrio*, including class A [113], class B [156], and class C [115] β-lactamases.

Efflux pumps are distributed amongst all domains of life and their genetic organization and structural features are well-conserved [21]. The Resistance Nodulation and cell Division (RND) superfamily of efflux pumps plays a prominent role in antimicrobial resistance (AMR) in Gram negative clinical isolates [157]. RND efflux pumps consist of a tripartite system including an outer membrane protein (OMP), a membrane fusion protein (MFP), and an inner membrane protein (IMP) [21]. Genes encoding for the MFP and IMP are usually found in an operonic structure, with or without the OMP gene, which may be located elsewhere in the genome [21]. One of the most well-studied RND systems, AcrAB, characterized in *Escherichia coli* with orthologs in many other members of the Enterobacteriaceae, has been shown to export dyes, detergents, chloramphenicol, tetracyclines, macrolides, β-lactams, fluoroquinolones, and organic solvents [18]. In addition to antimicrobial resistance, RND efflux pumps are involved in cell-to-cell communication and host colonization via the export of bile salts [18], as well are virulence [158, 159]. RND efflux pumps have been implicated in resistance to cephalosporins via the *mexAB* operon in *Pseudomonas* spp. and the *acrAB* operon in *E. coli* [21]. The interactions between some cephalosporin drugs and the

AcrAB proteins in *E. coli* have been extensively studied, and affinity of the drug for the membrane plays a role in determining substrate specificity of the pump [160]. Because members of the cephalosporin drug class have varied structures and chemical properties, they have different affinities for active sites in RND pumps. The over-expression of efflux pumps in combination with other factors such as porin deficiency and chromosomal resistance genes contributes to resistance [152].

To date, broad-substrate RND systems have been characterized in the following *Vibrio* spp.: *V. cholerae* [159], *V. parahaemolyticus* [161], and *V. vulnificus* [162], with each containing 6, 12, and 11, RND operons, respectively. The role of efflux pumps in MDR in *Vibrio* is important to understand, as efflux pumps contribute to AMR as well as virulence and host colonization.

We previously described two *Vibrio* strains (*V. parahaemolyticus* and *V. antiquarius*), isolated from the gut of the mummichog fish (*Fundulus heteroclitus*) (Lloyd et al., submitted; Chapter 3), an environment with an abundance of *Vibrio* [32]. The strains exhibited resistance to penicillins, cephalosporins, aminoglycosides, and in one case, a fluoroquinolone. Their genomes contained class A, class B, and class C β-lactamase genes, along with many efflux pump gene homologs. The importance of these findings stems from the known role of *V. parahaemolyticus* as an opportunistic pathogen, and while not much is known about the potential pathogenicity of *V. antiquarius*, it is genetically-related to other pathogenic *Vibrio* spp. [111]. With resistance to cephalosporins increasing globally [153], it is important to understand the mechanisms of AMR in *Vibrio* species. The aim of this paper is to examine the role of RND efflux

pumps in resistance to first- and third-generation cephalosporins, as well as increased virulence, in two *Vibrio* isolates from the gut microbiota of a forage-feeder fish.

Materials and Methods

Isolation and Species Determination

Vibrio spp. were isolated from mummichog gut microbiota [92]. The taxonomic identity of the isolates was determined based on the average nucleotide identity (ANI) [103] and confirmed by multi-locus sequence analysis (MLSA) that was performed on partial 16s rRNA, *gyrB*, *pyrH*, *recA*, *rpoD* genes from *Vibrio* sp. T9 and compared to reference MLSA patterns of these genes in *Vibrio* spp. [163].

Liquid MICs in Presence of Phenylalanine-Arginine-Beta-Napthylamide (PAβN)

Minimum inhibitory concentrations of various antibiotics were determined using the established broth microdilution method according to the guidelines of the Clinical Laboratory Standards Institute (CLSI) using microtiter plates [164] in the presence (50 μg/mL) or absence of efflux pump inhibitor PAβN. This concentration of PAβN was experimentally determined to not affect growth of the organisms (Figure 4.S1). Briefly, cultures were grown overnight at 28°C on Mueller-Hinton agar. The next day, cultures were diluted to a 0.5 McFarland standard as measured by the DensiCheck (bioMérieux, Craponne, France) system. The cultures were then used to inoculate a microtiter plate containing serial dilutions of antibiotics and 50 μg/mL PAβN. The plates were incubated for 24 h at 28°C before interpretation. MIC changes of 4-fold or greater were considered significant [165].

Effect of Efflux Inhibition on Growth Rates

Growth was monitored using the Bioscreen C (Oy Growth Ab Ltd), an automated microbiology growth curve analysis system. Pre-cultures were grown on solid media overnight at 28°C. Colonies were suspended in tryptic soy broth (TSB) media to a McFarland standard of ~1.5 measured using the DensiCheck system (Biomérieux). Approximately 4.5 x 10^6 CFU/mL were inoculated into Bioscreen C honeycomb plates containing serial dilutions of PAβN (0 – 100 µg/mL) in DMSO. Growth rates (µ) of the triplicate wells from the Bioscreen C assays were calculated from growth curves using the grofit package for R [100]. The averages and standard deviations of the growth rates were used to create graphs in Microsoft Excel (Figure 4.S1).

Identification of Putative RND Efflux Genes in the Vibrio *sp. T9 and* Vibrio *sp. T21 genomes*

RND efflux gene sequences characterized by Matsuo et al. [161] were extracted from the *V. parahaemolyticus* RIMD 2210633 genome sequence and used to create a blast database. This database was then used to blast search [96] our genome sequences for homologs. We further manually searched upstream and downstream of each RND gene hit to locate additional RND pump genes. In order to determine relatedness of the putative RND proteins in our *Vibrio* spp., we aligned them with translated reference genes to obtain % identity values. The following reference genes were used: *acrA*, *acrB*, and *acrD* from *E. coli* O157:H7 strain Sakai (NC_002695); *mexA* and *mexB* from *P. aeruginosa* PAO1 (NC_002516), and *vexA*, *vexB*, *vexC*, *vexD*, *vexK*, from *V. cholerae* O1 biovar El Tor strain N1696 (NC_002505 and NC_002506).

Predicted Pathogenicity

Genome sequences were uploaded to Pathogen Finder to predict pathogenicity from whole genome sequences, accessed in June 2018 [166].

Virulence Testing

Virulence of the *Vibrio* strains was determined as described by Froquet *et al.* [167] using the amoebal model, *D. discoïdeum*. Overnight bacterial cultures were adjusted to an OD_{600nm} of 1.5 by dilution in LB. One mL of each adjusted bacterial suspension was plated on SM Agar (Formedium, Hustanton, United Kingdom) medium. The plates were allowed to dry for one hour to obtain a dry bacterial layer. Cells of *D. discoïdeum* were washed twice in PAS (Page's amoeba saline) buffer by centrifugation at 1000 g for 10 minutes. The amoebal suspension was adjusted to 2×10^6 cells.mL^{-1} and serial dilutions were performed in order to obtain a final concentration of 7812 cells.mL^{-1} (in the most dilute sample). Five µL of each serial dilution of *D. discoïdeum* (containing from 39 - 14,000 cells per 5 µL aliquot) was spotted on the bacterial lawn. Plates were incubated at 22.5°C for five days and, appearance of phagocytic plaques was checked at the end of the incubation time. This assay was performed in triplicate. Strains of *P. aeruginosa* PT5 and *K. pneumoniae* KpGe [168] were used as negative (virulent *P. aeruginosa* PT5 should be non-permissive for *D. discoïdeum* growth) and positive controls (*K. pneumoniae* KpGe non-virulent strain should be permissive for *D. discoïdeum*) respectively, in each assay. Three categories of response were defined to interpret the results [169]: non-virulent (fewer than 400 amoebae were sufficient for lysis plaque formation), low-virulent (400-2500 amoebae for lysis plaque formation) and virulent (more than 2500 amoebae).

Results

Taxonomic Information

Vibrio sp. T9 was determined to be closely related to *Vibrio antiquarius*, based on an ANI value of 98.3% and 95% DNA identity in the MLSA analysis; values of >95% in each assay delineate the same species [170]. *Vibrio* sp. T21 was determined to be a closely related to *V. parahaemolyticus* (Table 4.1).

Table 4.1 – Taxonomic determination of *Vibrio* strains described in this study

	***Vibrio* sp. T9**	***Vibrio* sp. T21**
Most closely related organism and accession number	*Vibrio antiquarius* EX 25 (NC_013456, NC_013457)	*Vibrio parahaemolyticus* FORC 018 (NZ_CP013826, NZ_CP013827)
ANI (%)	98.3	98.2
MLSA (%)	94.5	Not tested
Probability of being a human pathogen (%)[1]	67.7	71.9

[1] as Determined by Pathogen Finder [166].

Antibiotic Resistance Profiles

Both *Vibrio* strains exhibited resistance to penicillins, cephalosporins, and intermediate resistance to aminoglycosides. *V. parahaemolyticus* T21 showed intermediate resistance to a fluoroquinolone (Lloyd *et al*., submitted; Chapter 3).

Effect of PAβN on Antibiotic Resistance Profiles

To assess the possible contribution of RND efflux pumps to drug resistance, we tested the MIC of 5 different cephalosporins in the presence and absence of the efflux pump inhibitor PAβN. Both *Vibrio* strains showed sensitivity to cefoperazone in the presence of the inhibitor, with *Vibrio* sp. T9 showing a 64-fold decrease in MIC and *V. parahaemolyticus* T21 showing a 128-fold decrease in MIC (Table 4.2). *V. parahaemolyticus* T21 showed a 32-fold decrease in MIC also to cephradine, while *V. antiquarius* T9 showed a 4-fold decrease in MIC to cefsulodin. Both strains had no change in MIC to ceftazidime, a third-generation drug used in treatments against *Pseudomonas* and *Enterobacteriaceae* [171]. Regarding cefazolin, a very hydrophobic molecule, shown not to enter the cell in *E. coli* [172], we saw a slight (4-fold) decrease in MIC in *V. parahaemolyticus* T21 and an 8-fold increase in *V. antiquarius* T9 (Table 4.2). Others have shown PAβN reduces resistance to cephalosporins in *E. coli*, speculated to be due to interactions between PAβN and substrates within the binding site [173]. *V. parahaemolyticus* T21 also showed reduced resistance to kanamycin (an aminoglycoside), with MIC decreasing 8-fold from 8 to 1 μg/mL and *V. antiquarius* showed a 4-fold decrease.

Table 4.2 – Effect of efflux pump inhibition (50 ug/mL PAβN) on cephalosporin and aminoglycoside resistance in *Vibrio* spp. T9 and T21

		Cephalosporins										Aminoglycoside	
		First-generation				Third-generation							
		Cefazolin		Cephradine		Cefoperazone		Cefsulodin		Ceftazidime		Kanamycin	
V. antiquarius T9	PAβN *	-	+	-	+	-	+	-	+	-	+	-	+
	MIC (ug/mL)	0.5	4 (**8**)‡	8	8	64	1 (**64**)	64	16 (**4**)	64	64	1	0.25 (**4**)
V. parahaemolyticus T21	PAβN	-	+	-	+	-	+	-	+	-	+	-	+
	MIC (ug/mL)	4	1 (**4**)	64	2 (**32**)	64	0.5 (**128**)	64	64	64	64	8	1 (**8**)

* Presence (+) or absence (-) of 50 ug/mL PAβN

‡ Fold changes in MIC are reported in bold and parentheses

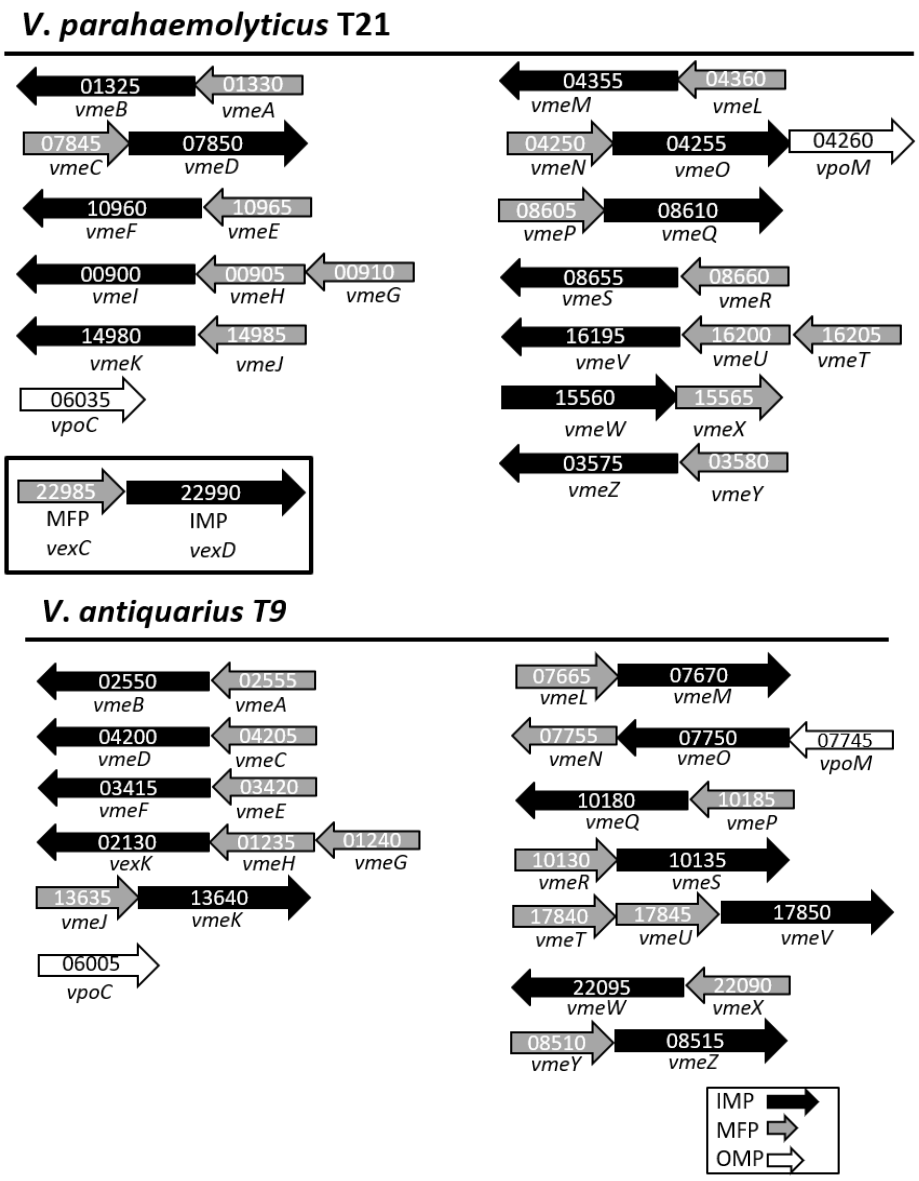

Figure 4.1 – Operon structure and gene loci of RND efflux pumps genes identified in *V. parahaemolyticus* T21 and *V. antiquarius* T9. Genes designations are based on the protein with highest % identity compared to reference proteins in *V. parahaemolyticus* (*vme*) or *V. cholerae* (*vex*). The operon with no homology to *V. parahaemolyticus* RIMD 2210633 is indicated by the black box.

Table 4.3A – Homology (% identity) of RND efflux pump proteins in *V. parahaemolyticus* T21

		Identity Against					Designation
Gene Locus in *V. parahaemolyticus* T21	**VmeA-Z[1,]**	**AcrA or AcrB[2]**	**MexA or MexB[3]**	**VexA or VexB[4]**	**VexC or VexD[4]**	**AcrD[2]**	
CCD93_01330	100	46	41	23	24		VmeA
CCD93_01325	100	63	61	29	20	58	VmeB
CCD93_07845	94	23	19	79	22		VmeC
CCD93_07850	97	30	30	88	20	29	VmeD
CCD93_01965	99	20	19	24	23		VmeE
CCD93_01960	100	28	29	35	21	29	VmeF
CCD93_00910	100	20	23	20	28		VmeG
CCD93_00905	99	17	19	18	27		VmeH
CCD93_00900	100	20	19	21	43	20	VmeI
CCD93_14985	99	18	20	19	18		VmeJ
CCD93_14980	100	21	20	20	21	22	VmeK
CCD93_04360	100	17	17	17	16		VmeL
CCD93_04355	100	18	19	18	17	18	VmeM
CCD93_04250	99	16	16	18	20		VmeN
CCD93_04255	100	18	20	20	36	18	VmeO
CCD93_04260	98	nt	nt	nt	nt		VpoM
CCD93_08605	100	31	30	21	21		VmeP
CCD93_08610	100	39	38	31	20	36	VmeQ
CCD93_08660	100	12	12	13	11		VmeR
CCD93_08665	100	21	19	21	22	19	VmeS
CCD93_16205	99	20	19	21	27		VmeT
CCD93_16200	99	19	17	15	25		VmeU
CCD93_16195	100	20	20	20	41	20	VmeV
CCD93_15560	100	20	21	20	20	21	VmeW
CCD93_15565	99	19	17	18	23		VmeX
CCD93_03580	100	31	26	22	25		VmeY
CCD93_03575	99	39	40	31	20	37	VmeZ
CCD93_22985	low %	20	19	20	70		VexC
CCD93_22990	low %	21	21	20	86	21	VexD
CCD93_06035	92	nt	nt	nt	nt		VpoC

The MFP (grey), IMP (black), and OMP (white) proteins from *V. parahaemolyticus* T21 were compared to reference proteins from *V. parahaemolyticus*[1], *E. coli*[2], *P. aeruginosa*[3], and *V. cholerae*[4]. Names were designated based on reference protein with highest % identity. They are listed according to their operonic affiliation (Fig. 4.1).
nt = not tested

Table 4.3B - Homology (% identity) of RND efflux pump proteins in *V. antiquarius T9*

Gene Locus in *V. antiquarius* T9	Identity Against VmeA-Z[1]	AcrA or AcrB[2]	MexA or MexB[3]	VexA or VexB[4]	VexC or VexD[4]	AcrD[2]	VexK[4]	Designation
CBX98_02555	88	46	45	22	23			VmeA
CBX98_02550	93	63	60	28	20	59		VmeB
CBX98_04205	95	22	21	86	24			VmeC
CBX98_04200	98	30	31	88	21	30		VmeD
CBX98_03420	93	21	21	23	23			VmeE
CBX98_03415	98	29	29	34	21	29		VmeF
CBX98_02140	87	21	25	17	26			VmeG
CBX98_02135	86	19	20	18	26			VmeH
CBX98_02130	low %	23	23	22	16	22	85	VexK
CBX98_13635	85	18	21	19	18			VmeJ
CBX98_13640	95	21	21	20	21	23		VmeK
CBX98_07665	94	18	18	16	15			VmeL
CBX98_07670	95	18	19	18	17	19		VmeM
CBX98_07755	99	17	16	18	21			VmeN
CBX98_07750	99	18	20	21	35	18		VmeO
CBX98_07745	98	nt	nt	nt	nt			VpoM
CBX98_10185	100	30	30	21	20			VmeP
CBX98_10180	99	39	38	31	20	36		VmeQ
CBX98_10130	93	11	12	13	13			VmeR
CBX98_10135	95	20	20	23	21	20		VmeS
CBX98_17840	85	19	20	20	28			VmeT
CBX98_17845	88	21	21	20	26			VmeU
CBX98_17850	94	21	22	21	40	20		VmeV
CBX98_22095	99	20	21	19	20	21		VmeW
CBX98_22090	99	20	16	17	23			VmeX
CBX98_08510	93	31	27	22	23			VmeY
CBX98_08515	97	39	40	31	20	36		VmeZ
CBX98_06005	91	nt	nt	nt	nt			VpoC

The MFP (grey), IMP (black), and OMP (white) proteins from *V. antiquarius* T9 were compared to reference proteins from *V. parahaemolyticus*[1], *E. coli*[2], *P. aeruginosa*[3], and *V. cholerae*[4]. Names were designated based on reference protein with highest % identity. They are listed according to their operonic affiliation (Fig. 4.1).
nt = not tested

Inventory of Putative RND Efflux Gene Homologs

In *V. parahaemolyticus* T21, we identified 13 RND operons, one additional compared to those described by Matsuo *et al*. in *V. parahaemolyticus* RIMD 2210633 [161] (Figure 4.1). This additional operon is indicated by a black box in Fig. 4.1. The % identities between the putative proteins and reference proteins are reported in Table 4.3A.

The *V. parahaemolyticus* T21 MFP and IMP efflux pump proteins had between 97-100% identity to pumps described by Matsuo *et al*. [161], except for the additional operon. The novel IMP (gene locus CCD93_22990) showed 86% amino acid identity by pairwise alignment to *V. cholerae* VexC (gene locus VC1756), and the MFP located just upstream of the IMP (gene locus CCD93_22990) showed 70% amino acid identity to VexD (gene locus VC1757) (Table 4.4). VexCD is known to transport bile in *V. cholerae* [159].

We identified 12 putative RND operons in *V. antiquarius* T9, consistent with the number and operon structure in *V. antiquarius* EX25 (NC_013456, NC_013457) (Table 4.S1), a reference strain. The % identity values of *V. antiquarius* T9 compared to the proteins described by Matsuo *et al*. [161] were between 85 and 100%, indicating strong homology between the two strains (Table 4.3B). However, one gene (CBX98_02130) showed very low homology to the *V. parahaemolyticus* pumps, and instead showed high homology (85%) to VexK from *V. cholerae* (Table 4.3B). VexK is involved in resistance to bile acids, detergents, and potentially required for pathogenesis in *V. cholerae* [174]. The genetic structure in both *Vibrio* spp. (location of genes, number of OMP, etc.) agrees with others' reports on the genetic arrangement of RND efflux pumps [161].

Table 4.4 – RND genes identified in *V. parahaemolyticus* T21, not present in *V. parahaemolyticus* RIMD 2210633

Gene Locus	Role in efflux pump	Length (nt)	%GC	*V. cholerae* homolog (NC_002505)	% Identity (AA) by pairwise alignment
CCD93_22985	MFP	1038	44	VexD (VC1757)	70
CCD93_22990	IMP	3045	47.6	VexC (VC1756)	86

To locate orthologs, we compared the efflux pump proteins to pumps characterized in reference organisms. Both *Vibrio* spp. contained proteins orthologous to the AcrAB and MexAB efflux pumps from *E. coli* and *P. aeruginosa* (Table 4.3 A-B), two systems shown to affect cephalosporin resistance [152]. Both *Vibrio* spp. also contained orthologs to VexAB, a typical RND broad spectrum efflux pump shown to be effective against antibiotics and detergents [159]. Both *Vibrio* strains contained VmeB, presumably an ortholog (58% identity) to AcrD, an *E. coli* IMP with activity against aminoglycosides [152].

Virulence

Both *Vibrio* strains showed non-virulent properties when tested with the *D. discoïdeum* virulence assay described above. Based on the genome sequences, Pathogen Finder predicts that *V. parahaemolyticus* T21 has a 71.9% probability of being a human pathogen and *V. antiquarius* T9 has a probability of 67.7% (Table 4.1).

Discussion

We isolated two *Vibrio* strains with phenotypic resistance to multiple classes of antibiotics. We hypothesized that the RND efflux pumps located within the organism contribute to the antibiotic resistance phenotype. Here, we report on the genome-facilitated discovery of efflux pump-mediated antibiotic resistance among *Vibrio* strains

isolated from the gut of a forage-feeder fish. While the two strains were isolated from the same environment and are both members of the *Vibrio* genus, their resistance phenotypes in the presence of an efflux pump inhibitor were dissimilar, indicating varying levels of RND efflux pump involvement in antibiotic resistance. Our findings suggest that resistance to first- and third-generation cephalosporins in these *Vibrio* spp. is mediated by RND efflux pumps. Genome sequences revealed that *V. antiquarius* T9 contained 12 and *V. parahaemolyticus* T21 contained 13 RND operons with homology to pumps characterized in *V. parahaemolyticus* RIMD 2210633. Furthermore, *V. parahaemolyticus* T21 harbored a supplementary RND operon, with strong homology to the *V. cholerae* efflux pump VexCD, suggesting this organism has the potential for increased virulence.

Comparisons between environmental and clinical strains of *Vibrio* show that environmental strains had a more diverse antibiotic resistance profile [148] suggesting the importance of understanding the evolution of resistance among environmental strains. Importantly, both *Vibrio* spp. strains in this study showed a significant decrease (64- to 128-fold) in MIC to cefoperazone, a third-generation cephalosporin (Table 4.2) when tested with PAβN. Resistance to cephalosporins via the AcrAB RND system in *E. coli* has been well-characterized [160]. The VmeB proteins located in both *Vibrio* spp. T9 and T21 showed 63% identity to AcrB from *E. coli* (Table 4.3); others have characterized VmeAB as an orthologue of AcrAB in *E. coli* [175], providing support for our hypothesis of RND involvement in cephalosporin resistance. Third-generation cephalosporins are currently part of the recommended treatment for Vibrionosis [155], and resistance to these drugs is emerging world-wide [153]. These results suggest that RND efflux pumps

in *Vibrio* in the fish gut microbiota, and more broadly, in the environment, may contribute to the emergence of resistance to third-generation cephalosporin drugs.

Using the power of genome sequencing, we can report on the number of RND proteins located in each strain and are further able to infer function based on homology. *Vibrio* species are known to contain between six [176] (*V. cholerae*) and 12 (*V. parahaemolyticus*) RND efflux pump operons. *V. antiquarius* T9 contained 12 RND operons, and almost all of those proteins showed homology (>85% identity) with *V. parahaemolyticus* RIMD 2210633. The only exception was one IMP that was most similar to VexK in *V. cholerae*. VexK is involved in resistance to bile acids, detergents, and potentially required for pathogenesis in *V. cholerae* [174]. Others have commented on the potential pathogenicity of *V. antiquarius* strains, noting that the genome harbors factors involved in human disease caused by Vibrios [111]. Our work adds to the understanding of the role of RND efflux pumps in the potential pathogenicity of this recently-discovered species of *Vibrio*, although virulence testing in an amoeba model suggested no virulence properties, but some features in the genome of *Vibrio* sp. T9 do suggest pathogenicity as determined by Pathogen Finder [166] (Table 4.1).

V. parahaemolyticus T21 contained 13 operons, one additional operon compared to *V. parahaemolyticus* RIMD 2210633. The extra RND operon shows high homology (70% in MFP; 86% in IMP) to VexCD from *V. cholerae* (Table 4.4). Notably, *V. antiquarius* T9 did not contain a homolog to VexD (Table 4.3). In *V. parahaemolyticus* T21, the addition of PAβN decreased the MIC of cephradine (first-generation cephalosporin) by 32-fold, while in *V. antiquarius* T9, it had no effect on sensitivity (Table 4.2). To explain this discrepancy, we speculate that either i) the extra RND

operon (VexCD) in *V. parahaemolyticus* T21 contributes to this resistance phenotype or ii) the *V. parahaemolyticus* VmeI protein, lacking in *V. antiquarius* T9, may be necessary for RND efflux pump-mediated resistance to cephradine. However, in *V. cholerae*, VexCD is not known to be involved in resistance to antibiotics [177]. VexCD is involved in virulence, as it pumps out bile acids, which aids in host colonization [177]. Bile acids are part of the antimicrobial barrier in enteric environments to prevent infections and are considered to be the primary substrate for RND efflux pumps [178]. Much like *V. cholerae* VexCD, VmeAB and VmeCD in *V. parahaemolyticus*, of which homologs were identified in both of our *Vibrio* spp., (Table 4.3A-B) are also involved in the export of bile acids [161].

Others have discussed the contributions of RND efflux pumps not only in resistance to antibiotics, but also to increased virulence and pathogenicity [179]. For example, bile enhances virulence gene expression in *V. parahaemolyticus* [180]. In *V. cholerae*, RND *vex* operons are required for colonization of infant mouse intestinal tracts [176] and, importantly, bile can induce regulators for VexCD, which can lead to overexpression [181]. While a survey of the genome predicted a 72% chance that this organism was pathogenic, the results of the amoebal virulence test suggested the strain is non-virulent. This result could indicate that the strain may not be digested by the amoeba, or the virulence may be mediated by a set of mechanisms that would manifest in a different organism, e.g. a rodent model [167]. Overall, we conclude that the additional RND operon (Table 4.4) may help *V. parahaemolyticus* T21 survive in its niche of the fish gut, an environment rich in the bile acids cholate and taurocholate [182]. The exact

role of the *V. cholerae*-like RND system, and the other RND systems, in antibiotic resistance and virulence, will require in vivo experimentation.

In some cases, RND efflux pumps were shown to not affect the resistance phenotype. For the first-generation cephalosporin ceftazidime, a drug typically used in the treatment of serious Gram-negative infections [171], we saw no change in MIC upon addition of PAβN in either *Vibrio* spp. Similarly, for the third-generation cefsulodin, a drug targeting *Pseudomonas* spp. [183], we saw no change in MIC in *V. parahaemolyticus* T21, and a 4-fold decrease in MIC in *V. antiquarius* T9. Both strains exhibited clinical-levels of resistance to these drugs, suggesting that resistance phenotypes are likely attributed to other mechanisms, e.g. degradation of the drugs by β-lactamases located within the genomes (Lloyd *et al*, submitted; Chapter 3).

Vibrio spp. T9 and T21 exhibited differing phenotypes for resistance to cefazolin (a first-generation cephalosporin). We observed an 8-fold increase in MIC in *V. antiquarius* T9 and a 4-fold decrease in *V. parahaemolyticus* T21. We note that the strains were sensitive [184] with a maximum MIC for each strain of only 4 μg/mL. The increase in *V. antiquarius* T9 is not entirely unexpected, as PAβN is known to result in increased MIC to cephalosporins in *E. coli* [173] and carbapenems in *Klebsiella pneumoniae* [185]. This increase has been attributed to altered expression of porin genes in *Enterobacteriaceae* [186]. Further, cefazolin is a very hydrophilic molecule and is known to not be effluxed by AcrB in *E. coli* [172]. Therefore, these two drugs are likely not affected by RND efflux pumps in these *Vibrio* strains.

Aminoglycosides are an important class of antibiotics known to be counter-acted by RND efflux pumps such as MexX (in *P. aeruginosa*) [187] and AcrD in *E. coli* [160].

In *V. parahaemolyticus* T21 and in *V. antiquarius* T9, we observed an 8- and 4-fold decrease, respectively, in MIC to kanamycin. However, the starting MIC was only 8 μg/mL for *V. parahaemolyticus* T21 and 1 ug/mL for *V. antiquarius* T9, which are considered sensitive according to [99]. Both strains contained proteins with some homology to AcrD (58% and 59% identity) (Table 4.3), which could potentially mediate efflux, a hypothesis that will need to be addressed by further testing. Interestingly, when RND efflux pump operons were individually knocked out in *V. parahaemolyticus* RIMD 2201633, MIC to kanamycin remained unchanged [161]. Our results suggest that RND efflux pumps are not involved in resistance to kanamycin in this organism, but may affect efflux of the drug.

The findings presented in this paper are important because RND efflux pumps allow bacteria to live in enteric environments, confer resistance to antibiotics used in therapy, and play a role in pathogenicity. Here, we report the potential involvement of such pumps in cephalosporin resistance in two *Vibrio* strains. We show that each *Vibrio* harbors a set of RND efflux genes, including those with homology to *V. cholerae*, suggesting that these genes may contribute to increased virulence. We wonder to what extent (if any) RND efflux pumps have contributed to the reported increase in *Vibrio* infections observed in recent years in the United States [188]. The increase in antibiotic resistance and virulence, may be related, for example, if there is an alteration in expression of RND efflux pumps leading to increase in both bile and antibiotic resistance, as suggested by the genome sequences. If the strains survive in the fish gut, they are likely able to live also in the human gut, as others have reported on the similarities in bile acids between the two [182]. This work demonstrates the connection between RND

efflux pumps, antibiotic resistance, bile resistance, and increased virulence in commensal fish gut bacteria. This work has implications for antibiotic usage in aquaculture, as *V. parahaemolyticus* is one of the leading causes of seafood-borne gastroenteritis. The overuse of antibiotics will not only contribute to the spread of resistance by applying selective pressure in an environment that is highly conducive to genetic exchange [120], but also for those over-expressing efflux pumps, which can, in turn, lead to populations with increased pathogenicity.

In addition to the roles previously mentioned, RND efflux pumps likely contribute to other aspects of microbial life in challenging environments. Vibrios are commonly found in brackish surface water environments, areas that tend to have high levels of anthropogenic input. Vibrios may depend on RND transporters, and other families of efflux pumps, to survive in these challenging environments with many stressors including: exposure to pollutants, and frequent changes in salinity concentration and temperature. We suggest that RND efflux pumps in environmental *Vibrio* are an area of needed research, as these pumps can contribute to antibiotic resistance and pathogenicity of environmental opportunistic pathogens and exposure to pathogenic *Vibrio* is possible through consumption of seafood and exposure to water.

Chapter 5: The Role of Efflux Pumps in Resistance to Arsenate and Antibiotics in *Shewanella* sp. BC20

Abstract

Cross-resistance of metals and antibiotics in bacteria occurs when resistance is mediated by the same mechanism via broad-spectrum efflux pumps. In this chapter, I studied cross-resistance to arsenate and antibiotics in a multi-drug resistant and metal resistant strain of *Shewanella*, isolated from the gut of a fish collected from an estuary contaminated with mercury and arsenic. The organism's genome contained genes involved in arsenate resistance and the strain grew at high levels (100 mM) of arsenate. Testing with an inhibitor of RND efflux pumps showed that RND efflux pumps may be involved in resistance to carbapenems and sulfonamide antibiotics as well as arsenate. I located several RND efflux pump operons with homology to characterized RND proteins in the genome. A transcriptomic study is in progress to understand gene regulation in response to arsenate stress. This experiment will allow us to determine if the resistance genes of interest are under control of the same regulatory systems, a phenomenon known as co-regulation. Overall, this chapter seeks to understand the role of efflux pumps in resistance to arsenate and antibiotics, and more broadly, to understand the effects metal contamination may have on antibiotic resistance in the environment.

Introduction

The Shewanellaceae, a family belonging to the gamma-proteobacteria, are commonly found in aquatic environments, and are increasingly being recognized as opportunistic human pathogens. *Shewanella* spp., primarily, *S. algae* and *S. putrefraciens*, have been implicated in human infections [35] and are known to harbor antibiotic resistance genes of public health concern [94]. Some species of *Shewanella* have been studied for their abilities to metabolize metals and survive in contaminated environments [189]. I have described a multi-drug and metal resistant *Shewanella* strain: *Shewanella* sp. BC20, isolated from the gut of the mummichog (*Fundulus heteroclitus*) collected from a mercury and arsenic-contaminated estuary.

Microbial resistance to antibiotics is a public health concern. Exposure to metals can indirectly select for antibiotic resistance through co-resistance, the genetic linkage between resistance genes. Co-resistance has been previously examined in this *Shewanella* strain (Chapter 3). In this chapter, I will focus on alternative mechanisms of co-selection: cross-resistance and co-regulation. In cross-resistance, the same mechanism facilitates resistance to both antibiotics and metals, mainly via broad-spectrum efflux pumps. In co-regulation, the expression of multiple resistance genes are under the control of a single regulatory gene [4].

Efflux pumps are distributed amongst all domains of life and their genetic organization and structural features are well-conserved [21]. Efflux pumps are divided into five families based on their structure and the mode by which they are energized. The ABC (ATP Binding Cassette) family, a few of which have been identified as multidrug exporters in prokaryotes, hydrolyzes ATP to transport substrates [21]. The Small Multidrug Resistance (SMR) transporters, several of which have been recognized for their role in antimicrobial resistance [190] dissipate proton motive force (PMF) during efflux. The Multidrug and Toxic compound Extrusion (MATE) family of efflux pumps uses a Na^+/H^+ antiporter transport system and is commonly associated with resistance in Gram positive organisms [21].

The Resistance Nodulation and cell Division (RND) superfamily of efflux pumps plays a prominent role in multi-drug resistance (MDR) in Gram negative pathogens [157]. As discussed in Chapter 1, these pumps consist of a tripartite system including an outer membrane protein (OMP), a membrane fusion protein (MFP), and an inner membrane protein (IMP) [21]. The MFP and IMP are usually found in an operon structure, with or without the OMP, which may be located elsewhere in the genome [21]. The most well-studied RND system, AcrAB, characterized in *Escherichia coli* with orthologs in many other members of the Enterobacteriaceae, has been shown to export dyes, detergents, chloramphenicol, tetracyclines, macrolides, β-lactams, fluoroquinolones, and organic solvents [18]. In addition to antimicrobial resistance, RND efflux

pumps are involved in cell-to-cell communication and host colonization [18], as well as virulence [158, 159].

The Membrane Facilitator Superfamily (MFS) of pumps, energized by the PMF, is also a key player in intrinsic antibiotic resistance. Intrinsic antibiotic resistance is resistance conferred by basal levels of efflux and causes antibiotics to be ineffective against some species of Gram negative bacteria [179]. Two examples of MFS pumps are the EmrAB-TolC complex in *E. coli*, and the Bcr/CflA protein complex, which will be discussed in more detail later.

Efflux pump genes are usually expressed at low levels [21]; however, various effectors may increase their expression. The expression of some efflux pumps is known to be under regulation by global regulator systems. For example, members of the TetR family control expression of some MFS pumps. Mutations may cause inherited high-level expression [21]. Further, one local regulator can act as a repressor or activator of different multidrug efflux systems [21].

Exposure to metal or antibiotics may affect the expression at the transcriptional or translational levels of various regulators, leading to a coordinated response to either stressor [4]. Thus, co-regulation in response to metals can affect antibiotic resistance, and vice versa. One example of co-regulation is the *Pseudomonas aeruginosa* RND efflux pump CzcCBA, providing resistance to cadmium, zinc, and cobalt. The regulator, CzcR, also regulates resistance to carbapenems in *P. aeruginosa* [191].

This study focuses on cross-resistance of arsenate and antibiotics in *Shewanella* sp. BC20. Biological arsenate reduction occurs via two distinct pathways: (i) the use of arsenate as a terminal electron acceptor in anaerobic conditions and (ii) intracellular reduction of arsenate to arsenite under aerobic conditions by arsenate reductase ArsC [192]; arsenite is then pumped out of the cell via a membranous efflux pump [193]. Resistance to arsenic is well-conserved and present in bacteria, archaea, and eukaryotes, while arsenate respiration is specific to the

prokaryotes [193]. Several genes involved in arsenic resistance and metabolism have been identified.

The *ars* system is the simplest set of co-transcribed genes that confer resistance to arsenate. The three essential genes are *arsR, arsB/acr3,* and *arsC.* ArsR is the regulator, ArsB/Acr3 is the arsenite efflux antiporter, and ArsC is the arsenate reductase. There are several non-essential proteins that are also involved in arsenate resistance. Two such proteins are occasionally found, ArsA, which is an ATPase that binds to ArsB to make efflux more effective, and *arsD*, encoding an arsenite chaperone that represses the operon. (For a more complete list of all genes involved, see Table 1 in [193].)

There are two unrelated families of arsenite transporters in bacteria: ArsB and Acr3, and there is limited amino acid sequence homology between the two [194]. ArsB has 2 membrane-spanning segments and extrudes both arsenite and antimonite, while Acr3 has 10 predicted transmembrane helices and is arsenite-specific. ArsB either functions alone using the PMF in the efflux of arsenite or it partners with ArsA (an ATPase) to form a highly efficient ATP-driven arsenite efflux pump. Acr3 utilizes membrane potential for the efflux of arsenite. It was once thought that the majority of arsenic resistant bacteria possessed ArsB, however, more recent studies suggest Acr3 is more commonly present than believed [194]. Importantly, bacteria require only one of the two transporter genes in order to be able to extrude arsenite from the cell.

The *Shewanella* genus is a reservoir of antibiotic resistance genes and is known to contain RND efflux pumps [195]. *Shewanella* sp. BC20 is a multi-drug resistant (MDR) organism isolated from a mercury and arsenite contaminated environment (Lloyd *et al*, submitted). The aim of this work is to understand cross-resistance, and more specifically, the effect metal exposure has on antibiotic resistance phenotypes via cross-resistance and co-regulation in *Shewanella* sp. BC20. I hypothesized that efflux pumps contribute to the observed resistance to arsenate and antibiotics. This work contributes to the understanding of efflux

pumps, especially RND-type, and further seeks to understand the effects metal contamination can have on antibiotic resistance gene pools in the environment.

Methods

Genomic Analyses

Protein sequences for genes involved in arsenate resistance and metabolism were downloaded from NCBI and the blastp [96] function was used to compare the protein sequences from NCBI to the predicted proteome of *Shewanella* sp. BC20. To identify efflux pump gene homologs, the *Shewanella* sp. BC20 genome was compared to the BacMet database [107], and was also manually searched. Potential efflux pump genes were manually confirmed by comparison against NCBI using blastp [96]. Potential efflux pump gene homologs were compared against the CARD protein homolog model database, accessed in April 2018 [196]. As an alternative method of searching, the potential efflux pump gene homologs were compared against the RND efflux pumps from *Vibrio parahaemolyticus* RIMD 2210633, as it is one of the more closely-related organism with characterized efflux pumps [161]. Efflux pump genes from *V. parahaemolyticus* RIMD 210633 are referred to as *vme* in Results.

Efflux Pump Inhibitor Assays

Efflux pump inhibitors (EPIs) are used to determine the physiological role of efflux in specific biological phenomena. Carbonyl cyanide 3-chlorophenylhydrazone (CCCP) uncouples oxidative phosphorylation which disrupts the proton gradient of all membranes in the cell and it has been found to increase the antibiotic susceptibility of several MDR bacteria [197]. Phenyl-arginine β-naphthylamide (PAβN) is a specific inhibitor of several RND efflux pumps which works by binding to the same site as the antibiotic substrate of the efflux pump. Specifically, PAβN (Chapter IV) is known to inhibit the *acrAB* system in *E. coli* and the *mex* efflux system in *P. aeruginosa* [152]. Both CCCP and PAβN have been used in numerous studies to assess the effect of efflux pumps on antimicrobial resistance (e.g. [165], [198]).

Growth of *Shewanella* sp. BC20 was monitored using the Bioscreen C (Oy Growth Ab Ltd), an automated microbiology growth curve analysis system. Pre-cultures were grown on solid media overnight at 28°C. Colonies were suspended in tryptic soy broth (TSB) media to a McFarland standard of ~1.5 measured using the DensiCheck system (bioMérieux, Craponne, France). Approximately 4.5 x 10^6 CFU/mL were inoculated into Bioscreen C honeycomb plates containing serial dilutions of potassium arsenate (KH_2AsO_4) (0-100 mM), and separately, PAβN and CCCP. Stock solutions of CCCP and PAβN were prepared by dissolving the appropriate amount of solid in DMSO. Final concentrations of 25 µg/mL (PAβN) and 3.15 µg/mL (CCCP) were used. These concentrations were experimentally determined to have no effect on the growth of the strain *Shewanella* sp. BC20 (Figure 5.S1). Growth rates under each condition were calculated from the growth curves using the GroFit package for R [100]. Graphs depict average and standard deviation of growth rates.

Liquid MICs

Minimum inhibitory concentrations of various antibiotics were determined using the established broth microdilution method according to the guidelines of the Clinical Laboratory Standards Institute (CLSI) using microtiter plates [164] in the presence (50 µg/mL) or absence of the efflux pump inhibitor PAβN. Briefly, cultures were grown overnight at 28°C on Mueller-Hinton agar. The next day, cultures were diluted to a ~0.5 McFarland standard as measured by the DensiCheck (bioMérieux, Craponne, France) system. The cultures were then used to inoculate a microtiter plate containing serial dilutions of antibiotics and PAβN. The plates were incubated for 24 h at 28°C before interpretation. MIC changes of 4-fold or greater were considered significant [165].

Virulence Testing

Virulence of the *Shewanella* strain was determined as described by Froquet *et al.* [167] using the amoebal model, *D. discoïdeum*. Overnight bacterial cultures were adjusted to an OD_{600nm} of 1.5 by dilution in LB. One mL of each adjusted bacterial suspension was plated on

SM Agar (Formedium, Hustanton, United Kingdom) medium. The plates were allowed to dry for one hour to obtain a dry bacterial layer. Cells of *D. discoïdeum* were washed twice in PAS (Page's amoeba saline) buffer by centrifugation at 1000 g for 10 minutes. The amoebal suspension was adjusted to 2 x 10^6 cells.mL^{-1} and serial dilutions were performed in order to obtain a final concentration of 7812 cells.mL^{-1} (in the most dilute sample). Five µL of each serial dilution of *D. discoïdeum* (containing from 39 - 14,000 cells per 5 µL aliquot) was spotted on the bacterial lawn. Plates were incubated at 22.5°C for five days and, appearance of phagocytic plaques was checked at the end of the incubation time. This assay was performed in triplicate. Strains of *P. aeruginosa* PT5 and *K. pneumoniae* KpGe [168] were used as negative (virulent *P. aeruginosa* PT5 should be non-permissive for *D. discoïdeum* growth) and positive controls (*K. pneumoniae* KpGe non-virulent strain should be permissive for *D. discoïdeum*) respectively, in each assay. Three categories of response were defined to interpret the results [169]: non-virulent (fewer than 400 amoebae were sufficient for lysis plaque formation), low-virulent (400-2500 amoebae for lysis plaque formation) and virulent (more than 2500 amoebae).

Gene Expression

Triplicate 50 mL tryptic soy broth (TSB) cultures of *Shewanella* sp. BC20 were prepared in 100 mL flasks by adding 100 µL of an overnight culture (OD_{600} of 2.0). The positive control was *Shewanella* sp. BC20 in 50 mL TSB with no additions, the arsenate treatment contained 12.5 mM potassium arsenate (KH_2AsO_4), and the final treatment contained 12.5 mM KH_2AsO_4 and 25 µg/mL PAβN, made freshly the week before. The exposure concentration of 12.5 mM arsenate was chosen in order to avoid complete suppression of cellular metabolism and *Shewanella* sp. BC20 showed moderate growth inhibition at this concentration. All samples were grown at 28°C with shaking at ~ 100 rpm. The OD_{600nm} was measured periodically using a spectrophotometer. Samples were taken in triplicate, spun down, and spent media was removed before being snap-frozen in liquid nitrogen and stored at -80°C until RNA extraction. RNA extraction was

performed on 57 of the samples (Table 5.S1) using the High Pure RNA Isolation Kit (Roche). RNA was stored at -80°C following extraction and purified using the DNA-free Kit (Ambion).

Results

Arsenate Resistance

The *Shewanella* genus has been studied for its ability to respire arsenate and other heavy metals [199] and often serves as a model organism in the study of microbe-metal interactions [200]. *Shewanella* sp. BC20 was able to grow in 100 mM arsenate (Fig. 3.2). The genome of *Shewanella* sp. BC20 contained the three required genes for arsenate resistance: *arsC*, *arsR*, and *acr3*. The genome additionally contains other gene homologs involved in arsenate metabolism, including *arrA* and *arrB*, genes for respiratory arsenate reduction (Table 5.1).

Table 5.1 - Gene homologs involved in metabolism of arsenate identified in *Shewanella* sp. BC20

Gene Homolog	Function	% Identity	Gene Locus in *Shewanella* sp. BC20
arsC [a]	Arsenate reductase	85	CBX96_17955
arsR [a]	Arsenical resistance operon repressor	83	CBX96_12160
arsB/*acr3* [a]	Transmembrane carrier pump	90	CBX96_12165
arrA [b]	Respiratory arsenate reductase large subunit	25	CBX96_18635
arrB [b]	Respiratory arsenate reductase small subunit	37	CBX96_15715
		33	CBX96_18630

Protein sequences from *Shewanella* sp. MR-1[a] and *Shewanella* sp. ANA-3[b] were compared to the genome of *Shewanella* sp. BC20 using the *blastp* function. The % identity and gene loci are reported.

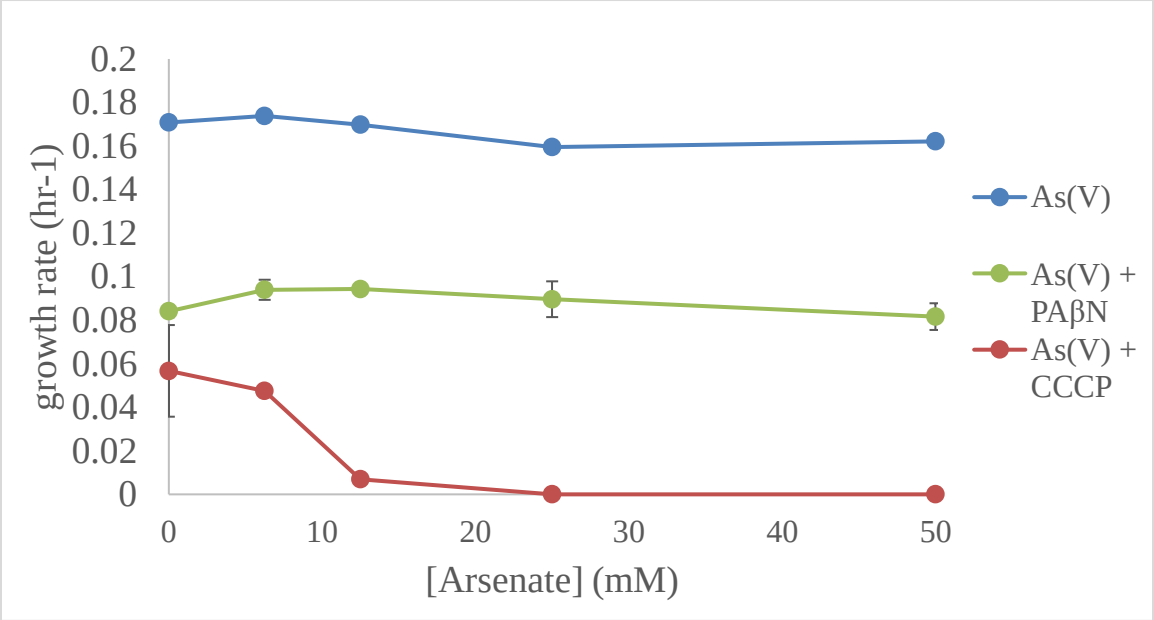

Figure 5.1 - Effect of (3.25 µg/mL) CCCP and (25 µg/mL) PAβN on resistance to arsenate in *Shewanella* sp. BC20. Growth rates in media containing increasing concentrations of arsenate are shown. Standard deviations of one or more determinations are shown.

Effects of Efflux Pump Inhibition of Arsenate Resistance

To assess the possible contribution of RND efflux pumps to arsenate resistance, I monitored growth in the presence of arsenate at various concentrations with two efflux pump inhibitors: PAβN (25 μg/mL), which inhibits RND-type pumps and CCCP (3.25 μg/mL), which dissipates the proton motive force. In the control treatment, *Shewanella* sp. BC20 was able to grow in as high a concentration as 100 mM arsenate (Fig. 5.1). With the addition of PAβN, the growth rate of *Shewanella* sp. BC20 was about half of the original. The organism was still able to grow with arsenate while RND efflux pumps were inhibited, RND efflux pumps are not involved in resistance to arsenate. However, the results do suggest some arsenate resistance mechanism is active. When challenged with CCCP, growth of *Shewanella* sp. BC20 was almost totally inhibited at 12.5 mM arsenate (Fig. 5.1). The results suggest that efflux likely contributed to the resistance of strain *Shewanella* sp. BC20 to arsenate. In the samples prepared for the transcriptome analysis (see below), I monitored growth in 12.5 mM arsenate and 25 μg/mL PAβN.

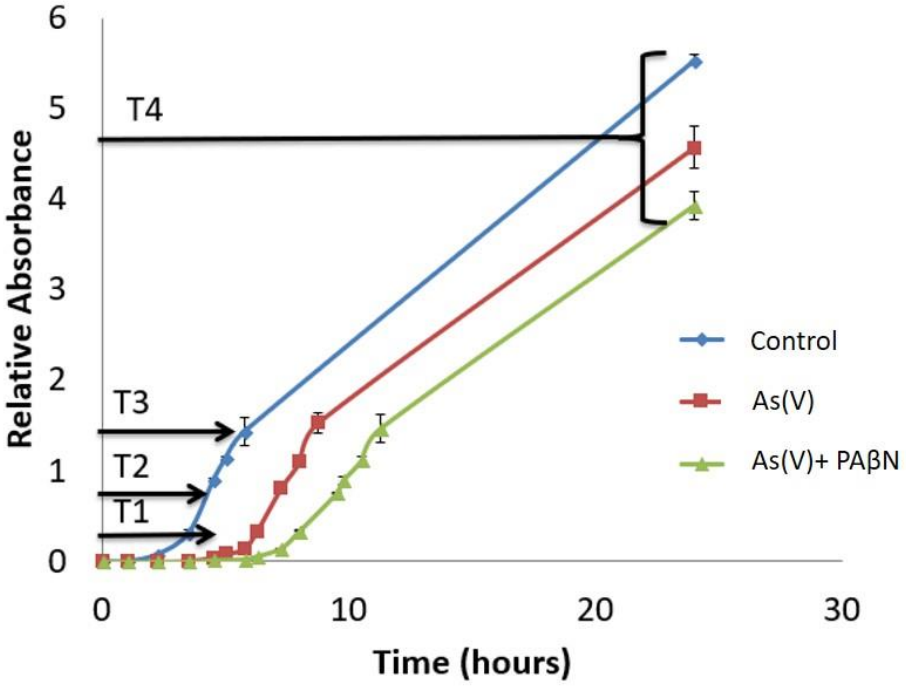

Figure 5.2 - Growth curve of samples prepared for gene expression study. Cultures were grown in TSB media at 28°C with amendments of 12.5mM arsenate and 25 µg/mL PAβN. Samples for transcriptome analysis were harvested at four time points, detailed in Table 5.S1.

Table 5.2 – Gene loci of ABC, MATE, and MFS efflux pump gene homologs in the *Shewanella* sp. BC20 genome

Family	Homolog	Location	Length (AA)	Annotation
ABC	*macB*	CBX96_07680	657	macrolide ABC transporter
ABC		CBX96_16535	250	ABC transporter ATP-binding protein
ABC		CBX96_18160	236	ABC transporter permease
ABC		CBX96_19275	610	multidrug ABC transporter ATP-binding protein
ABC		CBX96_19985	377	sulfate ABC transporter ATP-binding protein
ABC		CBX96_06405	352	hlyD
ABC		CBX96_12130	351	hlyD
ABC		CBX96_02665	262	ABC transporter ATP-binding protein
ABC		CBX96_07335	350	ABC transporter
ABC		CBX96_09215	322	ABC transporter
ABC		CBX96_07280	597	metal ABC transporter permease
ABC		CBX96_02675	297	antimicrobial peptide ABC transporter permease SapC
ABC		CBX96_15170	262	molybdate ABC transporter substrate-binding protein
ABC		CBX96_15180	362	molybdenum ABC transporter ATP-binding protein
ABC		CBX96_15165	260	molybdenum-dependent transcriptional regulator
ABC		CBX96_13795	472	nitrogen regulation protein NR(I)
ABC		CBX96_02670	336	peptide ABC transporter ATP-binding protein
ABC		CBX96_02680	344	peptide ABC transporter permease
ABC		CBX96_02685	542	peptide ABC transporter substrate-binding protein SapA
ABC		CBX96_00195	273	phosphate ABC transporter ATP-binding protein
ABC		CBX96_18155	275	tungsten ABC transporter substrate-binding protein
ABC		CBX96_07675	404	macA
MATE		CBX96_05585	460	MATE family efflux transporter
MATE		CBX96_07505	1371	MATE family efflux transporter
MATE		CBX96_10935	1368	MATE family efflux transporter
MATE		CBX96_18395	453	MATE family efflux transporter
MATE		CBX96_19440	1563	MATE family efflux transporter
MATE		CBX96_01170	451	MATE family efflux transporter
MFS	*emrD*	CBX96_05395	415	multidrug transporter EmrD
MFS		CBX96_05700	1272	Bcr/CflA family multidrug efflux transporter
MFS	*emrB/qacE*	CBX96_06400	528	EmrB/QacA family drug resistance transporter
MFS	*Bcr/CflA*	CBX96_06625	408	Bcr/CflA family drug resistance efflux transporter
MFS		CBX96_11200	1209	Bcr/CflA family drug resistance efflux transporter
MFS	*emrB/qacE*	CBX96_12135	536	EmrB/QacA family drug resistance transporter
MFS	*Bcr/Cfla*	CBX96_16080	396	MFS transporter
MFS	*qacE*	CBX96_19545	315	QacE family quaternary ammonium compound efflux SMR transporter

Table 5.3 - RND Efflux pump gene homologs in the *Shewanella* sp. BC20 genome.

Operon*	Location	Function	Top Hit**	% Identity
	CBX96_05410	MFP	VmeQ	43.9%
	CBX96_05415	IMP	MexB	41.5%
	CBX96_05420	OMP	OprM	34.0%
	CBX96_08220	IMP	VmeV	27.4%
	CBX96_08225	MFP	N/A	N/A
vmeLM	CBX96_09460	MFP	VmeL	34.8%
	CBX96_09465	IMP	VmeM	42.8%
vmeAB	CBX96_10705	MFP	VmeA	60.5%
	CBX96_10710	IMP	VmeB	72.1%
	CBX96_11030	IMP	VmeS	58.1%
	CBX96_11035	MFP	N/A	N/A
	CBX96_12100	OMP	N/A	N/A
	CBX96_12105	MFP	N/A	N/A
	CBX96_12110	IMP	CzcA	95.5%
vmeEF	CBX96_16070	MFP	VmeE	61.1%
	CBX96_16075	IMP	VmeF	76.4%
mexEF	CBX96_16120	IMP	MexF	71.0%
	CBX96_16125	MFP	MexE	52.8%
vmeEF	CBX96_18005	MFP	VmeE	34.0%
	CBX96_18010	IMP	VmeF	46.8%
	CBX96_18065	OMP	N/A	N/A
	CBX96_18070	MFP	N/A	N/A
	CBX96_18075	IMP	CzcA	35.0%
	CBX96_18405	MFP	VmeT	33.6%
	CBX96_18410	OMP	VmeI	54.1%
	CBX96_19135	MFP	N/A	N/A
	CBX96_19140	IMP	MexI	23.0%
	CBX96_19415	MFP	VmeC	23.6%
	CBX96_19420	IMP	VmeF	27.6%
	CBX96_19425	IMP	MdtC	25.0%
	CBX96_07685***	OMP	MtrE	30.1%
	CBX96_15260	OMP	VpoC	51.3%
	CBX96_14420	OMP	N/A	N/A

* Typical operon structure

**Top hit was determined by blast search against the Comprehensive Antibiotic Database (CARD) [196] and RND efflux pumps from the *V. parahaemolyticus* RIMD 210633 genome. Several genes did not return a hit, which are depicted by N/A.

***OMP genes that were not located in operonic structure

Efflux Pump Gene Inventory

Various efflux pump gene homologs were identified in the *Shewanella* sp. BC20 genome (Tables 5.2 and 5.3). The distribution and abundance of the different families of efflux pumps are similar between the genome sequence of *Shewanella* sp. BC20 and the reference genome of *Shewanella* sp. MR-4. Overall, I counted 66 efflux pump gene homologs in total, compared to 69 in *Shewanella* sp. MR-4 (Figure 3.S2)

Several gene homologs from the MFS family were located in the genome (Table 5.2). The MFS family of efflux pumps includes multiple copies of some multidrug exporters such as *emrB* and *bcr/cflA*. The *emr* family exports various substances including nalidixic acid, while the *bcr/cflA* group exports drugs such as chloramphenicol and sulfonamides [201]. *Shewanella* sp. BC20 was sensitive to both nalidixic acid and chloramphenicol when tested (Chapter 3).

Many RND efflux pump gene homologs were found in the genome (Table 5.3, Fig. 5.3), organized in 13 operons. Twelve of those were in a typical RND operon structure, i.e., the inner membrane protein (IMP) and membrane fusion protein (MFP) located together. One operon had an unusual structure, containing an MFP and two IMPs. The *Shewanella* sp. BC20 putative efflux protein with the highest homology to a known RND IMP is gene CBX96_12110, with 95% identity to *czcA*, which encodes for cadmium resistance (Table 4.3). When tested, *Shewanella* sp. BC20 was sensitive to 0.625 mM cadmium, a concentration commonly tolerated by resistant strains [37] under the growth conditions tested (Lloyd *et al*, submitted). I further classified the putative RND efflux pumps according to their similarity to other RND efflux pump genes into the following families: *mex*-like and MexEF (from *P. aeruginosa*) and several operons from *V. parahaemolyticus* (VmeAB, VmeEF, VmeLM). I further identified one operon with homology to the Mdt family, a unique operon with two IMPs, studied in members of the Enterobacteriaceae including *Salmonella* spp. and *E. coli*[202].

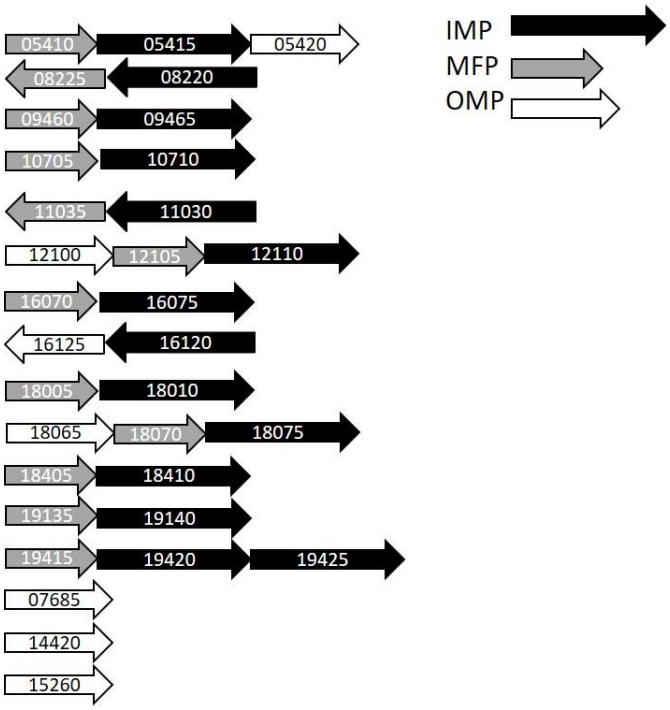

Figure 5.3 – **RND efflux transporter genes (13 total operons) encoded in the *Shewanella* sp. BC20 genome.** Numbers correspond to gene loci. Black genes represent IMPs, grey represent MFPs, and white are OMPs. Direction of arrow represents direction of transcription.

Table 5.4 - Effect of 50 µg/mL PAβN on antibiotic resistance in *Shewanella* sp. BC20

	Penicillins						Glycopeptides		Quinolones	
	Ticarcillin		Ticarcillin + Clavulanic acid		Penicillin		Vancomycin		Nalidixic Acid	
PAβN*	-	+	-	+	-	+	-	+	-	+
MIC (µg/mL)	64	64	64	64	64	64	32	32	2	0.5 (**4**)
	Aminoglycoside				Carbapenem		Tetracyclines		Sulfonamides	
	Streptomycin		Kanamycin		Meropenem		Tetracycline		Sulfamethoxazole	
PAβN	-	+	-	+	-	+	-	+	-	+
MIC (µg/mL)	1	NT	2	0.5 (**4**)	16	2 (**8**)	1	2 (**1**)	64	8 (**8**)
	Cephalosporins									
	Cefaperazone		Cefsulodin		Ceftazidime		Cefazolin		Cephradine	
PAβN	-	+	-	+	-	+	-	+	-	+
MIC (µg/mL)	32	16 (**2**)ǂ	64	64	64	64	64	64	2	16 (**8**)

***** Presence and absence of 50 µg/mL PAβN are shown.
ǂ Fold changes in MIC are reported in bold and parentheses.
MICs showing at least a 4-fold decrease from an initial MIC considered resistant are shaded.

Effect of PAβN on Antibiotic Resistance Profiles

To assess the possible contribution of RND efflux pumps to drug resistance, I tested the MIC of different antibiotics in the presence and absence of 50 µg/mL PAβN. Resistance of *Shewanella* sp. BC20 to meropenem and sulfamethoxazole decreased by 8-fold in presence of the inhibitor as indicated by the respective MIC values (Table 5.4). In contrast, resistance to cephradine increased 8-fold in the presence of the inhibitor. For other antibiotics that were tested, including penicillins, glycopeptides, and several cephalosporins, the MICs were unchanged (Table 4.4).

Virulence

Shewanella sp. BC20 showed a low virulent phenotype when tested with the amoebal model.

Discussion

I previously reported that *Shewanella* sp. BC20 had a varied antibiotic resistance profile, with resistance to carbapenems, penicillins, and cephalosporins (Lloyd *et al*. submitted), which is an unusual phenotype for *Shewanella* [93]. Chromosomally-located genes encoding resistance to these drugs were identified in the genome (Chapter 3). *Shewanella* sp. BC20 was also resistant to arsenate, and the genes necessary for arsenate resistance were located within the genome. Here, I wanted to test if cross-resistance to antibiotics and arsenate was mediated by RND efflux pumps. Work is in progress to assess the contribution of co-regulation, the phenomena of multiple resistance genes being under control the control of a single regulatory system. Strain *Shewanella* sp. BC20 is of particular interest for this study as it was isolated from an arsenic and mercury contaminated wetland in a densely-populated coastal region.

The identification of RND efflux pumps based on gene homology in *Shewanella* is challenging as so little is known about such pumps in this genus. By comparing *Shewanella* sp. BC20 sequences to RND genes of clinical origin (the CARD database), to genes from *V. parahaemolyticus*, and to the *czc* gene of *S. oneidensis*, I was able to identify several operons with high homology (~>60% identity) to known efflux pumps (Table 5.3).

I identified a total of 13 RND operons (Figure 5.3), a greater number than has been reported in other *Shewanella* species; *S. oneidensis* MR-1 contains nine copies of the AcrB/AcrD/AcrF RND multidrug efflux pump [203]. I found no potential homologs to the Acr family of RND efflux pumps, but, as already mentioned, it is difficult to distinguish amongst RND pumps based solely on sequence homology, and it is possible that *Shewanella* sp. BC20 does contain unrecognized homologs to the Acr family.

Typically, RND efflux pumps have homotrimeric organization: with one IMP, one MFP, and one OMP [202] (Reviewed in Chapter 1). However, the unusual MdtABC pump in *E. coli* encodes two IMPs, in addition to a MFP. I identified a putative RND operon with two IMPs (CBX96_19420 and CBX96_19425) and one MFP (CBX96_19415) (Fig. 5.3) in *Shewanella* sp.

BC20. The possession of the two IMP genes together, in addition to one of these RND proteins having ~25% identity to MdtC, suggests that *Shewanella* sp. BC20 may also contain an ortholog of this operon. The MdtABC operon has been implicated in resistance to β-lactams, copper, and zinc in *Salmonella* [204] and pumps out norfloxacin, novobiocin, cloxacillin, and deoxycholate when overexpressed in *E. coli* [152].

Two *Shewanella* sp. BC20 operons showed comparatively high (60-70% identity) homology to proteins characterized in *V. parahaemolyticus* (VmeAB and VmeEF) (Table 5.3). Both VmeAB and VmeEF are involved in drug resistance, including resistance to penicillins and erythromycin [161].

In order to assess the contribution of RND efflux pumps to antibiotic resistance, I tested resistance to antibiotics in the presence of an RND efflux pump inhibitor. I observed a significant decrease (≥ 4-fold decrease in MIC; [165]) in resistance to two antibiotics: meropenem and sulfamethoxazole. The MIC of several classes of antibiotics including penicillins, glycopeptides, and most cephalosporins, was not impacted by the presence of PAβN (Table 5.4), suggesting that resistance phenotypes are likely attributed to other mechanisms, e.g. degradation of the drugs by β-lactamases located within the genomes (Lloyd *et al*, submitted).

To relate the observed effect of PAβN on resistance to the genetic potential of *Shewanella* sp. BC20, I searched in its genome for genes homologous to RND efflux pumps. An inner-membrane protein (IMP) with high similarity (95.5% identity) to CzcA was identified (CBX96_12110) (Table 5.3). CzcA is part of a well-characterized efflux pump; substrates include cobalt, zinc, cadmium, and in *P. aeruginosa*, carbapenems [191]. *Shewanella* sp. BC20 was resistant to several carbapenems including doripenem, imipenem, and meropenem (Table 3.2); I further observed an 8-fold decrease in meropenem resistance in the presence of PAβN, suggesting that RND efflux pumps may be involved in resistance to this drug (Table 5.4). I previously reported that *Shewanella* sp. BC20 harbors a class D β-lactamase, $bla_{\text{OXA-48}}$, a carbapenemase gene of heightened public health concern [133]. This finding suggests that RND

efflux pumps may contribute to the increased carbapenem resistance profile. In *S. oneidensis* MR-1, strong induction of *czcABC*, was observed after exposure to UVA [203], suggesting that this operon may be involved in stress response to various stressors. The on-going analysis of *Shewanella* sp. BC20's transcriptome and its response to arsenate exposure may shed light on this specific aspect.

An 8-fold decrease in MIC to sulfamethoxazole in the presence of PAβN was observed (Table 5.4). The MexAB family has been implicated in resistance to sulfonamides in *Pseudomonas* [152]. I identified one protein (CBX96_05415) with 41.5% identity to MexB (Table 5.3), which supports the hypothesis of RND efflux mediated resistance to this drug. It should be noted that the genome contained genes for many other types of efflux pumps (Table 5.2) including the MFS pump Bcr/CflA, which is known to affect resistance to sulfonamides[205]. Studies in *Shewanella* have shown that UVA light induces expression of the EmrB/QacA family protein (in addition to the Czc protein discussed above) [203], which again suggests a role for efflux pumps in response to antibiotics and other stressors.

Interestingly, I observed a significant increase (8-fold) in MIC to cephradine, a first-generation cephalosporin drug. PAβN has been shown to increase MIC to cephalosporins in *E. coli* [173] and carbapenems in *Klebsiella pneumoniae* [185], which was attributed to altered expression of porin genes in Enterobacteriaceae [186]. This result suggests that RND efflux pumps do not affect resistance to this drug in *Shewanella* sp. BC20.

In order to test the effect of efflux pumps on arsenate resistance, I determined growth rates of *Shewanella* sp. BC20 exposed to increasing concentrations of arsenate in the presence and absence of two different efflux pump inhibitors. Typically, arsenate resistance is mediated by the *ars* system, which *Shewanella* sp. BC20 possesses (Table 5.1). The results (Fig. 5.1) show decreased growth rates in the presence of PAβN and clear reduction of growth in the presence of CCCP. The results of CCCP are expected, as CCCP is a general uncoupler of oxidative phosphorylation, and would thus prevent the arsenite pump (*acr3*) from functioning properly.

The results of the PAβN growth indicate that RND efflux pumps may not be involved in resistance to arsenate. Further testing will be needed to answer this question, and the results of the transcriptome study may allow us to identify potential gene targets.

To the best of our knowledge, the effects of arsenate on efflux pump gene expression have not been studied in *Shewanella* spp. A study from 2005 showed that genes encoding efflux pumps were up-regulated under chromate-reducing conditions in *S. oneidensis* MR-1 [206]. There seems to be a connection between arsenate resistance and efflux pumps in *S. oneidensis* MR-1 because one of the induced genes in that study was a homolog of a putative *czcA* gene. Beliaev *et al*. [207] reported that both the *ars* and *mexFE* genes were up-regulated during growth on metals as terminal electron acceptors in aerobic respiration (the effect of arsenate was not tested). Further, the *mexFE* genes were induced (on average) 4 to 40-fold under metal reducing conditions [207]. One operon in *Shewanella* sp. BC20 (CBX96_126120, CBX96_16125) (Table 5.3) was homologous to MexFE. MexFE substrates include various antibiotics such as trimethoprim and chloramphenicol [208]. This finding suggests a possible connection between arsenic resistance and the MexFE efflux pump in *Shewanella*.

Conclusion

In this chapter I have shown that *Shewanella* sp. BC20 has a unique metal and antibiotic resistance profile. The genome contained many efflux pump genes, including 13 RND operons, some of which may be involved in resistance to antibiotics including meropenem, a drug of clinical concern. Homology of the RND efflux proteins suggested *Shewanella* contained orthologs to several important RND genes characterized in other species. I further showed that RND efflux pumps likely do not mediate arsenate resistance in this strain. These findings contribute to the understanding of RND-mediated antibiotic and arsenate resistance in *Shewanella*, an emerging opportunistic human pathogen.

On-going Work – Transcriptome

I will sequence the transcriptome of *Shewanella* sp. BC20 samples grown under three conditions: i) no amendments, ii) in the presence of arsenate, iii) in the presence of arsenate and PAβN (Fig. 5.2). RNA was successfully extracted from withdrawn culture biomass and these samples are stored frozen in the Nazaret lab in Lyon while arrangements are being made for transcriptome sequencing.

This global transcriptomic profiling will allow me to elucidate molecular mechanisms of arsenate tolerance and to potentially assess the contribution of RND efflux pumps, notions suggested by our data. Overall, the transcriptome study will allow me to ask and answer many questions on the co-regulation of arsenate and antibiotic resistance (via global regulatory systems) in this *Shewanella* strain.

One transcriptomic study on the effects of arsenate in an uncharacterized Enterobacteriaceae strain with high resistance to heavy metals showed that approximately 10% of the genome was affected by growth in 4 mM arsenate, including the upregulation of the *ars* operon [209]. Genes encoding nitrate reductase were also up-regulated, suggesting this organism preferred nitrate respiration under arsenate stress. Other genes up-regulated included genes involved in oxidative stress response (but not ROS) and SoxRS, a regulator that modulates many diverse types of genes including efflux pumps. The up-regulation of oxidative stress response was expected, as metals are known to cause oxidative stress, and organisms need a mechanism to mediate cellular damage. The authors specifically showed up-regulation of three antibiotic resistance proteins, but it is unclear from their data and available sequence information if this was an RND efflux pump.

Another study addressing the effects of PAβN on transcription showed that PAβN down-regulated key virulence genes and up-regulated nitrogen metabolism genes in *P. aeruginosa* [210]. The authors concluded that RND efflux pumps contribute to establishment of infection in *P. aeruginosa* by inhibiting transcription of global regulators critical for the establishment of infection. I mentioned the connection between RND efflux pumps and virulence in Chapter 4.

Further, with the transcriptome data, I may be able to understand if there is a secondary mechanism of arsenate resistance in this organism. As shown in Figure 5.1, there was little decrease in growth rate as arsenate concentration increased in the cell, even with the addition of PAβN. This suggests that there may be a secondary mechanism active to tolerate the arsenate in the cell.

Summary and Concluding Remarks

The goal of this research was to investigate the co-selection of heavy metal and antibiotic resistance in bacteria isolated from the gut of a forage feeder fish, the mummichog (*Fundulus heteroclitus*). Prior to this work, co-selection had been studied in some types of fish, but never in the gut microbiota of a forage feeder fish. I chose to study the gut because it is an environment conducive to horizontal gene transfer (HGT) with its high population of bacteria and availability of growth substrates; I chose to study this fish because they are capable of surviving in contaminated environments and forage directly in the detritus, which exposes them to metal contamination. The results of this work add to the understanding of the genetic mechanisms underlying the relationship between metal and antibiotic resistance in the environment, including co-resistance, cross-resistance, and co-regulation, in the gut microbiota of the mummichog fish.

In Chapter II, I report the co-selection of mercury and antimicrobial resistance in gut ingesta microbiota of *F. heteroclitus* from mercury (Hg)-contaminated and control (non-polluted) waterways in New Jersey. I showed that the exposure to Hg indeed selected for Hg-resistant organisms, by quantifying *merA* gene abundance in DNA extracted from fish gut ingesta. I reported that ingesta from fish collected at a Hg-contaminated site contained significantly more copies of *merA* than those from a cleaner site, a finding consistent with the higher Hg concentration in fish tissue. Through phenotypic characterizations, we observed that Hg-resistant bacteria were more likely than Hg-sensitive isolates to be resistant to multiple antibiotics, suggesting co-selection, i.e. mercury toxicity might have selected for bacteria that were resistant to both metals and antibiotics. We hypothesized that this observation was due to co-resistance, because

the fish gut is an environment conducive to HGT and other studies have suggested co-resistance in bacteria from aquatic environments. This research contributes to the understanding of the mode and distribution of antibiotic resistant genes in environmental strains.

In Chapter III, I chose three multi-resistant strains from the fish gut for further characterization of the connection between metal and antibiotic resistance: two *Vibrio* spp. and one *Shewanella* sp., dominant genera in the mummichog fish gut [32]. To that end, I performed whole genome sequencing and clinical antibiotic resistance testing on the isolates. All three strains were resistant to various antibiotics, including β-lactams and in *Shewanella*, carbapenems, which is an usual phenotype for this organism [93]. All three organisms were resistant to one or more metals including arsenate, cadmium, and mercury. In analyzing the genomes, I found a few instances of metal and antibiotic resistance genes on mobile genetic elements (Fig. 3.1). We identified many resistance genes within the genomes including class A, B, C, and D β-lactamases (Table 3.3). Most of these genes, including some of public health concern, (e.g., a $bla_{OXA\text{-}48}$-like carbapenemase), were dispersed throughout the genomes. In addition to the chromosomal resistance genes, I identified many gene homologs encoding components of efflux pumps. Because I observed a large number of efflux pump genes in the three genomes and the known role of such pumps in antibiotic and metal resistances [211], I decided to separately investigate the contributions of cross-resistance in *Vibrio* (Chapter IV) and *Shewanella* (Chapter V).

In Chapter IV, I describe the role of RND efflux pumps in resistance to first- and third-generation cephalosporins in the two *Vibrio* spp. whose genome sequences were

obtained in Chapter III. *Vibrio* sp. T21 was identified as a strain of *V. parahaemolyticus*, and *Vibrio* sp. T9 was a strain of *V. antiquarius*. In *V. parahaemolyticus* T21, I observed decreased resistance to cefoperazone and cephradine, and in *V. antiquarius* T9, to cefoperazone and cefsulodin in the presence of phenylalanine-arginine beta-naphthylamide (PAβN), an inhibitor of the resistance-nodulation-division (RND) efflux pumps. Using genome sequences, I identified 13 and 12 RND operons, respectively, with *V. parahaemolyticus* T21 containing an additional RND operon compared to other *V. parahaemolyticus* strains. This operon has strong homology to the VexCD efflux pump in *V. cholerae*, which is involved in host colonization by mediating the efflux of bile salts. Considering the role of bile salts in host defense against intestinal pathogens [178], this finding indicates potential for increased virulence in *V. parahaemolyticus* T21. More generally, the RND proteins in our strains show homology to RND efflux pumps characterized in *E. coli* and *V. cholerae.* Our results suggest a role for RND efflux pumps in resistance to cephalosporins in *Vibrio*. This work highlights the need for further research into the unique *V. cholerae*-related RND operon in *V. parahaemolyticus* T21, and more generally, RND efflux pumps in *Vibrio* species, as *Vibrio* often cause seafood-borne illness.

In Chapter V, I studied cross-resistance to antibiotics and arsenate in *Shewanella* sp. BC20. The organism's genome contained the *ars* system, which mediates arsenate resistance, and grew at high levels of arsenate. Testing with the specific inhibitor of RND efflux pumps (PAβN) showed that such pumps may be involved in resistance to carbapenems, sulfonamides, and arsenate (Table 5.4). I observed several putative RND efflux-pump homologs in the genome including one protein with 96% identity to CzcA,

(Table 5.3) an efflux pump involved in resistance to cadmium, zinc, cobalt, and carbapenem antibiotics. A transcriptomic study of *Shewanella* sp. BC20 comparing gene expression in the absence of arsenate, presence of arsenate, and the presence of arsenate and PAβN is currently in progress. The transcriptomes will allow me to identify genes whose expression is affected by arsenate and PAβN. It will also allow me to identify genes upregulated in response to arsenate including those of the *ars* system and if the expression of RND efflux pumps may contribute to arsenate resistance, as suggested by our phenotypic data. Overall, the transcriptome study will further allow me to explore cross-resistance as a mechanism that promotes arsenate and potentially antibiotic resistance in this *Shewanella* strain.

Overall, this dissertation has contributed to the knowledge of antimicrobial resistance in the fish gut environment. In Chapter II, I established the mummichog fish gut as a reservoir of antibiotic and metal resistant organisms, shedding light on resistance gene pools in the environment. In Chapter III, I reported on the abundance of antimicrobial resistance genes in three strains isolated from the fish gut microbiota and analyzed the genetic mechanisms of co-selection. In Chapters IV and V, I reported on the contribution of RND efflux pumps to antibiotic resistances. These findings contribute to the understanding of RND-mediated antibiotic and metal resistances in known (*Vibrio* spp.) and emerging human pathogens (*Shewenella* spp.).

My results have direct implications to public health by identifying genes in environmental bacterial isolates that are of concern in the clinic (e.g. $bla_{\text{OXA-48}}$, *qnr* genes, various β-lactamases). Because such genes could be transferred from environmental to clinical strains, the environmental reservoir of resistance genes must be considered when

assessing the risk of the spread of antibiotic resistant pathogens. Further, the bacteria studied here are known to cause diseases in both humans and fish. The increase in antimicrobial resistance, in combination with increased virulence in bacteria such as those studies here, are cause for concern, and should drive future research.

APPENDIX A

Supplementary Material for Chapter 2

Supplementary Methods

Aquarium set up

Re-circulating aquariums (75 L) were set up one week prior to arrival of fish. Aquariums were filled with filtered bay water diluted with carbon/sand filtered municipal tap water to a salinity of 23 to 25 ppt. Aquariums were maintained in a chemical fume hood at an average room temperature of 24°C and an average water temperature of 25°C.

Analysis of total mercury (THg) and methylmercury (MeHg)

Water samples were oxidized using 0.2 N bromine monochloride (BrCl) for at least 24 h, while fish tissue and food were digested in hydrochloric and nitric acids (3:1) at 50 °C for 24 h. Total Hg was determined through stannous chloride reduction and cold vapor atomic fluorescence spectroscopy (CVAFS) [60] using a MERX-T Hg Analyzer (Brooks Rand Laboratories). Accuracy was evaluated by analysis of the standard reference material TORT-2 (*Lobster Hepatopancreas*-National Research Council Canada). The average measured concentration of THg in TORT-2 was 0.330 ± 0.006 µg g^{-1} dry wt. (n = 3), in comparison to the certified value (0.27 ± 0.06 µg g^{-1} dry wt.). The limit of detection for this method was 0.18 ng L^{-1} for water and 0.015 µg g^{-1} dry wt. for animal tissue.

Methylmercury (MeHg) was leached from 10 to 20 mg subsamples of dried fish muscle in 4 N nitric acid (Trace Metal Grade, Fisher) at 55°C for 16 hours [212]. Analysis was performed by CVAFS following isothermal gas chromatographic separation of ethylated derivates according to Liang et al. [61] using a Tekran 2500

spectrophotometer. Digestion efficiency was tested using TORT-2. The average measured concentration of methylmercury in TORT-2 (0.144 ± 0.014 µg g^{-1} dry wt., n = 6) was very similar to the certified value (0.152 ± 0.013 µg g^{-1} dry wt.) indicating recoveries of approximately 95%. All procedural and reagent blanks for MeHg were below the detection limit of 0.005 µg g^{-1} dry weight for animal tissue.

Estimating percentage of Hg resistant (Hg^R) bacteria in the fish gut microbiome

Pooled fish gut ingesta samples were aseptically sheared by at least 10 passages through an 18-gauge 1.5-inch syringe needle (BD brand) and then 10 fold diluted in 0.85% buffered saline solution (pH ~7). A hundred µl of the serial dilutions were plated on both tryptic soy agar (TSA) and TSA-Hg plates (12.5 µM $HgCl_2$). Colonies were counted after a 5 day incubation period at 23°C. For each sample, percentage of colonies resistant to Hg was calculated by:

$$\frac{\text{No. of CFUs on TSA-Hg Plates}}{\text{No. of CFUs on TSA Plates}} \cdot 100$$

qPCR

Each 25 µL qPCR reaction contained: 1.2 µL of each forward and reverse primers (10 µM), 7.5 µL water, 12.5 µL SYBR Green Jumpstart Taq Mix (Sigma-Aldirch), and 2 µL of the sample DNA template. Standard curves for *glnA* and *merA* were constructed according to [67] and were included in each run. Samples were analyzed in triplicate with a positive control (*Pseudomonas aeruginosa* containing the Hg resistance plasmid pVS1), and a negative control (only reagents).

merA qPCR conditions included an initial denaturation step consisting of a 5 min incubation at 95°C, followed by 40 cycles of 1 min at 95°C, 30 s at 61°C, 1 min at 70°C with a final cycle of 7 min at 72°C. qPCR conditions of *glnA* included an initial

denaturation step consisting of a 10 min incubation at 95°C, followed by 40 cycles of 1 min at 95°C, 30 s at 58°C, and 1 min at 72°C, with a final cycle of 7 min at 72°C

Supplementary Results

Selection of Hg^R microbes in fish ingesta – lab exposure study

To determine if bacteria in the fish GI tract were adapted to Hg toxicity, we counted the number of cultured colonies on media with and without Hg. The number of cultured aerobic heterotrophic bacteria in the fish ingesta varied by more than two orders of magnitude ranging from 1.4E+07 CFU g_{ww}^{-1} for the high exposure aquarium to 6.6E+05 CFU g_{ww}^{-1} for the low exposure (Table 2.S7). The number of colonies that grew on media with 12.5 µM Hg ranged from $1.1\pm1.5x10^4$ to $1.3\pm1.5x10^5$ per g ingesta plated with the highest counts observed for ingesta that was extracted from the high exposure fish. However, the difference in percent Hg resistance (Hg^R) counts, a measure of adaptation to Hg [9], ranged from 0.8±1.0 to 1.4±1.0 % for the control and the high Hg exposures, respectively, was not significantly different (two-way ANOVA, $p > 0.05$). The high standard deviations reported in Table S7 may be attributed to the natural variability of samples collected from many different fish. The results suggest that aerobic cultured ingesta microbes were not adapted to Hg even though the fish were clearly impacted by exposure as indicated by accumulation of Hg in their tissue.

Supplementary Figures

Figure 2.S1 - Map of New Jersey depicting the two sampling sites: Berry's Creek (BC) and Great Bay (GB).

Table 2.S1 - Concentrations of THg in mummichog muscle tissue, and fish lengths and weights at the end of a 15 day laboratory feeding experiment. Fish were exposed to untreated fish food with a mean measured Hg concentration of 0.08 µg/g.

Fish ID	Length (mm)	Weight (g)	Hg concentration (µg g_{ww}^{-1})
0-1	37	1.06	0.027
0-2	40	1.75	NA
0-3	42	1.42	NA
0-4	49	2.45	0.025
0-5	40	1.26	0.041
0-6	34	0.88	0.012
0-7	39	1.25	NA
0-8	40	1.81	NA
0-9	35	0.96	NA
0-10	36	1.12	NA
0-11	40	1.52	NA
0-12	37	1.29	NA
0-13	38	1.26	NA
0-14	40	2.02	NA
0-15	35	0.89	NA
0-16	38	1.62	NA
0-17	34	0.87	NA
0-18	36	1.23	0.050
0-19	32	0.85	NA

Table 2.S2 - Concentrations of Hg (THg) in mummichog muscle tissue, and fish lengths and weights at the end of a 15 day laboratory feeding experiment. Fish were exposed to amended fish food with a mean measured Hg concentration of 24.4 µg/g.

Fish ID	Length (mm)	Weight (g)	Hg concentration (µg g_{ww}^{-1})
1-1	51	2.43	NA
1-2	47	1.66	NA
1-3	38	0.96	NA
1-4	40	2.07	NA
1-5	35	0.92	NA
1-6	56	3.99	0.012
1-7	41	1.27	NA
1-8	37	1.51	NA
1-9	43	2.33	NA
1-10	50	2.04	NA
1-11	50	3.26	NA
1-12	46	2.31	0.046
1-13	31	0.96	NA
1-14	45	1.81	0.051
1-15	35	0.95	NA
1-16	34	0.94	NA
1-17	38	1.31	NA
1-18	87	13.62	0.027

Table 2.S3 - Concentrations of Hg (THg) in mummichog muscle tissue, and fish lengths and weights at the end of a 15 day laboratory feeding experiment. Fish were exposed to amended fish food with a mean measured Hg concentration of 131.6 µg/g.

Fish ID	Length (mm)	Weight (g)	Hg concentration (µg g_{ww}^{-1})
2-1	45	1.98	NA
2-2	39	1.15	NA
2-3	47	2.22	NA
2-4	44	1.91	NA
2-5	40	1.36	0.141
2-6	41	1.23	NA
2-7	39	1.40	0.148
2-8	37	1.04	NA
2-9	42	1.37	NA
2-10	35	1.10	NA
2-11	36	1.07	NA
2-12	34	0.97	NA
2-13	35	0.84	0.141
2-14	39	1.26	NA
2-15	35	0.73	NA
2-16	34	0.88	NA
2-17	36	16.76	0.167

Table 2.S4 - Concentrations of Hg (THg) in mummichog muscle tissue, and fish lengths and weights of individual fish collected from Great Bay (June sampling)[1]

Fish ID	Length (mm)	Weight (g)	Hg concentration ($\mu g\ g_{ww}^{-1}$)
3-1	75	6.50	0.067
3-2	80	8.10	0.044
3-3	81	8.30	0.091
3-4	75	6.60	0.048
3-5	72	5.10	0.069
3-6	56	4.10	0.044
3-7	59	4.30	0.045
3-8	57	3.80	0.066
3-9	56	4.20	0.074
3-10	56	4.00	0.032
3-11	62	5.00	0.051
3-12	58	4.70	0.067
3-13	47	2.50	NA
3-14	62	5.00	NA
3-15	56	4.30	NA
S3-16	67	6.50	NA
3-17	59	5.80	NA
3-18	56	4.20	NA

[1] As stated in the manuscript, fish were sampled from Great Bay twice, once in June and once in August 2014. The June sampling was used for determination of tissue Hg concentrations, while the August sampling was used for the determination of the Hg^R and antibiotic resistance.

Table 2.S5 - Concentrations of Hg (THg) in mummichog muscle tissue, and fish lengths and weights of individual fish collected from Berry's Creek

Fish ID	Length (mm)	Weight (g)	Hg concentration ($\mu g\ g_{ww}^{-1}$)
4-1	84	15	0.097
4-2	93.5	18.2	0.106
4-3	69	7	0.131
4-4	84	13.7	0.154
4-5	69	7.3	0.109
4-6	70	7.9	0.181
4-7	67	7.3	0.156
4-8	62	5.4	0.175
4-9	68	6.7	0.247
4-10	63	6	0.131
4-11	64	6.1	0.150
4-12	63	5.9	0.354
4-13	64	6.5	NA
4-14	64	5.6	NA
4-15	73	8.7	NA
4-16	76	9.8	NA
4-17	56	4.6	NA
4-18	62	6.2	NA

Table 2.S6 - Number of colonies and type and concentrations of antibiotics tested in the aquarium and field studies

Sample	Number of Colonies Tested	Antibiotics Tested (μg mL^{-1})
Aquariums	136	ampicillin (100), kanamycin (50), tetracycline (50), rifampicin (100)
GB	106	ampicillin (100), kanamycin (50), gentamycin (50), ciprofloxacin (10), sulfisoxazole (50)
BC	181	ampicillin (100), kanamycin (50), gentamycin (50), ciprofloxacin (10), sulfisoxazole (50), trimethoprim (10)

Table 2.S7 - Targets and mechanisms of action for the antibiotics used in this study

Antibiotic	Target	Mechanism of Action
Ampicillin	Cell wall synthesis	Binds to specific penicillin-binding proteins (PBPs) to inhibit the third and last stage of cell wall synthesis
Ciproflaxacin	DNA replication and repair	Inhibits topoisomerase II (DNA gyrase) and topoisomerase IV
Gentamycin	Protein synthesis (30S subunit)	Irreversibly binds to specific 30S-subunit proteins and 16S rRNA
Kanamycin	Protein synthesis (30S subunit)	Irreversibly binds to specific 30S-subunit proteins and 16S rRNA
Rifampicin	DNA-dependent RNA polymerase	Inhibits DNA-dependent RNA polymerase, leading to suppression of RNA synthesis and cell death
Sulfisoxazole	Folic acid synthesis	Competitively inhibits dihydropteroate synthetase
Tetracycline	Protein synthesis (30S subunit)	Diffuses through porins to bind to 30S subunit, interfering with protein synthesis
Trimethoprim	Folic acid synthesis	Binds to dihydrofolate reducatse and inhibits reduction of dihydrofolic acid (DHF) to tetrahydrofolic acid (THF), an essential precursor in thymidine synthesis

Source: [213]

Table 2.S8 - Mercury resistance among aerobic heterotrophic microorganisms isolated from ingesta of mummichogs exposed to three different Hg concentrations in their food. Values are means of colony forming units (CFUs) ± 1SD.

Treatment (µg g_{dw}^{-1} in food)	**Total counts (CFUs g^{-1})[1]**	**Hg^R counts (CFUs g^{-1})[2]**	**Percent Resistance to Hg[3]**
0.08	3.7E ± 5.5E +06	1.8E ± 2.0E+04	0.8 ± 1.0%
24.4	6.6E ± 4.3E+05	1.1E ± 1.5E+04	1.3 ± 1.1%
131.6	1.4E ± 2.4E+07	1.3E ± 1.5E+05	1.4 ± 1.0%

[1] Number of colony forming units per g of diluted and plated ingesta observed on TSA plates

[2] Number of colony forming units per g of diluted and plated ingesta observed on TSA plates containing 12.5 µM Hg

[3] Calculated by: $\frac{\text{No. of CFUs on TSA-Hg Plates}}{\text{No. of CFUs on TSA Plates}} \cdot 100$

Table 2.S9 - Mercury resistant CFUs in ingesta from fish collected from BC and GB. Values are means ± 1SD.

Site	Total counts (CFU g^{-1})[1]	Hg^R (CFU g^{-1})[2]	Percent Resistance to Hg^3
BC	1.6E ±2.0E+08	8.8E ± 9.7E+07	58.9 ± 16.9%
GB	1.2E ±1.6E+08	5.4E ± 5.7E+07	47.6 ± 17.1%

[1] Number of colony forming units per g of diluted and plated ingesta observed on TSA plates

[2] Number of colony forming units per g of diluted and plated ingesta observed on TSA plates containing 12.5 µM Hg

[3] Calculated by: $\frac{\text{No. of CFUs on TSA-Hg Plates}}{\text{No. of CFUs on TSA Plates}} \cdot 100$

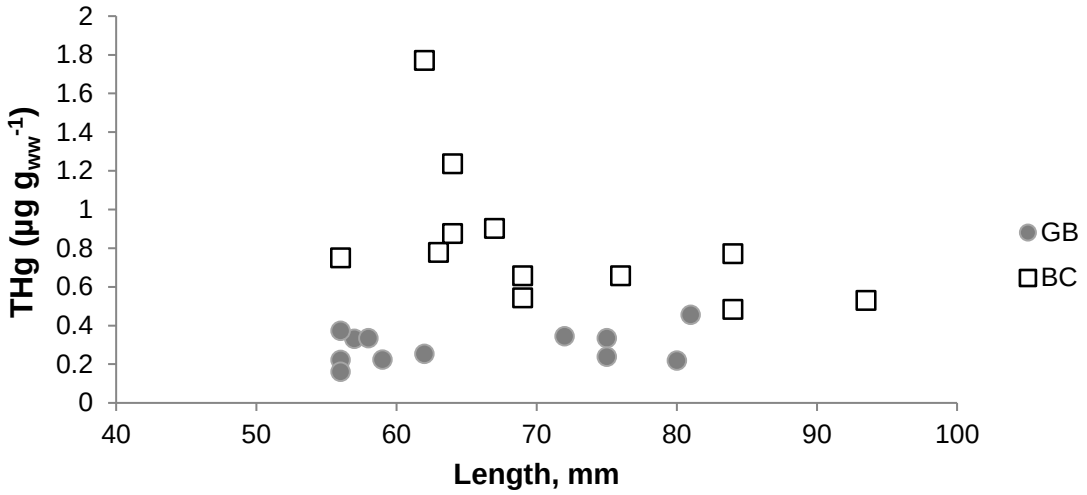

Figure 2.S2 - Relationship between fish length in mm and muscle tissue THg. Concentration in µg g_{ww}^{-1}. Data points are 12 individual fish from each site: Great Bay (GB) and Berry's Creek (BC).

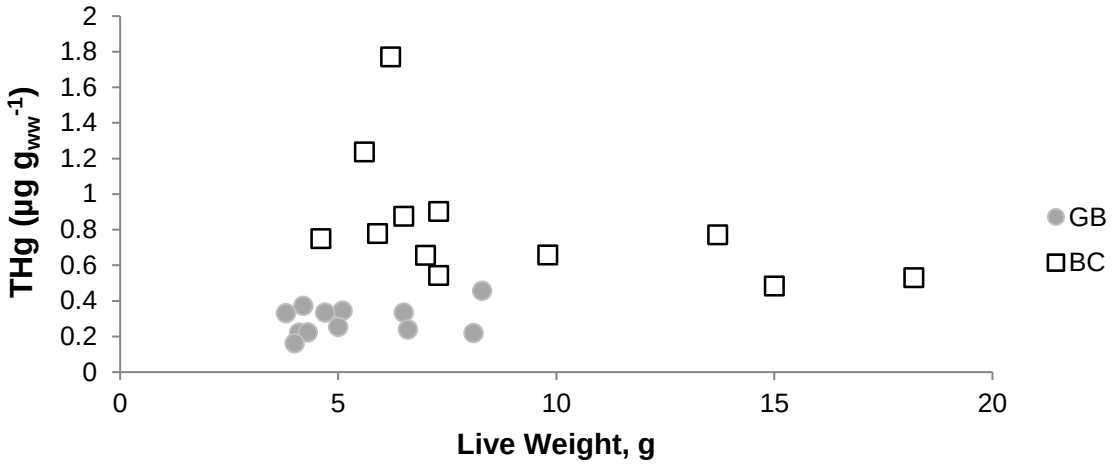

Figure 2.S3 - Relationship between fish weight in g and muscle tissue THg. Concentration in µg g_{ww}^{-1}. Data points are 12 individual fish from each site: Great Bay (GB) and Berry's Creek (BC).

APPENDIX B

Supplementary Material for Chapter 3

Supplementary Results

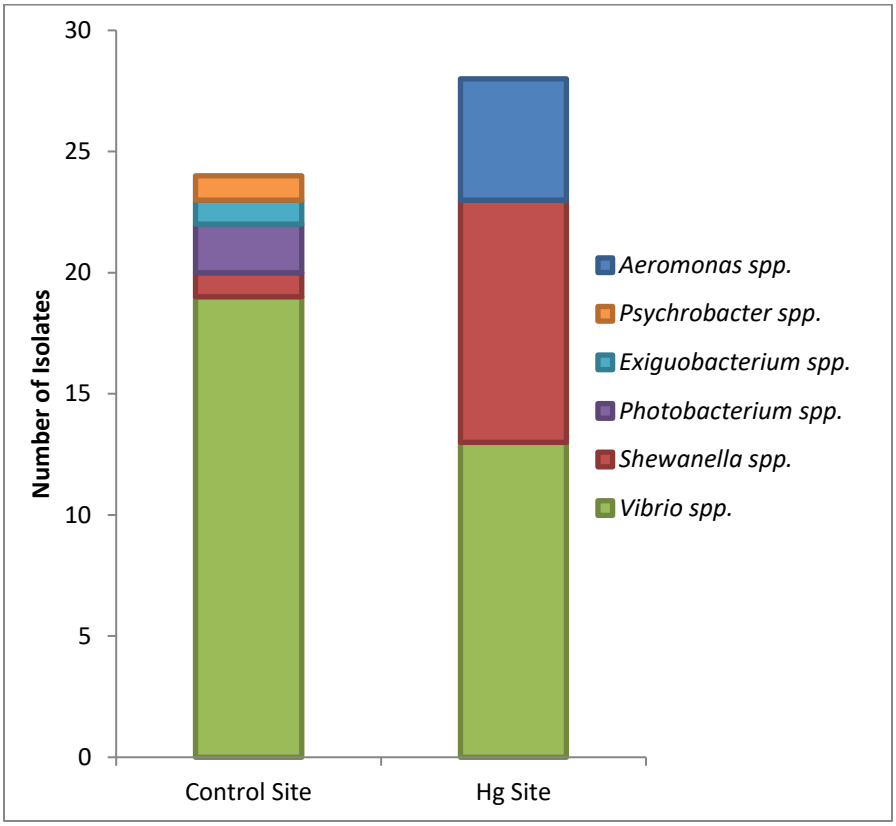

Figure 3.S1 - Genera of organisms cultered from mummichog fish gut microbiomes

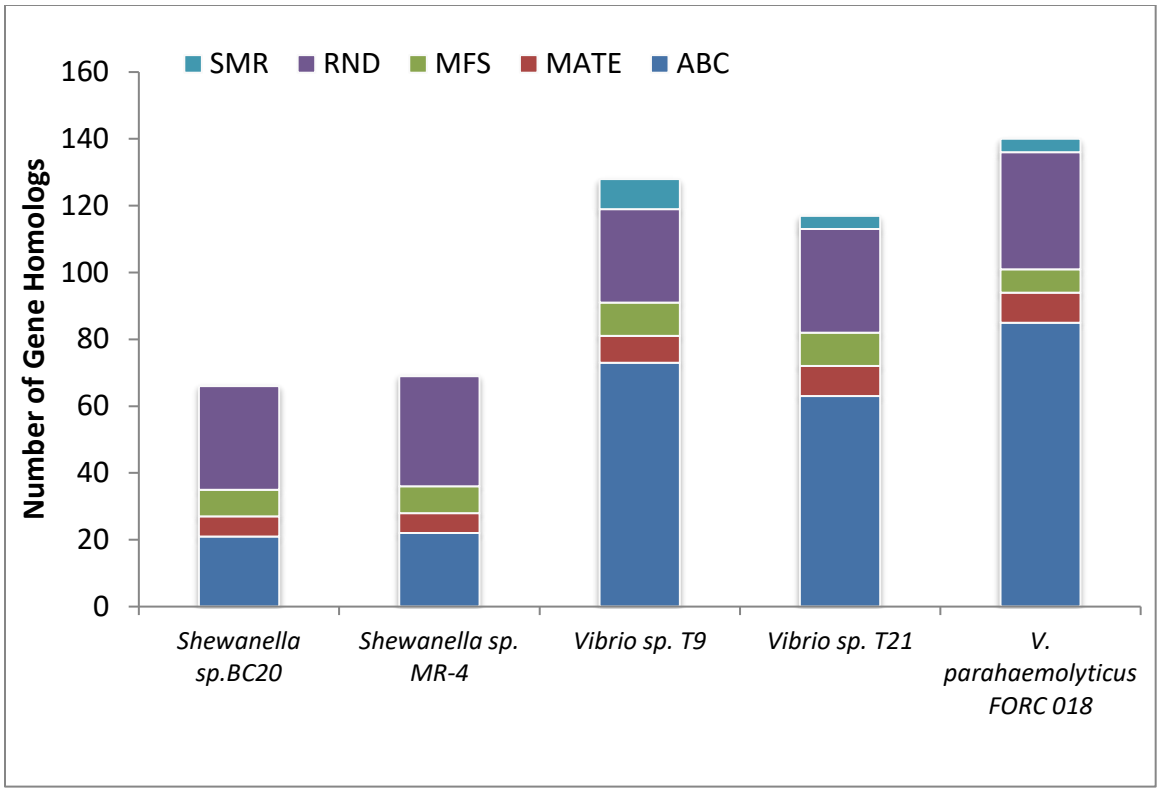

Figure 3.S2 - Distribution of abundance and type of efflux pump gene homologs in our 3 genomes and in 2 reference strains

Table 3.S1 – Results and interpretation of antimicrobial resistance testing for all drugs tested in both microdilution and disk diffusion assays

				T9		T21		BC20	
Target		**Class**	**Drug**	**MIC**		**MIC**		**MIC**	
Cell Wall	Betalactams	Carbapenems	Doripenem	≥ 24	S	≥ 24	S	≤ 21	R
			Imipenem	≥ 22	S	≥ 22	S	≤ 16	R
			Meropenem	≥ 22	S	≥ 22	S	≤ 16	R
			Meropenem	0	S	0	S	16	R
		Cephalosporins	Cefoxitin (2)	≥ 18	S	≥ 18	S	≥ 18	S
			Cefepime (4)	≥ 25	S	≥ 25	S	≥ 25	S
			Cefoperazone (3)	64	*	64	*	32	*
			Cefsulodin (3)	64	*	64	*	64	*
			Ceftazidime (3)	≥ 21	S	≥ 21	S	≥ 21	S
			Ceftazidime (3)	64	R	64	R	64	R
			Cefazolin (1)	0.5	S	4	S	64	R
			Cefradine (1)	8		64		2	
		Penicillins	Ampicillin		R		R		R
			Piperacillin	≤ 17	R	≤ 17	R	≤ 17	R
			Piperacillin – Tazobactam	≥ 20	S	≥ 20	S	≤ 17	R
			Ticarcillin	64	R	64	R	64	R
			Ticarcillin	≤ 23	R	≤ 23	R	≤ 23	R
			Penicillin	64	R	64	R	64	R
			Ticarcillin – Culvanic Acid	≤ 23	R	≤ 23	R	≤ 23	R
			Ticarcillin - Culvanic Acid	16	R	32	R	64	R
	Glycopeptides		Vancomycin	2	S	8	S	32	R
	Monobactams		Aztreonam	≥ 24	S	≥ 24	S	≥ 24	S
DNA Topoisomerase	Fluoroquinolones		Ciproflaxacin	≥ 22	S	≥ 22	S	≥ 22	S
			Pefloxacin	≥ 24	S	≥ 24	S	≥ 24	S
			Levofloxacin	≥ 22	S	≥ 22	S	≥ 22	S
			Ofloxacin	≥ 22	S	≤ 22	I	≥ 22	S
	Quinolones		Nalidixic Acid	0.5	S	1	S	2	S
Folic Acid Synthesis	Sulfonamides		Sulfamethoxazole	2	*	8	*	64	*
	DHFR / Sulfonamides		Trimethoprim-Sulfamethoxazole	≥ 16	S	≥ 16	S	≥ 16	S
Protein Synthesis	30S	Aminoglycosides	Amikacin	≥ 17	S	≤ 17	I	≥ 17	S
			Gentamicin	≥ 17	S	≥ 17	S	≥ 17	S
			Netilmicin	≥ 15	S	≥ 15	S	≥ 15	S
			Tobramicin	≤ 17	I	≤ 17	I	≥ 17	S
			Kanamycin	1	S	8	S	2	S
			Streptomycin	0.125	S	2	S	1	S
		Tetracyclines	Tetracycline	≥ 15	S	≥ 15	S	≥ 15	S
			Tetracycline	0	S	0.125	S	1	S
	50S	Phenicols	Chloramphenicol	≥ 17	S	≥ 17	S	≥ 17	S

Table 3.S8 - Arsenate resistance and metabolism genes located in *Shewanella* sp. BC20

	Query Sequence		*Shewanella* sp. BC20		
Gene	**Organism**	**Accession**	**E value**	**% Identity**	**Location**
arsC	*S. sp. ANA-3*	ABK4788.1	1.00E-82	*99*	CBX96_17955
arsR	*S. sp. ANA-3*	ABK46772.1	5.00E-80	98	CBX96_12160
ACR3	*S. oneidensis MR-1*	AAN53615.1	0	90	CBX96_12165
aioA	*V. alginolyticus*	ARP40250.1	2.00E-28	23	CBX96_09280
arrA	*S. sp. ANA-3*	AAQ01672.1	3.00E-50	25	CBX96_18635
arrB	*S. sp. ANA-3*	AAQ01673.1	2.00E-46	37	CBX96_15715
arrC	*Sulfurospirillum sp. SL2-1*	ARU48174.1	4.00E-12	36	CBX96_11135
arsP	*S. oneidensis MR-1*	AAN53584.1	2.00E-11	21	CBX96_11725

Table 3.S9 - Arsenate resistance and metabolism genes located in *Vibrio* spp. T9 and T21.

	Query Sequence		*Vibrio* sp. T9			*Vibrio* sp.T21		
Gene	**Organism**	**Accession**	**E value**	**% I***	**Location**	**E value**	**% I**	**Location**
arsC	*V. parahaemolyticus*	OYR36499.1	7.00E-80	96	CBX98_14680	1.00E-83	99	CCD93_13985
arsR	*S. sp. ANA-3*	ABK46772.1	9.00E-33	53	CBX98_22910	1.00E-33	54	CCD93_21850
ACR3	*V. alginolyticus 40B*	EEZ83533.1	0	94	CBX98_10060	0	95	CCD93_08740
aioA	*V. alginolyticus*	ARP40250.1	2.00E-29	23	CBX98_10110	5.00E-28	23	CCD93_08680
arrA	*S. sp. ANA-3*	AAQ01672.1	3.00E-22	24	CBX98_00560	6.00E-30	27	CCD93_10470
arrB	*S. sp. ANA-3*	AAQ01673.1	2.00E-41	36	CBX98_15490	2.00E-40	36	CCD93_13040
arrC	*Sulfurospirillum sp. SL2-1*	ARU48174.1	3.00E-16	26	CBX98_15055	2.00E-14	25	CCD93_13480

* %I = % identity

Table 3.S10 - Metal transporting p-type ATPase gene homologs in the 3 genomes

Gene Locus	**Type of ATPase**
***Vibrio* sp. T9**	
CBX98_00455	1B-1
CBX98_03340	1B-2
CBX98_18425	1B-1
***Vibrio* sp. T21**	
CCD93_01870	1B-2
CCD93_18010	1B-1
CCD93_10890	1B-1 (genomic island)
***Shewanella* sp. BC20**	
CBX96_05915	1B-1
CBX96_00355	1B-1

APPENDIX C

Supplementary Material for Chapter 4

Supplementary Results

Table 4.S1 – RND efflux pump gene loci in *V. antiquarius* EX25

Gene name in *V. parahaemolyticus*	locus_tag in *V. antiquarius* EX25	Gene name in *V. parahaemolyticus*	locus_tag in *V. antiquarius* EX25
vmeA	VEA_003895	*vmeP*	VEA_001385
vmeB	VEA_003894	*vmeQ*	VEA_001386
vmeC	VEA_001980	*vmeR*	VEA_001396
vmeD	VEA_001981	*vmeS*	VEA_001395
vmeE	VEA_004022	*vmeT*	VEA_000228
vmeF	VEA_004021	*vmeU*	VEA_000227
vmeG	VEA_003811	*vmeV*	VEA_000226
vmeH	VEA_003810	*vmeW*	VEA_000104
vmeI	VEA_003809	*vmeX*	VEA_000105
vmeJ	VEA_002593	*vmeY*	VEA_000504
vmeK	VEA_002594	*vmeZ*	VEA_000503
vmeL	VEA_000669	*vpoC*	VEA_004522
vmeM	VEA_000668		
vmeN	VEA_000654		
vpoM	VEA_000655		
vmeO	VEA_000656		

The table above shows the locations of the RND efflux pump genes identified in *V. antiquarius* EX25, the strain most closely-related to *V. antiquarius* T9. The table shows that the number and structure of RND efflux pumps between strains T9 and EX25 are comparable.

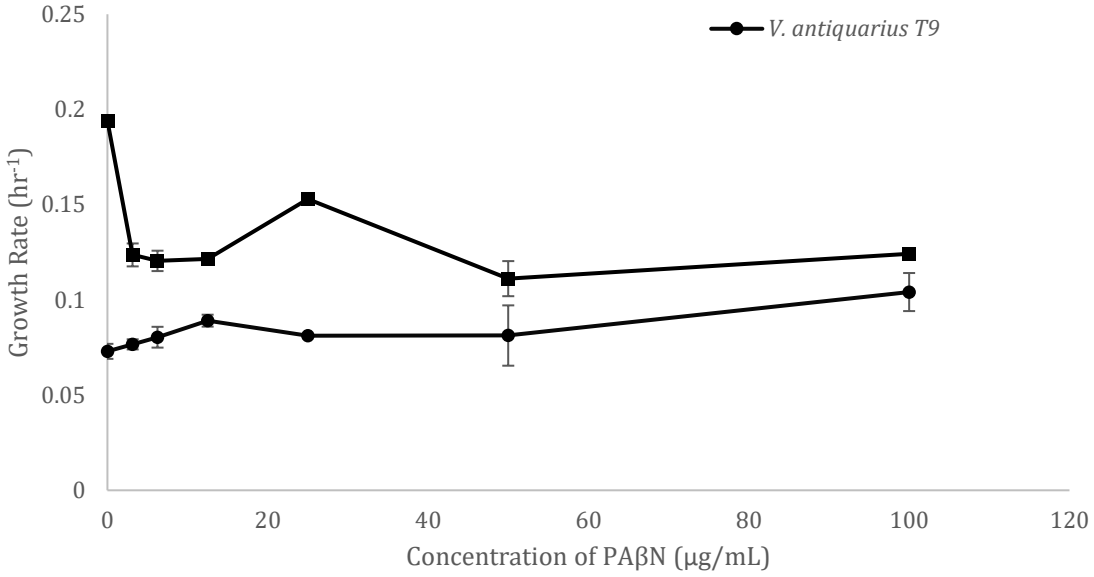

Figure 4.S1 – Growth rates of *Vibrio* spp. strains T9 and T21 in presence of PAβN (0-100 µg/mL). Each point represents average growth rates and standard deviations of 1 or more replicate wells.

APPENDIX D

Supplementary Material for Chapter 5

Supplementary Results

Table 5.S1 – Time points of *Shewanella* sp. BC20 selected for RNA extraction. This table shows the OD (at 600 nm) readings as well as time points for the duplicate samples taken of *Shewanella* growing under three different conditions.

	Positive Control BC20				BC20 + 12.5 mM Ars				BC20 + 12.5 mM Ars + 25 µg/mL PABN			
	Name		Time (h)	OD	Name		Time (h)	OD	Name		Time (h)	OD
T1	1A	1	3.5	0.35	2A	1	6.25	0.28	3A	1	8	0.34
					2A	2	6.25	0.28	3A	2	8	0.34
	1B	1	3.5	0.31	2B	1	6.25	0.37	3B	1	8	0.35
					2B	2	6.25	0.37	3B	2	8	0.35
	1C	1	3.5	0.29	2C	1	6.25	0.33	3C	1	8	0.33
					2C	2	6.25	0.33	3C	2	8	0.33
T2	1A	4	4.5	0.9	2A	4	7.25	0.74	3A	4	9.75	0.93
					2A	5	7.25	0.74	3A	5	9.75	0.93
	1B	4	4.5	0.92	2B	4	7.25	0.87	3B	4	9.75	0.89
					2B	5	7.25	0.87	3B	5	9.75	0.89
	1C	4	4.5	0.88	2C	4	7.25	0.82	3C	4	9.75	0.86
					2C	5	7.25	0.82	3C	5	9.75	0.86
T3					2A	7	8	1.09	3A	7	10.5	1.15
					2A	8	8	1.09	3A	8	10.5	1.15
					2B	7	8	1.14	3B	7	10.5	1.12
					2B	8	8	1.14	3B	8	10.5	1.12
					2C	7	8	1.07	3C	7	10.5	1.08
					2C	8	8	1.07	3C	8	10.5	1.08
T5	1A	13	24	5.6	2A	13	24	4.7	3A	13	24	3.8
					2A	14	24	4.7	3A	14	24	3.8
	1B	13	24	5.5	2B	13	24	4.7	3B	13	24	4.1
					2B	14	24	4.7	3B	14	24	4.1
	1C	13	24	5.5	2C	13	24	4.3	3C	13	24	3.9
					2C	14	24	4.3	3C	14	24	3.9

Figure 5.S1 – Effect of efflux pump inhibitors on growth rate in *Shewanella* sp. BC20. This graph shows the growth rate of Shewanella sp. BC20 grown with increasing concentrations of the efflux pump inhibitors CCCP and PAβN.

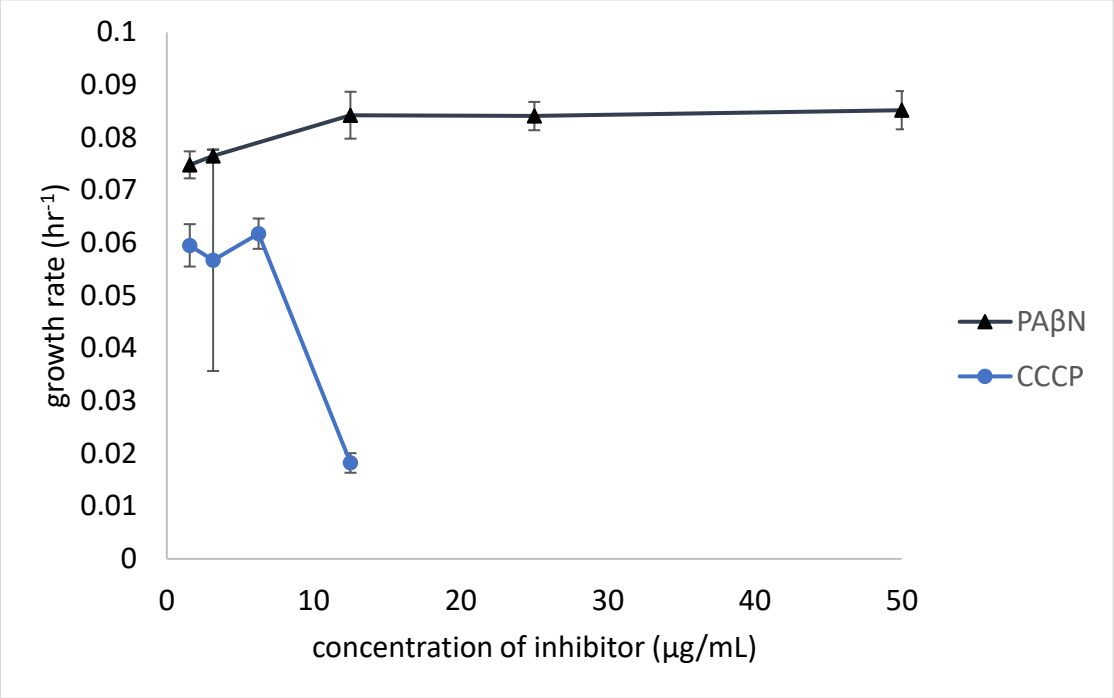

Appendix E

Supplementary Material Located in Supplementary Excel File

The supplementary Excel file containing these tables is available for download from the RUcore: Rutgers University Community Repository.

Table 3.S2 – Proteins involved in antibiotic resistance in *Shewanella* sp. BC20
Table 3.S3 – Proteins involved in antibiotic resistance in *Vibrio* sp. T21
Table 3.S4 – Proteins involved in antibiotic resistance in *Vibrio* sp. T9
Tables 3.S2-3.S4 show the blast results for the putative antibiotic resistance genes (and associated genes) for each of the three genomes identified using the ARGANNOT database.

Table 3.S5 – Proteins involved in efflux pumps in *Shewanella* sp. BC20
Table 3.S6 – Proteins involved in efflux pumps in *Vibrio* sp. T21
Table 3.S7 – Proteins involved in efflux pumps in *Vibrio* sp. T9
Tables 3.S5-3.S7 depict the putative efflux pump proteins and their location in the three genomes.

Table 3.S11 – Proteins involved in metal resistance in *Shewanella* sp. BC20
Table 3.S12 – Proteins involved in metal resistance in *Vibrio* sp. T21
Table 3.S13 – Proteins involved in metal resistance in *Vibrio* sp. T9

Tables 3S11-3S12 depict the blast results for the putative metal resistance proteins encoded in the three genomes identified using the experimentally-determined BacMet database.
Table 3.S14 – Predicted genomic islands located in *Shewanella* sp. BC20
Table 3.S15 – Predicted genomic islands located in *Vibrio* sp. T21
Table 3.S16 – Predicted genomic islands located in *Vibrio* sp. T9

Tables 3.S14-3.S16 show the predicted genomic islands in each of the three genomes identified using IslandViewer.

References

1. Centers for Disease Control, *Antibiotic resistance threats in the United States*. 2013.
2. Lushniak, B.D., *Antibiotic resistance: a public health crisis.* Public Health Reports, 2014. **129**: 1-3.
3. de Kraker, M.E.A., *et al.*, *Will 10 million people die a year due to antimicrobial resistance by 2050?* PLoS Medicine, 2016. **13**(11): e1002184.
4. Baker-Austin, C., *et al.*, *Co-selection of antibiotic and metal resistance.* Trends in Microbiology, 2006. **14**(4): 176-182.
5. Lu, Z., *et al.*, *Fate of sulfonamide resistance genes in estuary environment and effect of anthropogenic activities.* Science of the Total Environment, 2015. **527-528**: 429-438.
6. Allen, H.K., *et al.*, *Call of the wild: antibiotic resistance genes in natural environments.* Nature Reviews Microbiology, 2010. **8**: 251-259.
7. Selin, N.E., *Global biogeochemical cycling of mercury: a review.* Annual Review of Environment and Resources, 2009. **34**(1): 43-63.
8. Hobman, J.L., *et al.*, *Bacterial mercury resistance genes*, in *Metal Ions in Biological Systems*. 1997, Dekker Inc. p. 527-568.
9. Barkay, T., *Adaptation of aquatic microbial communities to Hg stress.* Applied and Environmental Microbiology, 1987. **53**(12): 2725-2732.
10. Barkay, T., *et al.*, *Bacterial mercury resistance from atoms to ecosystems.* FEMS Microbiology Reviews, 2003. **27**(2-3): 355-384.
11. Boyd, E.S., *et al.*, *The mercury resistance operon: from an origin in a geothermal environment to an efficient detoxification machine.* Frontiers in Microbiology, 2012. **3**(349).
12. Hardy, K., *Bacterial Plasmids*, in *Aspects of Microbiology*. 1981, American Society for Microbiology.
13. Summers, A.O., *Genetic linkage and horizontal gene transfer, the roots of the antibiotic multi-resistance problem.* Animal Biotechnology, 2006. **17**(2): 125-135.
14. Summers, A.O., *Generally overlooked fundamentals of bacterial genetics and ecology.* Clinical Infectious Diseases, 2002. **34 Suppl 3**: S85-92.
15. McIntosh, D., *et al.*, *Transferable, multiple antibiotic and mercury resistance in Atlantic Canadian isolates of Aeromonas salmonicida subsp. salmonicida is associated with carriage of an IncA/C plasmid similar to the Salmonella enterica plasmid pSN254.* Journal of Antimicrobial Chemotherapy, 2008. **61**(6): 1221-1228.
16. Pal, C., *et al.*, *Metal resistance and its association with antibiotic resistance.* Advances in Microbial Physiology, 2017. **70**: 261-313.
17. Pal, C., *et al.*, *Co-occurrence of resistance genes to antibiotics, biocides and metals reveals novel insights into their co-selection potential.* BMC Genomics, 2015. **16**(964): 1-14.
18. Blanco, P., *et al.*, *Bacterial multidrug efflux pumps: much more than antibiotic resistance determinants.* Microorganisms, 2016. **4**(1): 1-19.
19. Webber, M.A., *et al.*, *The importance of efflux pumps in bacterial antibiotic resistance.* Journal of Antimicrobial Chemotherapy, 2003. **51**(1): 9-11.

20. Anes, J., *et al., The ins and outs of RND efflux pumps in Escherichia coli.* Frontiers in Microbiology, 2015. **6**(7).
21. Hernando-Amado, S., *et al., Multidrug efflux pumps as main players in intrinsic and acquired resistance to antimicrobials.* Drug Resistance Updates, 2016. **28**: 13-27.
22. Martínez, J.L., *et al., Functional role of bacterial multidrug efflux pumps in microbial natural ecosystems.* FEMS Microbiology Reviews, 2013. **33**(2): 430-449.
23. Seiler, C., *et al., Heavy metal driven co-selection of antibiotic resistance in soil and water bodies impacted by agriculture and aquaculture.* Frontiers in Microbiology, 2012. **3**(399): 1-10.
24. Pathak, S., *et al., Occurrence of antibiotic and metal resistance in bacteria from organs of river fish.* Environmental Research, 2005. **98**(1): 100-103.
25. Meredith, M.M., *et al., Concomitant antibiotic and mercury resistance among gastrointestinal microflora of feral brook trout, Salvelinus fontinalis.* Current Microbiology, 2012. **65**(5): 575-582.
26. Akinbowale, O.L., *et al., Antibiotic and heavy metal resistance in motile aeromonads and pseudomonads from rainbow trout (Oncorhynchus mykiss) farms in Australia.* International Journal of Antimicrobial Agents, 2007. **30**(2): 177-182.
27. Wardwell, L.H., *et al., Co-selection of mercury and antibiotic resistance in sphagnum core samples dating back 2000 years.* Geomicrobiology Journal, 2009(26): 351-360.
28. Johnson, T.J., *et al., Expansion of the IncX plasmid family for improved identification and typing of novel plasmids in drug-resistant Enterobacteriaceae.* Plasmid, 2012. **68**(1): 43-50.
29. Henriques, I., *et al., Co-selection of antibiotic and metal(loid) resistance in gram-negative epiphytic bacteria from contaminated salt marshes.* Marine Pollution Bulletin, 2016. **109**(1): 427-434.
30. Teixeira, P., *et al., Antibiotic and metal resistance in a ST395 Pseudomonas aeruginosa environmental isolate: A genomics approach.* Marine Pollution Bulletin, 2016. **110**(1): 75-81.
31. Flach, C.-F., *et al., Does antifouling paint select for antibiotic resistance?* Science of the Total Environment, 2017. **590-591**: 461-468.
32. Givens, C.E., *et al., Comparison of the gut microbiomes of 12 bony fish and 3 shark species.* Marine Ecology Progress Series, 2015. **518**: 209-223.
33. Yousfi, K., *et al., A novel plasmid, pSx1, harboring a new Tn 1696 derivative from extensively drug-resistant Shewanella xiamenensis encoding OXA-416.* Microbial Drug Resistance, 2017. **23**(4): 429-436.
34. Thompson, F.L., *et al., Phylogeny and molecular identification of Vibrios on the basis of multilocus sequence analysis.* Applied and Environmental Microbiology, 2005. **71**(9): 5107-5115.
35. Cimmino, T., *et al., Whole genome sequence to decipher the resistome of Shewanella algae, a multidrug-resistant bacterium responsible for pneumonia, Marseille, France.* Expert Review of Anti-infective Therapy, 2016. **14**(2): 269-275.

36. Dang, H., *et al., Molecular characterizations of chloramphenicol- and oxytetracycline-resistant bacteria and resistance genes in mariculture waters of China.* Marine Pollution Bulletin, 2009. **58**(7): 987-994.
37. He, Y., *et al., Antibiotic and heavy-metal resistance of Vibrio parahaemolyticus isolated from fresh shrimps in Shanghai fish markets, China.* Environmental Science and Pollution Research, 2016. **23**(15): 15033-15040.
38. Heuer, H., *et al., IncP-1ε plasmids are important vectors of antibiotic resistance genes in agricultural systems: diversification driven by class 1 integron gene cassettes.* Frontiers in Microbiology, 2012. **3**: 2.
39. Gullberg, E., *et al., Selection of a multidrug resistance plasmid by sublethal levels of antibiotics and heavy metals.* mBio, 2014. **5**(5).
40. Hölzel, C.S., *et al., Heavy metals in liquid pig manure in light of bacterial antimicrobial resistance.* Environmental Research, 2012. **113**: 21-27.
41. Ji, X., *et al., Antibiotic resistance gene abundances associated with antibiotics and heavy metals in animal manures and agricultural soils adjacent to feedlots in Shanghai, China.* Journal of Hazardous Materials, 2012. **235-236**: 178-185.
42. Tuckfield, R.C., *et al., Spatial analysis of antibiotic resistance along metal contaminated streams.* Microbial Ecology, 2007. **55**(4): 595-607.
43. Skurnik, D., *et al., Is exposure to mercury a driving force for the carriage of antibiotic resistance genes?* Journal of Medical Microbiology, 2010. **59**(7): 804-807.
44. Ready, D., *et al., Oral bacteria resistant to mercury and to antibiotics are present in children with no previous exposure to amalgam restorative materials.* FEMS Microbiology Letters, 2003. **223**(1): 107-111.
45. Summers, A.O., *et al., Mercury released from dental "silver" fillings provokes an increase in mercury-and antibiotic-resistant bacteria in oral and intestinal floras of primates.* Antimicrobial Agents and Chemotherapy, 1993. **37**(4): 825-834.
46. Wireman, J., *et al., Association of mercury resistance with antibiotic resistance in the gram-negative fecal bacteria of primates.* Applied and Environmental Microbiology, 1997. **63**(11): 4494-4503.
47. Liebert, C.A., *et al., Transposon Tn21, flagship of the floating genome.* Microbiology and Molecular Biology Reviews, 1999. **63**(3): 507-522.
48. Bass, L., *et al., Incidence and characterization of integrons, genetic elements mediating multiple-drug resistance, in avian Escherichia coli.* Antimicrobial Agents and Chemotherapy, 1999. **43**(12): 2925-2929.
49. Ball, M.M., *et al., Mercury resistance in bacterial strains isolated from tailing ponds in a gold mining area near El Callao (Bolívar State, Venezuela).* Current Microbiology, 2007. **54**(2): 149-154.
50. Hill, K.E., *et al., Isolation and screening of plasmids from the epilithon which mobilize recombinant plasmid pD10.* Applied and Environmental Microbiology, 1992. **58**(4): 1292-1300.
51. Smit, E., *et al., Self-transmissible mercury resistance plasmids with gene-mobilizing capacity in soil bacterial populations: influence of wheat roots and mercury addition.* Applied and Environmental Microbiology, 1998. **64**(4): 1210-1219.

52. Chen, C.Y., *et al.*, *Benthic and pelagic pathways of methylmercury bioaccumulation in estuarine food webs of the northeast United States.* PLoS ONE, 2014. **9**(2).
53. Kwon, S.Y., *et al.*, *Absence of fractionation of mercury isotopes during trophic transfer of methylmercury to freshwater fish in captivity.* Environmental Science and Technology, 2012. **46**(14): 7527-7534.
54. Cardona-Marek, T., *et al.*, *Mercury speciation, reactivity, and bioavailability in a highly contaminated estuary, Berry's Creek, New Jersey Meadowlands.* Environmental Science and Technology, 2007. **41**(24): 8268-8274.
55. Cardona-Marek, T., *Mercury cycling in Berry's Creek (Hackensack Meadowlands) and the Delaware River Estuary*. 2005, Rutgers University.
56. Hepher, B., *Nutrition of pond fishes*. 1988: Cambridge University Press.
57. Wright, V.A., *et al.*, *Berry's Creek: a glance backward and a look forward.* International Journal of Soil, Sediment and Water, 2010. **3**: 1-10.
58. Weis, P., *et al.*, *Effects of environmental factors on release of mercury from Berry's Creek (New Jersey) sediments and its uptake by killifish (Fundulus heteroclitus).* Environmental Pollution Series A, Ecological and Biological, 1986. **40**(4): 303-315.
59. American Veterinary Medical Association, *AVMA Guidelines for the euthanasia of animals (2013 Edition)*. 2013.
60. US Environmental Protection Agency, *Method 1631 Revision E*. 2002. p. 1-46.
61. Liang, L., *et al.*, *Simultaneous determination of mercury speciation in biological materials by GC/CVAFS after ethylation and room-temperature precollection.* Clinical Chemistry, 1994. **40**(4): 602-607.
62. Kummerer, K., *Resistance in the environment.* Journal of Antimicrobial Chemotherapy, 2004. **54**(2): 311-320.
63. Ovchinnikov, Y.A., *et al.*, *RNA polymerase rifampicin resistance mutations in Escherichia coli: sequence changes and dominance.* Molecular Genetics and Genomics, 1983. **190**(2): 344-348.
64. Stepanauskas, R., *et al.*, *Elevated microbial tolerance to metals and antibiotics in metal-contaminated industrial environments.* Environmental Science and Technology, 2005. **39**(10): 3671-3678.
65. Wright, M.S., *et al.*, *Bacterial tolerances to metals and antibiotics in metal-contaminated and reference streams.* FEMS Microbiology Ecology, 2006. **58**(2): 293-302.
66. Hurt, R.A., *et al.*, *Simultaneous recovery of RNA and DNA from soils and sediments.* Applied and Environmental Microbiology, 2001. **67**(10): 4495-4503.
67. Poulain, A.J., *et al.*, *Microbial DNA records historical delivery of anthropogenic mercury.* The ISME Journal, 2015. **9**: 2541-2550.
68. Weis, J.S., *et al.*, *Living in a contaminated estuary: behavioral changes and ecological consequences for five species.* BioScience, 2011. **61**(5): 375-385.
69. Hugenholtz, P., *Exploring prokaryotic diversity in the genomic era.* Genome Biology, 2002. **3**(2).
70. Barkay, T., *et al.*, *The relationships of Hg(II) volatilization from a freshwater pond to the abundance of mer genes in the gene pool of the indigenous microbial community.* Microbial Ecology, 1991. **21**: 151-161.

71. Goto, D., *et al., Altered feeding habits and strategies of a benthic forage fish (Fundulus heteroclitus) in chronically polluted tidal salt marshes.* Marine Environmental Research, 2011. **72**(1): 75-88.
72. Ellis, R.H., *et al., A comprehensive monitoring and assessment program for selected heavy metals in New Jersey aquatic fauna.* 1980.
73. Wang, W.X., *Biodynamic understanding of mercury accumulation in marine and freshwater fish.* Advances in Environmental Research, 2012. **1**(1): 15-35.
74. Dutton, J., *et al. Bioaccumulation of As, Cd, Cr, Hg(II), and MeHg in killifish (Fundulus heteroclitus) from amphipod and worm prey*. Science of the Total Environment, 2011. **409**, 3438-3447.
75. Rudd, J.W., *et al., Mercury methylation by fish intestinal contents.* Applied and Environmental Microbiology, 1980. **40**(4): 777-782.
76. Müller, A.K., *et al., Adaptation of the bacterial community to mercury contamination.* FEMS Microbiology Letters, 2001. **204**(1): 49-53.
77. Rasmussen, L.D., *et al., Effects of mercury contamination on the culturable heterotrophic, functional and genetic diversity of the bacterial community in soil.* FEMS Microbiology Ecology, 2001. **36**(1): 1-9.
78. Nazaret, S., *et al., merA gene expression in aquatic environments measured by mRNA production and Hg (II) volatilization.* Applied and Environmental Microbiology, 1994. **60**(11): 4059-4065.
79. Schaefer, J.K., *et al., Role of the bacterial organomercury lyase (MerB) in controlling methylmercury accumulation in mercury-contaminated natural waters.* Environmental Science and Technology, 2004. **38**(16): 4304-4311.
80. Whitman, W.B., *et al., Prokaryotes: The unseen majority.* Proceedings of the National Academy of Sciences of the United States of America, 1998. **95**(12): 6578-6583.
81. Barkay, T., *et al., A thermophilic bacterial origin and subsequent constraints by redox, light and salinity on the evolution of the microbial mercuric reductase.* Environmental Microbiology, 2010. **12**(11): 2904-2917.
82. Kiviat, E., *et al., Hackensack Meadowlands, New Jersey, Biodiversity: a review and synthesis*. 2002.
83. Murphy, E.A., *et al., Mercury species in potable ground water in southern New Jersey*. Water Air and Soil Pollution, 1994. **78**(1): 61-72.
84. Shin, J.Y., *et al., Assessment of anthropogenic influences on surface water quality in urban estuary, northern New Jersey: multivariate approach.* Environmental Monitoring and Assessment, 2012. **185**(3): 2777-2794.
85. Ventola, C.L., *The antibiotic resistance crisis: part 1: causes and threats.* Pharmacy and Therapeutics, 2015. **40**(4): 277-83.
86. Pal, C., *et al., The structure and diversity of human, animal and environmental resistomes.* Microbiome, 2016. **4**(1): 54.
87. D'Costa, V.M., *et al., Sampling the antibiotic resistome.* Science, 2006. **311**(5759): 374-377.
88. Kang, C.-H., *et al., Antibiotic and heavy metal resistance in Shewanella putrefaciens strains isolated from shellfishes collected from West Sea, Korea.* Marine Pollution Bulletin, 2016. **112**(1-2): 111-116.

89. Culliton, T.J., *Population: Distribution, density and growth* 1998, National Oceanic and Atmospheric Administration. p. 1-33.
90. Zhu, Y.-G., *et al.*, *Continental-scale pollution of estuaries with antibiotic resistance genes.* Nature Microbiology, 2017. **2**(16270): 1-7.
91. Lima-Bittencourt, C.I., *et al.*, *Multiple antimicrobial resistance in Enterobacteriaceae isolates from pristine freshwater.* Genetics and Molecular Research, 2007. **6**(3): 510-521.
92. Lloyd, N.A., *et al.*, *Co-selection of mercury and multiple antibiotic resistances in bacteria exposed to mercury in the Fundulus heteroclitus gut microbiome.* Current Microbiology, 2016. **73**(6): 834-842.
93. Janda, J., *Shewanella: a marine pathogen as an emerging cause of human disease.* Clinical Microbiology Newsletter, 2014. **36**(4): 25-29.
94. Yousfi, K., *et al.*, *Current trends of human infections and antibiotic resistance of the genus Shewanella.* European Journal of Clinical Microbiology and Infectious Disease, 2017. **36**(8): 1353-1362.
95. Lane, D.J., *16S/23S rRNA sequencing.* Nucleic Acids Techniques in Bacterial Systematics, 1991: 115-147.
96. Madden, T., *Chapter 16: The BLAST Sequence Analysis Tool*, in *The NCBI Handbook*. 2002, National Center for Biotechnology Information. p. 1-15.
97. Soussy, C.J., *et al.*, *Antibiotic Resistance Committee Recommendations 2013*. 2013, French Society of Microbiology. p. 1-62.
98. Clincal Laboratory Standards Institute, *Methods for Dilution Antimicrobial Susceptibility Tests for Bacteria That Grow Aerobically; Approved Standard—Ninth Edition*. 2012.
99. Bier, N., *et al.*, *Survey on antimicrobial resistance patterns in Vibrio vulnificus and Vibrio cholerae non-O1/non-O139 in Germany reveals carbapenemase-producing Vibrio cholerae in coastal waters.* Frontiers in Microbiology, 2015. **6**(1179): 1-11.
100. Kahm, M., *et al.*, *Grofit: Fitting biological growth curves with R.* Journal of Statistical Software, 2010. **33**(7): 1-21.
101. Bankevich, A., *et al.*, *SPAdes: A new genome assembly algorithm and its applications to single-cell sequencing.* Journal of Computational Biology, 2012. **19**(5): 455-477.
102. Tatusova, T., *et al.*, *NCBI prokaryotic genome annotation pipeline.* Nucleic Acids Research, 2016. **44**(14): 6614-6624.
103. Yoon, S.-H., *et al.*, *Introducing EzBioCloud: a taxonomically united database of 16S rRNA gene sequences and whole-genome assemblies.* International Journal of Systematic and Evolutionary Microbiology, 2017. **67**(5): 1613-1617.
104. Kearse, M., *et al.*, *Geneious Basic: An integrated and extendable desktop software platform for the organization and analysis of sequence data.* Bioinformatics, 2012. **28**(12): 1647-1649.
105. Bertelli, C., *et al.*, *IslandViewer 4: expanded prediction of genomic islands for larger-scale datasets.* Nucleic Acids Research, 2017. **45**(W1): W30-W35.
106. Gupta, S.K., *et al.*, *ARG-ANNOT, a new bioinformatic tool to discover antibiotic resistance genes in bacterial genomes.* Antimicrobial Agents and Chemotherapy, 2013. **58**(1): 212-220.

107. Pal, C., *et al., BacMet: antibacterial biocide and metal resistance genes database.* Nucleic Acids Research, 2013. **42**(D1): D737-D743.
108. Smith, A.T., *et al., Diversity of the metal-transporting P1B-type ATPases.* Journal of Biological Inorganic Chemistry, 2014. **19**(6): 947-960.
109. Bairoch, A., *et al., The universal protein resource (UniProt).* Nucleic Acids Research, 2007. **35**: D193-D197.
110. Nealson, K.H., *et al., Isolation and identification of manganese-reducing bacteria and estimates of microbial Mn(IV)-reducing potential in the Black Sea.* Deep Sea Research, 1991. **38**: S907-S920.
111. Hasan, N.A., *et al., Deep-sea hydrothermal vent bacteria related to human pathogenic Vibrio species.* Proceedings of the National Academy of Sciences of the United States of America, 2015. **112**(21): E2813-E2819.
112. Lehtopolku, M., *et al., Inaccuracy of the disk diffusion method compared with the agar dilution method for susceptibility testing of Campylobacter spp.* Journal of Clinical Microbiology, 2011. **50**(1): 52-56.
113. Chiou, J., *et al., CARB-17 family of β-lactamases mediates intrinsic resistance to penicillins in Vibrio parahaemolyticus.* Antimicrobial Agents and Chemotherapy, 2015. **59**(6): 3593-3595.
114. Palzkill, T., *Metallo-beta-lactamase structure and function.* Annals of the New York Academy of Sciences, 2013. **1277**: 91-104.
115. Bush, K., *et al., Updated functional classification of β-Lactamases.* Antimicrobial Agents and Chemotherapy, 2010. **54**(3): 969-976.
116. Nonaka, L., *et al., New Mg2+-dependent oxytetracycline resistance determinant tet 34 in Vibrio isolates from marine fish intestinal contents.* Antimicrobial Agents and Chemotherapy, 2002. **46**(5): 1550-1552.
117. Teo, J.W., *et al., Genetic determinants of tetracycline resistance in Vibrio harveyi.* Antimicrobial Agents and Chemotherapy, 2002. **46**(4): 1038-1045.
118. Hooper, D.C., *et al., Mechanisms of drug resistance: quinolone resistance.* Annals of the New York Academy of Sciences, 2015. **1354**(1): 12-31.
119. Liao, V.H.-C., *et al., Arsenite-oxidizing and arsenate-reducing bacteria associated with arsenic-rich groundwater in Taiwan.* Journal of Contaminant Hydrology, 2011: 1-10.
120. Marti, E., *et al., The role of aquatic ecosystems as reservoirs of antibiotic resistance.* Trends in Microbiology, 2014. **22**(1): 36-41.
121. Guo, J., *et al., Metagenomic analysis reveals wastewater treatment plants as hotspots of antibiotic resistance genes and mobile genetic elements.* Water Research, 2017. **123**: 468-478.
122. Berendonk, T.U., *et al., Tackling antibiotic resistance: the environmental framework.* Nature Reviews Microbiology, 2015. **13**(5): 310-317.
123. Perry, J.A., *et al., The antibiotic resistance "mobilome": searching for the link between environment and clinic.* Frontiers in Microbiology, 2013. **138**: 1-7.
124. Versluis, D., *et al., Mining microbial metatranscriptomes for expression of antibiotic resistance genes under natural conditions.* Scientific Reports, 2015: 1-10.
125. Hawkey, P.M., *Multidrug-resistant Gram-negative bacteria: a product of globalization.* Journal of Hospital Infection, 2015. **89**(4): 241-247.

126. Tacao, M., *et al.*, *Shewanella species as the origin of blaOXA-48 genes: insights into gene diversity, associated phenotypes and possible transfer mechanisms.* International Journal of Antimicrobial Agents, 2018. **51**(3): 340-348.
127. Poirel, L., *et al.*, *Chromosome-encoded Ambler class D beta-lactamase of Shewanella oneidensis as a progenitor of carbapenem-hydrolyzing oxacillinase.* Antimicrobial Agents and Chemotherapy, 2003. **48**(1): 348-351.
128. Almuzara, M., *et al.*, *Genetic analysis of a Per-2 Producing Shewanella spp. strain harboring a variety of mobile genetic elements and antibiotic resistant determinants.* . Journal of Global Antimicrobial Resistance, 2017. **11**: 81-86.
129. Singh, P., *et al.*, *Prevalence of gyrA and B gene mutations in fluoroquinolone-resistant and -sensitive clinical isolates of Mycobacterium tuberculosis and their relationship with MIC of ofloxacin.* The Journal of Antibiotics, 2015. **68**(1): 63-66.
130. Chenia, H.Y., *Prevalence and characterization of plasmid-mediated quinolone resistance genes in Aeromonas spp. isolated from South African freshwater fish.* International Journal of Food Microbiology, 2016. **231**: 26-32.
131. Wong, K.C., *et al.*, *Antibiotic use for Vibrio infections: important insights from surveillance data.* BMC Infectious Diseases, 2015. **15**(226): 1-9.
132. Rasheed, J., *et al.*, *New Delhi Metallo-β-Lactamase–producing Enterobacteriaceae, United States.* Emerging Infectious Diseases, 2013. **19**(6): 870-878.
133. Gudeta, D.D., *et al.*, *The soil microbiota harbors a diversity of carbapenem-hydrolyzing beta-lactamases of potential clinical relevance.* Antimicrobial Agents and Chemotherapy, 2016. **60**(1): 151-60.
134. Potron, A., *et al.*, *Occurrence of the carbapenem-hydrolyzing β-lactamase gene blaOXA-48 in the environment in Morocco.* Antimicrobial Agents and Chemotherapy, 2011. **55**(11): 5413-5414.
135. Clowes, R.C., *Molecular structure of bacterial plasmids.* Bacteriological Reviews, 1972. **36**(3): 361-405.
136. Sorensen, S., *et al.*, *Studying plasmid horizontal transfer in situ: a critical review.* Nature Reviews Microbiology, 2005. **3**(9): 700-710.
137. Forsberg, K.J., *et al.*, *Bacterial phylogeny structures soil resistomes across habitats.* Nature, 2014. **509**(7502): 612-616.
138. Lo, S.W., *et al.*, *Breaking the code of antibiotic resistance.* Nature Reviews Microbiology, 2018. **16**(5): 262-262.
139. Allen, H.K., *et al.*, *Call of the wild: antibiotic resistance genes in natural environments.* Nature Reviews Microbiology, 2010. **8**(4): 251-259.
140. Allen, S.E., *et al.*, *Antimicrobial resistance in generic Escherichia coli isolates from wild small mammals living in swine farm, residential, landfill, and natural environments in southern Ontario, Canada.* Applied and Environmental Microbiology, 2011. **77**(3): 882-888.
141. Heuer, O.E., *et al.*, *Human health consequences of use of antimicrobial agents in aquaculture.* Clincal Infectious Diseases, 2009. **49**(8): 1248-1253.
142. Cabello, F.C., *Heavy use of prophylactic antibiotics in aquaculture: a growing problem for human and animal health and for the environment.* Environmental Microbiology, 2006. **8**(7): 1137-1144.

143. Letchumanan, V., *et al.*, *Prevalence and antimicrobial susceptibility of Vibrio parahaemolyticus isolated from retail shrimps in Malaysia.* Frontiers in Microbiology, 2015. **6**(33): 1-11.
144. Cabello, F.C., *et al.*, *Antimicrobial use in aquaculture re-examined: its relevance to antimicrobial resistance and to animal and human health.* Environmental Microbiology, 2013. **15**(7): 1917-1942.
145. Zeng, Q., *et al.*, *Genetic adaptation of microbial populations present in high-intensity catfish production systems with therapeutic oxytetracycline treatment.* Scientific Reports, 2017. **7**: 1-13.
146. Elmahdi, S., *et al.*, *Antibiotic resistance of Vibrio parahaemolyticus and Vibrio vulnificus in various countries: A review.* Food Microbiology, 2016. **57**: 128-134.
147. Centers for Disease Control. *Increase in Vibrio parahaemolyticus illnesses associated with consumption of shellfish from several Atlantic coast harvest areas, United States, 2013*. 2017; Available from: https://www.cdc.gov/vibrio/investigations/vibriop-09-13/index.html.
148. Shaw, K.S., *et al.*, *Antimicrobial susceptibility of Vibrio vulnificus and Vibrio parahaemolyticus recovered from recreational and commercial areas of Chesapeake Bay and Maryland coastal bays.* PLoS ONE, 2014. **9**(2): e89616.
149. Letchumanan, V., *et al.*, *Vibrio parahaemolyticus: a review on the pathogenesis, prevalence, and advance molecular identification techniques.* Frontiers in Microbiology, 2014. **5**: 705.
150. Letchumanan, V., *et al.*, *Occurrence and antibiotic resistance of Vibrio parahaemolyticus from shellfish in Selangor, Malaysia.* Frontiers in Microbiology, 2015. **6**(1417).
151. Kalman, D., *et al.*, *Review of the pharmacology, pharmacokinetics, and clincal use of cephalosporins.* Texas Heart Institute Journal, 1990. **17**(3): 203-215.
152. Li, X.Z., *et al.*, *The challenge of efflux-mediated antibiotic resistance in gram-negative bacteria.* Clinical Microbiology Reviews, 2015. **28**(2): 337-418.
153. Obaidat, M.M., *et al.*, *Virulence and antibiotic resistance of Vibrio parahaemolyticus isolates from seafood from three developing countries and of worldwide environmental, seafood, and clinical isolates from 2000 to 2017.* Journal of Food Protection, 2017. **80**(12): 2060-2067.
154. Park, S.H., *Third-generation cephalosporin resistance in gram-negative bacteria in the community: a growing public health concern.* The Korean Journal of Internal Medicine, 2014. **29**(1): 27-30.
155. Centers for Disease Control. *Management of Vibrio vulnificus wound infections after a disaster*. 2017; Available from: https://www.cdc.gov/disasters/disease/vibriofaq.html.
156. Palzkill, T., *Metallo-β-lactamase structure and function.* Annals of the New York Academy of Sciences, 2012. **1277**(1): 91-104.
157. Poole, K., *Bacterial stress responses as determinants of antimicrobial resistance.* Journal of Antimicrobial Chemotherapy, 2012. **67**(9): 2069.
158. Venter, H., *et al.*, *RND-type drug eux pumps from Gram-negative bacteria: molecular mechanism and inhibition.* Frontiers in Microbiology, 2015. **28**(6): 377.

159. Bina, J.E., *et al., Characterization of the Vibrio cholerae vexAB and vexCD efflux systems.* Archives of Microbiology, 2006. **186**(3): 171-181.
160. Anes, J., *et al., The ins and outs of RND efflux pumps in Escherichia coli.* Frontiers in Microbiology, 2015. **6**(587).
161. Matsuo, T., *et al., Characterization of all RND-type multidrug efflux transporters in Vibrio parahaemolyticus.* Microbiologyopen, 2013. **2**(5): 725-742.
162. Lee, S., *et al., Functional analysis of Vibrio vulnificus RND efflux pumps homologous to Vibrio cholerae VexAB and VexCD, and to Escherichia coli AcrAB.* Journal of Microbiology, 2015. **53**(4): 256-261.
163. Pascual, J., *et al., Multilocus sequence analysis of the central clade of the genus Vibrio by using the 16S rRNA, recA, pyrH, rpoD, gyrB, rctB and toxR genes.* International Journal of Systematic and Evolutionary Microbiology, 2010. **60**(1): 154-165.
164. CLSI, *M07-A9: Methods for Dilution Antimicrobial Susceptibility Tests for Bacteria That Grow Aerobically; Approved Standard—Ninth Edition*. 2012. p. 1-88.
165. Bina, X.R., *et al., Effect of the efflux inhibitors 1-(1-naphthylmethyl)-piperazine and phenyl-arginine-β-naphthylamide on antimicrobial susceptibility and virulence factor production in Vibrio cholerae.* Journal of Antimicrobial Chemotherapy, 2008. **63**(1): 103-108.
166. Cosentino, S., *et al., PathogenFinder - Distinguishing friend from foe using bacterial whole genome sequence data.* PLoS ONE, 2013. **8**(10): e77302.
167. Froquet, R., *et al., Dictyostelium discoideum: a model host to measure bacterial virulence.* Nature Protocols, 2008. **4**: 25.
168. Lima, W.C., *et al., Genome sequencing and functional characterization of the non-pathogenic Klebsiella pneumoniae KpGe bacteria.* Microbes and Infection, 2018. **20**(5): 293-301.
169. Adamek, M., *et al., Genotyping of environmental and clinical Stenotrophomonas maltophilia isolates and their pathogenic potential.* PLoS ONE, 2011. **6**(11): e27615.
170. Steinum, T.M., *et al., Multilocus sequence analysis of close relatives Vibrio anguillarum and Vibrio ordalii.* Applied and Environmental Microbiology, 2016. **82**(18): 5496-504.
171. Arnold, C.J., *et al., Cefepime and ceftazidime safety in hospitalized infants.* The Pediatric Infectious Disease Journal, 2015. **34**(9): 964-968.
172. Nagano, K., *et al., Kinetic behavior of the major multidrug efflux pump AcrB of Escherichia coli.* Proceedings of the National Academy of Sciences of the United States of America, 2009. **106**(14): 5854-5858.
173. Kinana, A.D., *et al., Some ligands enhance the efflux of other ligands by the Escherichia coli multidrug pump AcrB.* Biochemistry, 2013. **52**(46): 8342-8351.
174. Taylor, D.L., *et al., Vibrio cholerae vexH Encodes a multiple drug efflux pump that contributes to the production of cholera toxin and the toxin co-regulated pilus.* PLoS ONE, 2012. **7**(5): e38208.
175. Matsuo, T., *et al., VmeAB, an RND-type multidrug efflux transporter in Vibrio parahaemolyticus.* Microbiology, 2007. **153**(12): 4129-4137.

176. Bina, X.R., *et al., Vibrio cholerae RND family efflux systems are required for antimicrobial resistance, optimal virulence factor production, and colonization of the infant mouse small intestine.* Infection and Immunity, 2008. **76**(8): 3595-3605.
177. Rahman, M.M., *et al., Molecular cloning and characterization of all RND-Type efflux transporters in Vibrio cholerae Non-O1.* Microbiology and Immunology, 2007. **51**(11): 1061-1070.
178. Hay, A.J., *et al., In sickness and in health: the relationships between bacteria and bile in the human gut.* Advances in Applications of Microbiolgy, 2016. **96**: 43-64.
179. Piddock, L.J., *Multidrug-resistance efflux pumps - not just for resistance.* Nature Reviews Microbiology, 2006. **4**(8): 629-36.
180. Gotoh, K., *et al., Bile acid-induced virulence gene expression of Vibrio parahaemolyticus reveals a novel therapeutic potential for bile acid sequestrants.* PLoS One, 2010. **5**(10): e13365.
181. Cerda-Maira, F.A., *et al., The bile response repressor BreR regulates expression of the Vibrio cholerae breAB efflux system operon.* Journal of Bacteriology, 2008. **190**(22): 7441-52.
182. Honkanen, R.E., *et al., Bile salt absorption in killifish intestine.* American Journal of Physiology-Gastrointestinal and Liver Physiology, 1987. **253**(6): G730-G736.
183. Routman, A., *et al., Cefsulodin treatment for serious Pseudomonas aeruginosa infections.* Journal of International Medical Research, 1986. **14**(5): 242-253.
184. CLSI, *M45-P - Methods for Antimicrobial Dilution and Disk Susceptibility Testing of Infrequently Isolated or Fastidious Bacteria; Proposed Guideline*. 2014. p. 1-68.
185. Vera-Leiva, A., *et al., The efflux pump inhibitor phenylalanine-arginine beta-naphthylamide (PAβN) increases resistance to carbapenems in Chilean clinical isolates of KPC-producing Klebsiella pneumoniae.* Journal of Global Antimicrobial Resistance, 2018. **12**: 73-76.
186. Saw, H.T.H., *et al., Inactivation or inhibition of AcrAB-TolC increases resistance of carbapenemase-producing Enterobacteriaceae to carbapenems.* Journal of Antimicrobial Chemotherapy, 2016. **71**(6): 1510-1519.
187. Morita, Y., *et al., MexXY multidrug efflux system of Pseudomonas aeruginosa.* Frontiers in Microbiology, 2012. **3**(408).
188. Bennish, M.L., *et al., Antimicrobial Resistance in Vibrio*, in *Antimicrobial Drug Resistance*, D.L. Mayers, Editor. 2017, Springer International Publishing.
189. Malasarn, D., *et al., Characterization of the arsenate respiratory reductase from Shewanella sp. strain ANA-3.* Journal of Bacteriology, 2007. **190**(1): 135-142.
190. Srinivasan, V.B., *et al., Role of AbeS, a novel efflux pump of the SMR family of transporters, in resistance to antimicrobial agents in Acinetobacter baumannii.* Antimicrobial Agents and Chemotherapy, 2009. **53**(12): 5312-5316.
191. Perron, K., *et al., CzcR-CzcS, a two-component system involved in heavy metal and carbapenem resistance in Pseudomonas aeruginosa.* Journal of Biological Chemistry, 2004. **279**(10): 8761-8768.
192. Cai, L., *et al., Genes involved in arsenic transformation and resistance associated with different levels of arsenic-contaminated soils.* BMC Microbiology, 2009. **8**(9): 4.

193. Andres, J., *et al.*, *The microbial genomics of arsenic.* FEMS Microbiology Reviews, 2016. **40**(2): 299-322.
194. Wang, L., *et al.*, *Identification of an arsenic resistance and arsenic-sensing system in Campylobacter jejuni.* Applied and Environmental Microbiology, 2009. **75**(15): 5064-5073.
195. Yin, J., *et al.*, *Stress Responses of Shewanella.* International Journal of Microbiology, 2011. **2011**: 863623.
196. McArthur, A.G., *et al.*, *The comprehensive antibiotic resistance database.* Antimicrobial Agents and Chemotherapy, 2013. **57**(7): 3348-3357.
197. Ardebili, A., *et al.*, *Effect of efflux pump inhibitor carbonyl cyanide 3-chlorophenylhydrazone on the minimum inhibitory concentration of ciprofloxacin in Acinetobacter baumannii clinical isolates.* Jundishapur Journal of Microbiology, 2014. **7**(1): e8691.
198. Lamers, R.P., *et al.*, *The efflux inhibitor phenylalanine-arginine beta-naphthylamide (PAβN) permeabilizes the outer membrane of gram-negative bacteria.* PLoS ONE, 2013. **8**(3): e60666.
199. Saltikov, C.W., *et al.*, *The ars detoxification system is advantageous but not required for As(V) respiration by the genetically tractable Shewanella species strain ANA-3.* Applied and Environmental Microbiology, 2003. **69**(5): 2800-2809.
200. Saffarini, D., *et al.*, *Shewanella oneidensis and extracellular electron transfer to metal oxides*, in *Bacteria-Metal Interactions*, D. Saffarini, Editor. 2015, Springer.
201. Youenou, B., *et al.*, *Comparative genomics of environmental and clinical Stenotrophomonas maltophilia strains with different antibiotic resistance profiles.* Genome Biology and Evolution, 2015. **7**(9): 2484-2505.
202. Kim, H.S., *et al.*, *Multidrug efflux pump MdtBC of Escherichia coli is active only as a B2C heterotrimer.* Journal of Bacteriology, 2010. **192**(5): 1377-1386.
203. Qiu, X., *et al.*, *Comparative analysis of differentially expressed genes in Shewanella oneidensis MR-1 following exposure to UVC, UVB, and UVA radiation.* Journal of Bacteriology, 2005. **187**(10): 3556-3564.
204. Nishino, K., *et al.*, *Regulation of multidrug efflux systems involved in multidrug and metal resistance of Salmonella enterica serovar Typhimurium.* Journal of Bacteriology, 2007. **189**(24): 9066-9075.
205. Lee, S.-Y., *et al.*, *Proteogenomic characterization of antimicrobial resistance in extensively drug-resistant Acinetobacter baumannii DU202.* Journal of Antimicrobial Chemotherapy, 2014. **69**(6): 1483-1491.
206. Bencheikh-Latmani, R., *et al.*, *Global transcriptional profiling of Shewanella oneidensis MR-1 during Cr(VI) and U(VI) reduction.* Applied and Environmental Microbiology, 2005. **71**(11): 7453-7460.
207. Beliaev, A.S., *et al.*, *Global transcriptome analysis of Shewanella oneidensis MR-1 exposed to different terminal electron acceptors.* Journal of Bacteriology, 2005. **187**(20): 7138-7145.
208. Fetar, H., *et al.*, *mexEF-oprN multidrug efflux operon of Pseudomonas aeruginosa: regulation by the MexT activator in response to nitrosative stress and chloramphenicol.* Anitmicrobial Agents and Chemotherapy, 2011. **55**(2): 508-514.

209. Zhang, Y., *et al.*, *Transcriptomic analysis reveals adaptive responses of an Enterobacteriaceae strain LSJC7 to arsenic exposure.* Frontiers in Microbiology, 2016. **7**: 636.
210. Rampioni, G., *et al.*, *Effect of efflux pump inhibition on Pseudomonas aeruginosa transcriptome and virulence.* Scientific Reports, 2017. **7**(1): 11392.
211. Martinez, J.L., *et al.*, *Functional role of bacterial multidrug efflux pumps in microbial natural ecosystems.* FEMS Microbiology Reviews, 2009. **33**(2): 430-49.
212. Hintelmann, H., *et al.*, *Extraction of methylmercury from tissue and plant samples by acid leaching.* Analytical and Bioanalytical Chemistry, 2005. **381**(2): 360-365.
213. Law, V., *et al.*, *DrugBank 4.0: shedding new light on drug metabolism.* Nucleic Acids Research, 2013. **42**(D1): D1091-D1097.